

Characterization and Modeling of a 30 KiloHertz Transformer

by
Anne M. Mitzel

Submitted to the Department of Electrical Engineering and Computer Science

in partial fulfillment of the requirements for the degree of
Master of Engineering in Electrical Science and Engineering

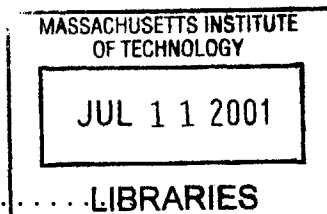
at the

MASSACHUSETTS INSTITUTE OF TECHNOLOGY

January 2001 [February 2001]

© Anne M. Mitzel, MMI. All rights reserved.

The author hereby grants to MIT permission to reproduce and distribute publicly paper and electronic copies of this thesis document **BARKER** in whole or in part.



Author
Department of Electrical Engineering and Computer Science
October 2, 2000

Certified by
Jeffrey H. Lang
Professor, EECS
Thesis Supervisor

Certified by
Mouhoub Mekhiche, Ph.D.
Electro Magnetics/Mechanical Group Leader, Satcon Technology Corporation
Thesis Supervisor

Accepted by
Arthur C. Smith
Chairman, Department Committee on Graduate Students

Characterization and Modeling of a 30 Kilohertz Transformer

by

Anne M. Mitzel

Submitted to the Department of Electrical Engineering and Computer Science
on October 2, 2000, in partial fulfillment of the
requirements for the degree of
Master of Engineering in Electrical Science and Engineering

Abstract

A 30 kilohertz transformer for a power conditioning unit was characterized through extensive experimental measurements. Measurements of the driving-point impedance of the transformer were used to create an equivalent circuit model of the transformer, and the model was optimized for close correspondence between the measured impedance and the impedance of the equivalent circuit. While the impedance predicted by the model bore a close resemblance to the actual driving point impedance of the transformer, the model was unable to predict the transient behavior of the transformer in its operational environment. The model was evaluated to be an impractical method of simulating transformer behavior in a power electronics circuit.

Thesis Supervisor: Jeffrey H. Lang
Title: Professor, EECS

Thesis Supervisor: Mouhoub Mekhiche, Ph.D.
Title: Electro Magnetics/Mechanical Group Leader, Satcon Technology Corporation

Acknowledgments

I would like to thank Mouhoub Mekhiche at SatCon for his invaluable help throughout this project. I would also like to thank Evgeny Holmansky at SatCon for providing the data for the transformer and Professor Lang for his advice and help.

Funding for this project was provided by SatCon Technology Corporation.

Contents

1	Introduction	9
1.1	Background	10
1.2	Technical approach	13
2	Previous Work	16
3	Methods	19
3.1	Equivalent circuit model	19
3.2	Experimental measurements	22
3.2.1	Configuration BD	23
3.2.2	Configuration AB CD	26
3.2.3	Configurations AC, BC, and AD	26
3.2.4	Equipment	27
4	Identification of the Equivalent Circuit Parameters	29
4.1	Modification of the equivalent circuit	30
4.1.1	Coupling coefficient	32
4.1.2	Loss parameters	33
4.2	Optimization procedure	34
4.3	Calculation of six capacitor values	37
5	Simulation	40
5.1	Simulation tool	40
5.2	The transformer as a stand-alone circuit	41

5.3	The transformer in its operational environment	47
5.3.1	Transient simulation results	50
6	Results and Conclusions	58
6.1	Interpretation of results	58
6.2	Conclusion	59
A	Maple Code	62
A.1	Short-circuit impedance	62
A.2	Open-circuit impedance	64
A.3	Open-circuit resonant frequencies	68
B	Matlab Scripts	72
B.1	Minimization script for inductances, capacitances, and resistances . .	72
B.1.1	lxiter.m	72
B.1.2	reserr.m	76
B.1.3	reserrsimpl.m	77
B.1.4	magnerr.m	79
B.1.5	finaldrivingpoint.m	80
B.1.6	finaldrivingcc.m	83
B.2	Determination of six capacitors	85
C	Equivalent Model for Remaining Transformer Configurations	93
C.1	Measured Data	93
C.2	Equivalent Circuit Model	97

List of Figures

1-1	DC to DC converter	11
1-2	Connections to primary and secondary windings	11
1-3	Magnetic structure of transformer	12
1-4	Block diagram of procedure	14
3-1	Equivalent circuit model of transformer	20
3-2	Three independent voltages of a two-winding transformer	20
3-3	Six capacitors of the equivalent circuit model	21
3-4	Impedance of secondary, primary open	23
3-5	Impedance of secondary, primary shorted	24
3-6	Impedance of primary, secondary open	25
4-1	Simplified equivalent circuit model of the transformer	30
4-2	Simplified circuit with additional inductance	31
4-3	Simplified circuit with additional inductance	31
4-4	Open circuit impedance, measured and predicted	36
4-5	Short circuit impedance, measured and predicted	36
5-1	Circuit model of transformer	41
5-2	Open circuit simulation, configuration BD	42
5-3	Short circuit simulation, configuration BD	43
5-4	Simulated impedance from secondary, primary open, various capacitor values	44

5-5	Impedance of secondary, primary open, using six capacitors from Table 5.1	45
5-6	Impedance of secondary, primary shorted, using six capacitors from Table 5.1	46
5-7	Impedance of secondary, primary open, for three-capacitor circuit . . .	47
5-8	Impedance of secondary, primary shorted, for three-capacitor circuit .	48
5-9	Equivalent circuit used for simulation	48
5-10	Connections to external circuit	49
5-11	Test waveforms from the rectifier circuit, 2 kW output power	51
5-12	Test waveforms from the rectifier circuit, 6 kW output power	51
5-13	Transient simulation, 6 kW output power	52
5-14	Transient simulation, $C_1 = 0.1nF$	53
5-15	Transient simulation, $C_1 = 85nF$	54
5-16	Transient simulation, $C_3 = 150nF$	55
5-17	Transient simulation, $C_3 = 15nF$	55
5-18	Transient simulation	56
5-19	Transient simulation	56
C-1	Impedance of full secondary, full primary shorted	94
C-2	Impedance of half secondary, primary open	94
C-3	Impedance of half secondary, full primary shorted	95
C-4	Impedance of half secondary, half primary shorted	95
C-5	Impedance of full primary, secondary open	96
C-6	Full secondary, full primary. Impedance of secondary, primary open .	98
C-7	Full secondary, full primary. Impedance of secondary, primary shorted	98
C-8	Half secondary, full primary. Impedance of secondary, primary open .	99
C-9	Half secondary, full primary. Impedance of secondary, primary shorted	99
C-10	Half secondary, half primary. Impedance of secondary, primary open .	100
C-11	Half secondary, half primary. Impedance of secondary, primary shorted	100

List of Tables

3.1	Experimental measurements	22
3.2	Experimental measurements	27
4.1	Optimized circuit parameter values	37
4.2	Equations relating capacitance values for various measurement configurations	38
4.3	Values for six capacitors	38
5.1	Altered capacitor values	45
5.2	New capacitor values	57
C.1	Measured resonant frequencies	96
C.2	Optimized circuit parameter values	97

Chapter 1

Introduction

The technology of power electronic components has seen many improvements over the past several years, stemmed from the market needs for light weight, compact, and power dense systems, allowing for power circuits that can operate at high frequencies with high efficiency.

A transformer is a device frequently used in power electronic circuits due to its ability to transform voltages and currents while preserving power. In high-power circuits, it is necessary for the transformer to be able to operate at high frequencies and yet with the lowest losses.

To aid in the design and development of power electronic systems, circuit simulation programs exist that can model diodes, transistors, and many other components. However, due to the variety of topologies available for transformers, it is not easy to include a transformer as part of a circuit simulation program. Thus there is a need for an in-depth understanding of the physical phenomena taking place in and generated by wound components such as transformers in order to improve and optimize the design of various power electronic systems.

The goal of this project was to extensively characterize the physical behavior of a transformer operating in a high frequency power conversion and conditioning unit. The analysis was to account for all relevant physical phenomena that affect the performance of the transformer. Such an analysis could then be used to optimize the transformer and the entire power conditioning unit for efficiency and size. The

terminal behavior of the transformer was measured and characterized. An equivalent circuit model for the transformer was developed to be included in a circuit simulation for the study of the system as a whole.

1.1 Background

The transformer in question is part of a power electronics circuit that is currently being developed for use in a fuel cell based commercial product. The circuit is a power conditioning unit that requires the transformer to run at a switching frequency of 30 kHz while transforming 7 kilowatts of output power. It will transform a variable voltage of 40 to 80 volts on the primary to 215 volts on the secondary, carrying an average current of 193 amps on the primary and 32 amps on the secondary. It is part of a push-pull DC to DC converter. A simplified diagram of the push-pull converter is shown in Figure 1-1. The transformer primary has a center tap which is connected to the positive DC bus. Switches control the voltage across each half of the primary winding. When the top switch is closed, the bus voltage is applied across the top half of the transformer. When the bottom switch is closed, the bus voltage is applied across the bottom half of the transformer, with opposite polarity. The effect of the switching will be to place alternating positive and negative voltages across the transformer. Current will alternately flow in opposite directions in the transformer secondary. The diodes and inductors maintain current in one direction across the load at a DC voltage that is higher than the bus voltage at the primary.

The transformer has a primary winding of four turns and a secondary winding with 24 turns. The primary winding is constructed with 24 turns, in bundles of six in parallel to form the equivalent of four total turns. The secondary turns are all connected in series. Each winding has an additional center-tapped connection, resulting in six electrical connections to the transformer as a whole. Figure 1-2 shows the electrical connections to the windings of the transformer.

The magnetic structure of the transformer consists of a ferrite E-core with the windings surrounding the center post, as shown in Figure 1-3. The windings are made

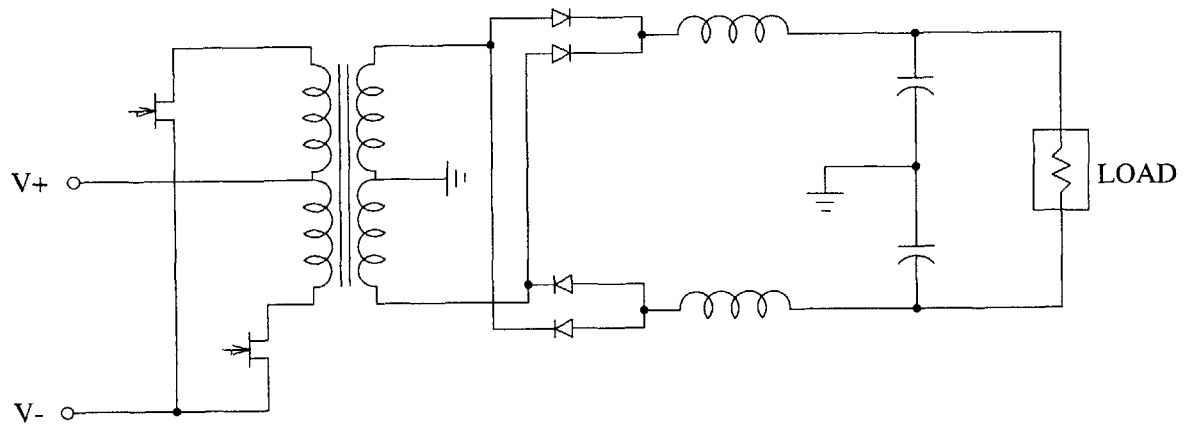


Figure 1-1: DC to DC converter

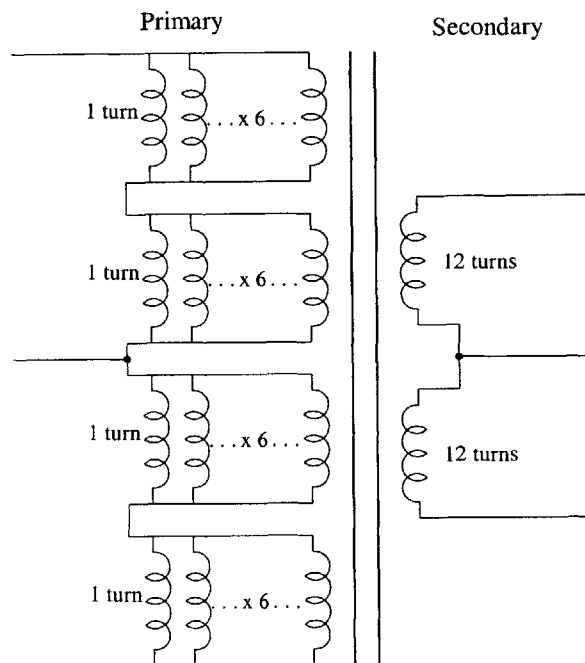


Figure 1-2: Connections to primary and secondary windings

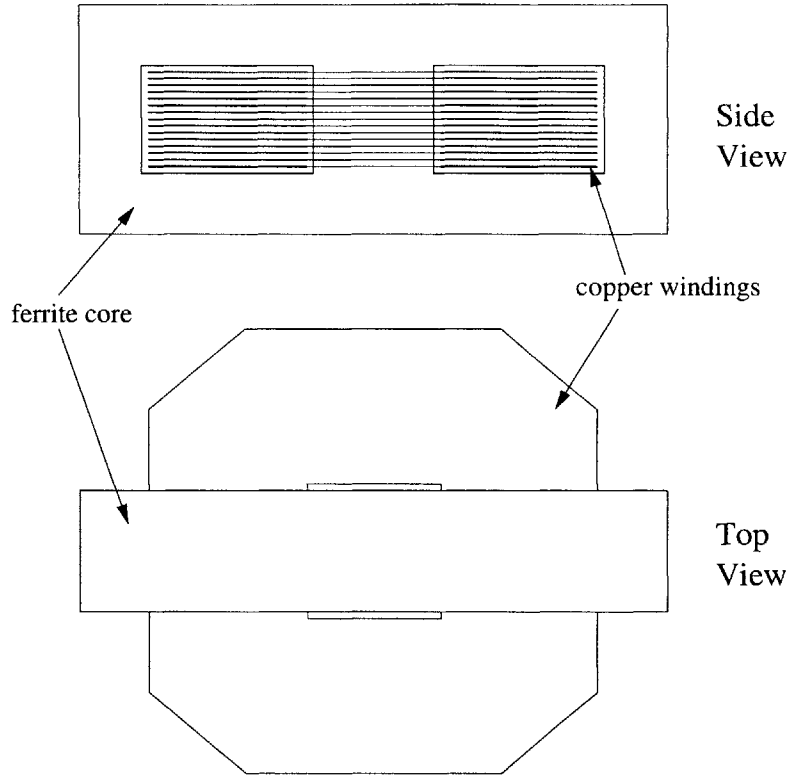


Figure 1-3: Magnetic structure of transformer

of flat copper sheets separated by thin layers of insulating material. The structure of the windings is designed to increase the current density handling capability that is required during normal operation at high frequencies. This is due to the fact that the flat-winding construction of the transformer has several advantages over conventional windings for carrying high current density at a high frequency. Copper sheets with thin layers of insulation between them allow for a much higher packing factor than conventional windings made of rounded insulated wire, as the fill factor is higher for the flat sheets. The resulting effective area of the windings is higher, allowing the windings to carry greater current density. The shape of the windings also has the effect of giving the transformer better performance at high frequency. The thickness of the windings is less than the skin depth of the copper at 30 kHz, so the skin effect is reduced at high frequencies as well as the proximity effect.

However, the use of flat copper conductors in the windings raises other design issues. The flat windings running parallel to each other behave as parallel plate ca-

pacitors, causing inter- and intra-winding capacitances to become significant. The primary and secondary windings are interleaved in order to reduce the leakage inductance of the transformer. However, interleaving the windings greatly increases the parasitic capacitance between the primary and secondary windings, resulting in unplanned resonant frequencies affecting the behavior of the transformer. Capacitance was therefore one of the more important transformer characteristics considered by this thesis.

An attempt was made to analyze the transformer using three-dimensional finite element analysis. However, the geometry of the transformer did not lend itself well to construction of the finite element analysis mesh. Each of the flat windings is about three inches in length and width but only 0.016 inches in thickness. The large difference between the largest and smallest dimension means that a very fine mesh is needed over a large surface area in order to accurately analyze the model. The amount of memory needed to run the simulation exceeded that found in the average computer. The difficulty of performing a physical analysis of the transformer behavior demonstrated the need for a simpler way to accurately predict transformer behavior.

1.2 Technical approach

Preliminary tests of the power conditioning circuit indicated that the transformer was overheating under normal operating conditions. The transformer needed to be made more efficient in order to function effectively as a power transfer device. The objective of this thesis was to allow the transformer and its surrounding circuitry to be improved for efficiency based on a complete description of its behavior.

The procedure for characterizing and optimizing the model is outlined in Figure 1-4. Extensive experimental impedance measurements were carried out, leading to the initial calculation of parameter values for an equivalent circuit model of the transformer. The parameter values were then modified by an optimization procedure to minimize the difference between the equivalent circuit behavior and experimental data points. Simulations were run on the equivalent circuit model in order to rep-

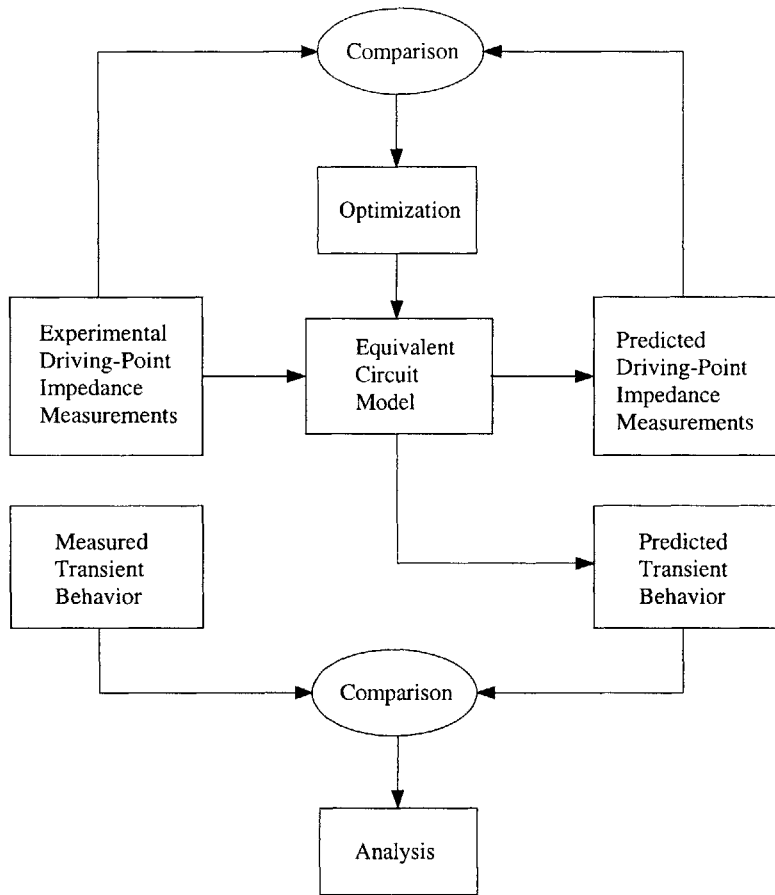


Figure 1-4: Block diagram of procedure

resent the behavior of the transformer in its operating environment. The modeling technique was analyzed for its ability to predict the impedance characteristics of the transformer and its performance in its operating environment.

The procedure for carrying out impedance measurements on the transformer is described in Chapter 3. Open circuit and short circuit driving-point impedance measurements were recorded for various measurement configurations.

The impedance measurements were used to identify parameters for an equivalent circuit representation of the transformer. Chapter 4 describes how the inductance, resistance, and capacitance values were calculated based on the measurements. The equivalent model was optimized for close correspondence between the simulated and measured impedances using error minimization techniques.

After the model was developed, simulations were run on the equivalent circuit

model. Chapter 5 describes the circuit simulation software and the equivalent circuit model. The transformer was simulated both as a stand-alone unit and with inputs that simulate its operating environment. The simulations were compared to the various measurement results as well as actual waveforms recorded from tests on the power electronics unit.

The performance of the model was checked against data taken from testing the transformer, and the effectiveness of the equivalent circuit to predict the transformer properties was analyzed. The results of this analysis are described in Chapter 6.

Chapter 2

Previous Work

Many different approaches have been taken to modeling transformers. Developing an equivalent circuit model for a given transformer is a particularly important task, as it allows the circuit containing the transformer to be simulated and tested for performance before circuit construction. Some of the methods involve using the physical characteristics of a transformer to explain its behavior, while others attempt to describe the transformer using equivalent circuit parameters not dependent on the physical transformer.

Extensive work in this field has been done by the magnetics group at the Laboratoire d'Electrotechnique de Grenoble, France. An experimental method for producing an equivalent circuit model for a transformer is presented in [4]. The method relies only on external open-circuit and short-circuit driving-point impedance measurements taken at the primary and secondary of the transformer. The equivalent circuit includes terms for parallel and series inductance, losses, and parasitic capacitances. The advantage of the model is that it is valid for a wide range of frequencies but is independent of the geometry and construction of the transformer. Transformers of different shape or technology can be represented by the same model with different circuit parameters.

Calculation of capacitances in the equivalent circuit is treated more thoroughly in [1]. The total electrostatic energy stored in a two-winding transformer is shown to depend on six coefficients and three independent voltages. Therefore, the capacitive

effects seen from the terminals of the transformer can be completely described by six capacitors, appropriately placed in the circuit. The six values can be obtained using different measurement configurations in which certain terminals of the transformer are electrically connected. The model then simplifies to a partial equivalent circuit with three capacitor values. An expression for the energy stored by the capacitors is obtained in each case, and this can be used to calculate the six capacitance values of the total equivalent circuit. The capacitor values for the partial equivalent circuits can be found using resonance frequencies, once the open-circuit and short-circuit inductance values of transformer are known. Similarly, once the capacitor values are known, the resonant frequencies can be predicted. The paper also presents a microscopic approach to calculating capacitances and general rules for reducing capacitance in windings.

The equivalent circuit representation of transformers is also given extensive treatment in [3]. Each component of the lumped-parameter equivalent circuit model is discussed, including elements for magnetic coupling; winding resistance, core losses, and eddy current losses; and capacitance between the windings. Calculation of the component values for a two-winding transformer is demonstrated through an example, and a comparison of experimental and theoretical results is presented. The paper also discusses measurement techniques and configurations and issues of accuracy that may arise from impedance measuring equipment.

Transformers of more than two windings are described in [7], which presents a different method for calculating equivalent circuits, related to the method described by the previous work in [4], [1], and [3]. The method allows for transformers with an arbitrary number of windings to be modeled. It also accounts for situations where certain resonant frequencies, which are needed to calculate component values, are out of the range of the measuring apparatus. Rough equivalent circuit models of the transformer are refined in successive steps to make a more and more accurate model.

Multiwinding transformers have also been treated in [6], [8], and [2]. [6] uses a network of circuit elements to model the frequency dependence of resistance and inductance values in the equivalent circuit. This allows the ac winding resistance and

leakage inductance to be calculated over a range of frequencies for high-frequency transformers with any number of windings. A physically-based approach to modeling a multiwinding transformer is given in [8]. The method described was used to more accurately predict leakage inductances in high-voltage multiwinding transformers. The transformers described in the paper all have coaxial windings, however. Leakage inductances are also the focus of [2], which uses the finite element method to relate each parameter of the model to a specific flux in the physical transformer. The form of the model, however, does not depend on the physical geometry of the transformer.

Modeling of a magnetic system with a complicated geometry was performed in [5]. The paper develops a lumped-parameter model to calculate the voltage distribution in a helical armature winding. The model uses electrical cells to represent the windings, including self and mutual inductance between the cells, capacitance between the cells, and capacitance to ground. The values of the parameters are calculated based on the physical structure of the system.

The previous work serves as a basis for this thesis. The method described in [4], [1], and [3] is used here to develop an equivalent circuit model for the transformer. The method had not been previously applied to a transformer with flat windings, and thus it was of interest to determine if the methods extend to this particular topology. Capacitance values were expected to play a particularly large role in the behavior of the transformer, while other factors such as eddy current losses were expected to have a much smaller effect. The equivalent circuit model was simplified in order to focus on the effects which were expected to dominate the transformer's behavior.

Chapter 3

Methods

A circuit model of the transformer was selected, and the values of the circuit components were identified through experimental measurements on the transformer. The equivalent circuit chosen to model the transformer was the one described by Cogitore [3]. A set of measurements was taken at the various transformer terminals in order to determine the parameters representing transformer behavior. The parameters to be determined included magnetic constants, losses, and electrostatic constants. These constants were determined through open-circuit and short-circuit impedance measurements at the various terminals.

3.1 Equivalent circuit model

The equivalent circuit model used for the analysis is shown in Figure 3-1 and includes all the components to be identified. Each circuit element represents a different physical phenomenon affecting the behavior of the transformer. L_p represents the parallel inductance of the transformer, while L_s represents the series inductance. The resistor R_p represents core loss, and DC winding resistances are accounted for in r_1 and r_2 . Eddy current and proximity effects are neglected in this circuit as a simplification, since the expected eddy current losses are low due to the winding structure. The six capacitors in the circuit represent all possible capacitive couplings observed at the terminals of the transformer [1].

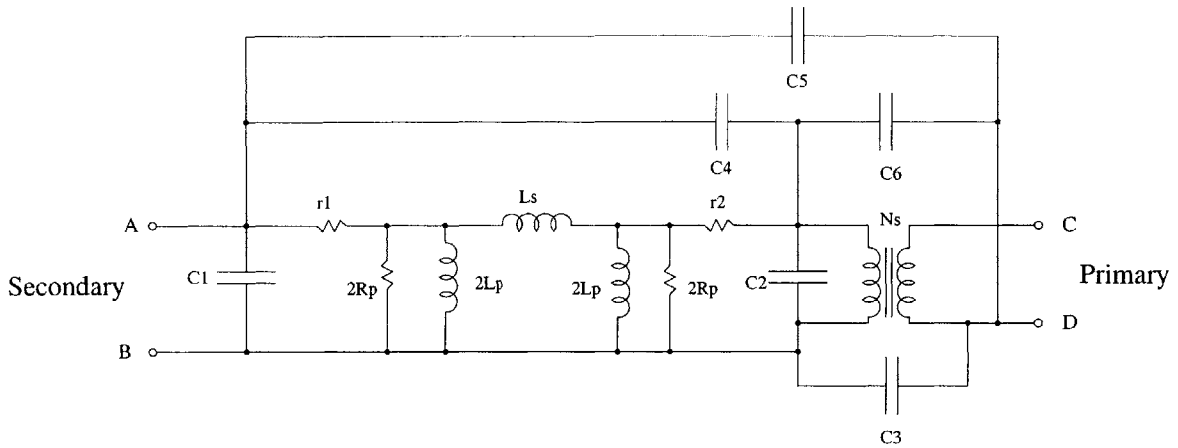


Figure 3-1: Equivalent circuit model of transformer

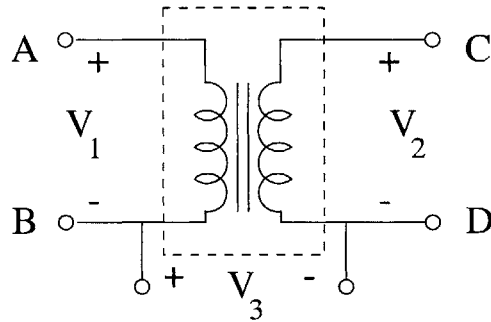


Figure 3-2: Three independent voltages of a two-winding transformer

A two-winding transformer has at most three independent voltages, depicted in Figure 3-2: the voltage on the primary, the voltage on the secondary, and the voltage difference between one terminal of the primary and one terminal of the secondary. The stored electrostatic energy of the system is a function of the three voltages:

$$W_E = \frac{1}{2}C_{11}V_1^2 + \frac{1}{2}C_{22}V_2^2 + \frac{1}{2}C_{33}V_3^2 + C_{12}V_1V_2 + C_{13}V_1V_3 + C_{23}V_2V_3 \quad (3.1)$$

The six coefficients $C_{11} - C_{23}$ completely characterize the electrostatic behavior of the transformer. [1]

Figure 3-3 is a simplified version of Figure 3-1 showing the six capacitors of the

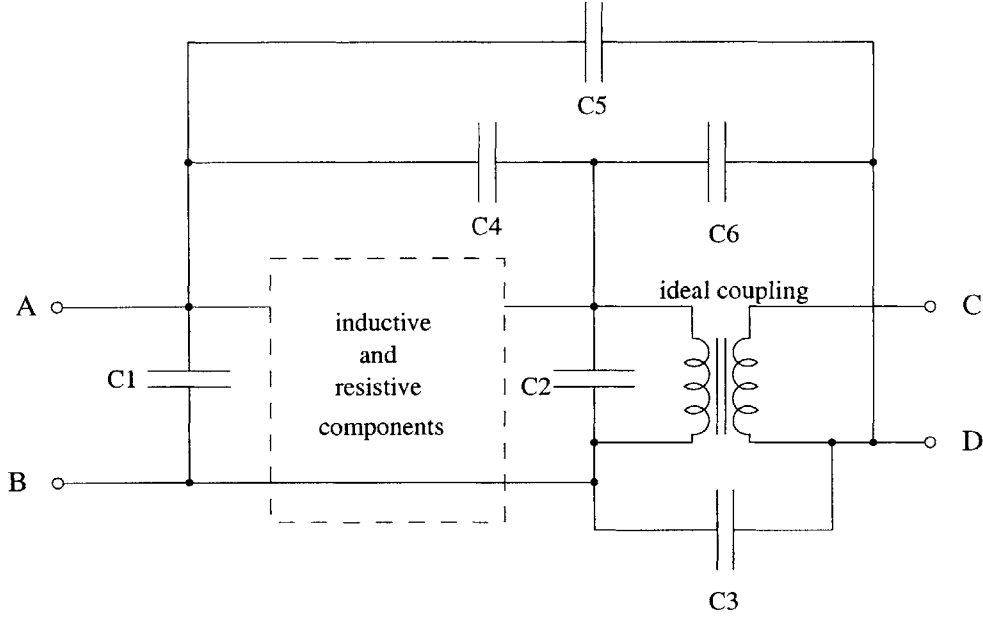


Figure 3-3: Six capacitors of the equivalent circuit model

equivalent circuit model. The stored electrostatic energy in this circuit is given by

$$W_E = \frac{1}{2}C_1V_1^2 + \frac{1}{2}C_2\left(\frac{V_2}{N}\right)^2 + \frac{1}{2}C_3V_3^2 + C_4\left(V_1 - \frac{V_2}{N}\right)^2 + \frac{1}{2}C_5(V_1 - V_3)^2 + \frac{1}{2}C_6(V_2 - V_3)^2 \quad (3.2)$$

Equating the expressions of Equations 3.1 and 3.2 gives expressions for the six capacitors of the equivalent circuit model in terms of the coefficients $C_{11} - C_{23}$. [3]

$$C_1 = C_{11} + NC_{12} + C_{13}$$

$$C_2 = N^2C_{22} + NC_{12} + NC_{23}$$

$$C_3 = C_{33} + C_{13} + NC_{23}$$

$$C_4 = -NC_{12}$$

$$C_5 = -C_{13}$$

$$C_6 = -NC_{23}$$

Configuration	Experiment	Shorted connections	Driving point impedance port
BD	1	BD	AB
	2	BD, CD	AB
	3	BD	CD
AB CD	4	AB, CD	BD
AC	5	AC	AB
	6	AC, CD	AB
BC	7	BC	AB
	8	BC, CD	AB
AD	9	AD	AB
	10	AD, CD	AB

Table 3.1: Experimental measurements

3.2 Experimental measurements

Identification of the equivalent circuit parameters involved the use of driving point impedance measurements. Different conditions of the impedance measurements were used to compute the various circuit elements. Low frequency values of the inductance, resonant frequencies, and peak impedance values were observed from the measurements and used to calculate the parameter values.

There were four possible models that could be developed for the transformer under study, depending on whether the center tap was used as a connection. The measurements could utilize half or all of the primary or secondary winding. The model using the full secondary winding and half of the primary winding was chosen for its significance in later simulations, using the secondary as port AB and half of the primary as port CD. For completeness and to verify the accuracy of the modeling method, measurements were recorded for the three other transformer models. A description of those measurements can be found in Appendix C.

Several sets of driving point impedance measurements were taken at the terminals of the transformer. The various experiments are listed in Table 3.1.

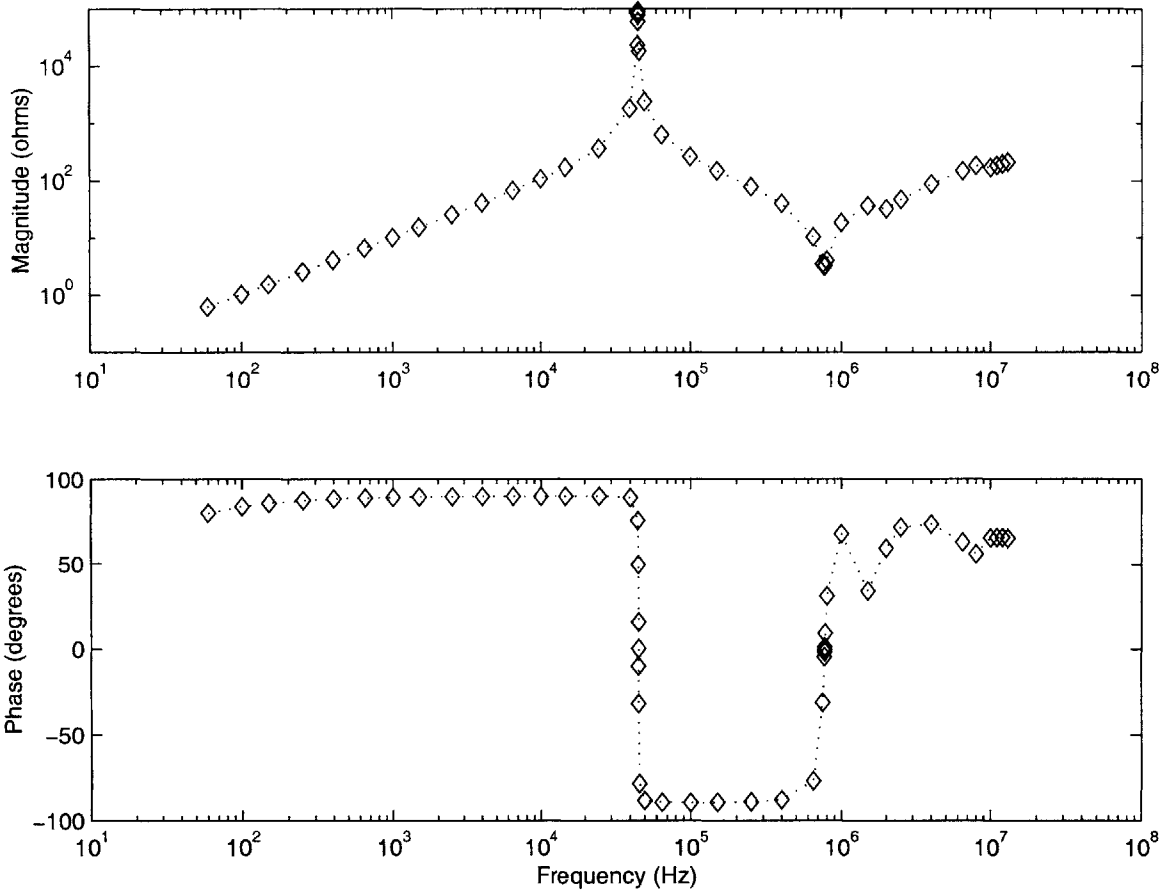


Figure 3-4: Impedance of secondary, primary open

3.2.1 Configuration BD

Three full plots of the driving point impedance were made for the configuration in which B was connected to D. The first plot measured the impedance seen from the secondary (AB) with the primary (CD) open, the second the impedance seen from AB with CD shorted, and the third the impedance seen from CD with AB open. The magnitude and phase of the impedance were recorded over a range of frequencies from 60 Hz to 13 MHz. Plots of the measured impedance are found in Figures 3-4, 3-5, and 3-6.

The experiments performed with configuration BD allowed for the calculation of the inductive and resistive parameters in the equivalent circuit model and provided information relevant to the calculation of the capacitor values, as described in Chap-

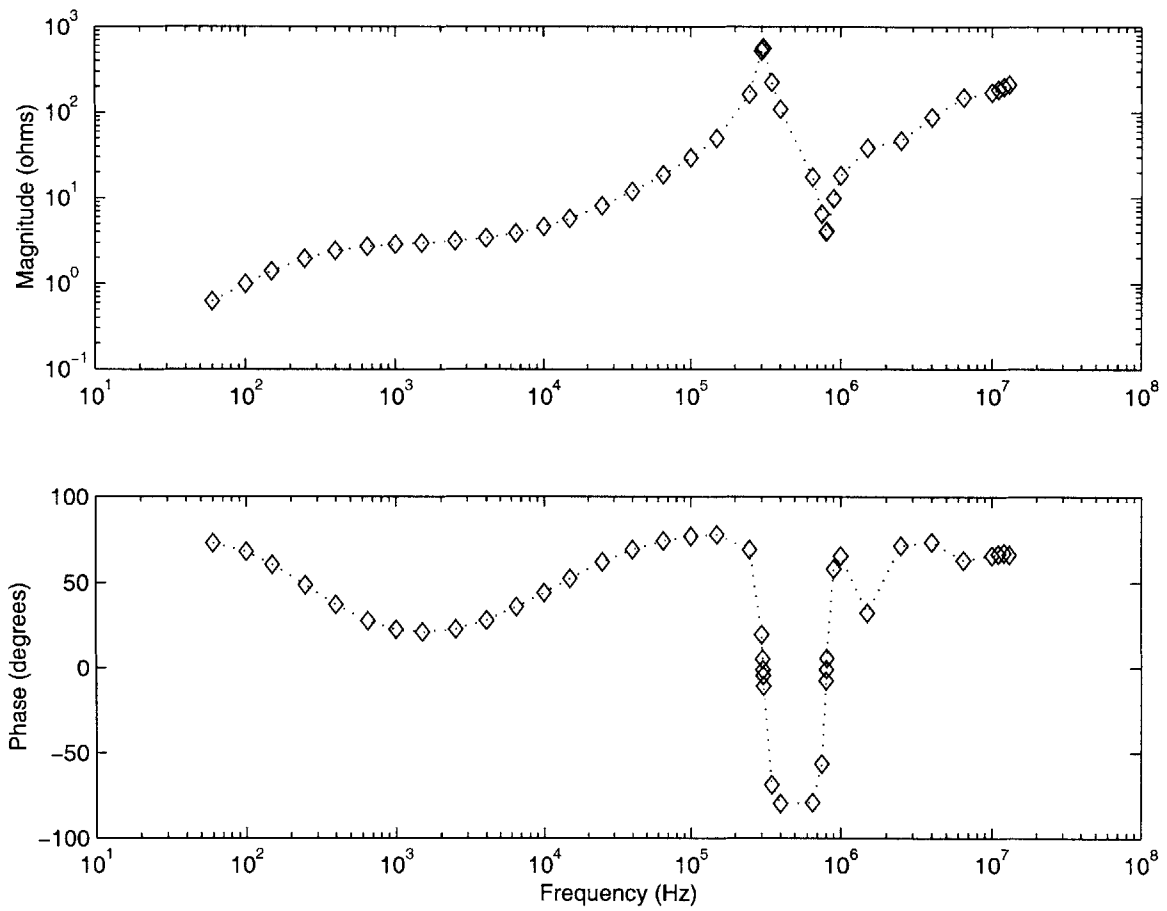


Figure 3-5: Impedance of secondary, primary shorted

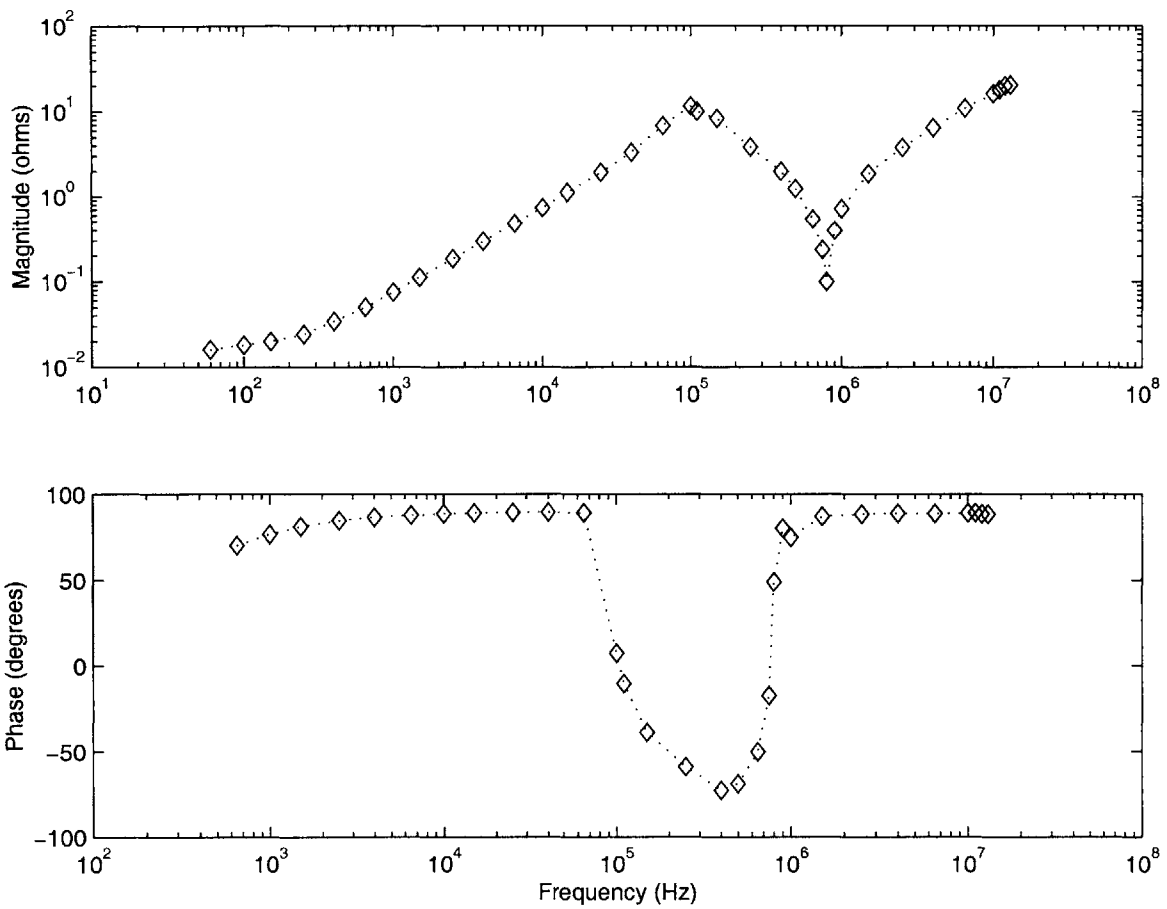


Figure 3-6: Impedance of primary, secondary open

ter 4.

The measurements using this configuration were later compared to bode plots of the impedance of the equivalent circuit model in order to verify the accuracy of the model.

3.2.2 Configuration AB CD

When the ports AB and CD are shorted, $V_1 = 0$ and $V_2 = 0$. Equation 3.1 reduces to

$$W_E = \frac{1}{2}C_{33}V_3^2 \quad (3.3)$$

Measuring the capacitance between terminals B and D gave the capacitive coefficient C_{33} . The measurement was taken at several low frequencies in order to confirm the accuracy of the measurement.

$$C_{33} = 12.8nF$$

3.2.3 Configurations AC, BC, and AD

Open-circuit and short-circuit driving point impedance measurements were taken for each of the remaining configurations in Experiments 5 through 10. In each case the impedance was measured from the transformer secondary, AB, while the primary, CD, was either open or shorted. The first two resonant frequencies were recorded for each open-circuit experiment, and the first resonant frequency was recorded for each short-circuit experiment. The point where the phase of the impedance crossed zero was observed and used to precisely determine the resonant frequency. Capacitor values for the equivalent circuit model depend on the resonant frequencies of the various measurement configurations.

The measured frequencies are listed in Table 3.2. The resonant frequencies of configuration BD are also listed. f_p is the frequency of the parallel resonance, or peak in the impedance graph. f_s is the frequency of the series resonance, or valley in the impedance graph.

Configuration	$f_{p,open}$	$f_{s,open}$	$f_{p,short}$
BD	45.43kHz	773kHz	307kHz
AC	41.96kHz	723kHz	317kHz
BC	51.05kHz	850kHz	330kHz
AD	48.72kHz	814kHz	337kHz

Table 3.2: Experimental measurements

The ten experiments gave enough data to overdetermine the eleven equivalent circuit parameters. With more than the necessary amount of data, redundant results could be compared against each other for consistency.

3.2.4 Equipment

The relatively low impedance of the transformer made impedance measurements difficult. Preliminary impedance characteristics were measured using a Hewlett-Packard 4395A network analyzer. The frequency characteristics measured by the network analyzer showed significant differences from measurements taken using a current probe and oscilloscope. High frequency resonances occurred at different frequencies and the shape of the waveform differed slightly at low frequencies. It was speculated that impedances internal to the network analyzer and its probe were changing with frequency in a way that could not be measured or compensated. These speculations were supported by similar problems related in [3]. Since the test configuration for using the HP4395A as an impedance analyzer was not available, measurements were instead carried out on a Hewlett-Packard 4192A impedance analyzer. The impedance analyzer can measure low impedances with greater accuracy than a network analyzer.

The method of [3] required that various driving-point impedance measurements be taken over a swept range of frequencies. Two impedance measurements were to be taken from side AB of the transformer (one with the leads CD open and one with the leads CD shorted together) and one impedance measurement was to be taken from side CD (with the port AB open). The equivalent circuit parameters depended more heavily on the measurements taken from side AB than on those taken from

the side CD. The accuracy of the model may depend on the choice of which side of the transformer is considered as AB and which is CD. Since measurements of lower impedances run a greater risk of error due to equipment inaccuracies, more accurate results are likely to be obtained when the side chosen as port AB has a higher impedance. It was expected that more accurate results would be obtained by choosing the side of the transformer with the greater number of turns to represent AB, since a greater number of turns made the impedance seen from this side of the transformer slightly higher.

The secondary side of the transformer in question was chosen to correspond to the port AB. The secondary of the transformer had a higher number of turns and therefore the expected impedance was higher.

The HP4395A did not have automatic sweep measurement or data recording capability in the configuration that was available to perform the testing. Individual data points had to be read and recorded manually. As a result, measurements are discrete rather than continuous, and the data is not as thorough as the measurements recorded in [3].

Chapter 4

Identification of the Equivalent Circuit Parameters

The values of the circuit components were calculated using external impedance measurements. The experimental method described in [3] for creating a lumped-parameter equivalent circuit depends on the open-circuit impedance measured from both sides of the transformer and the short-circuit impedance measured from one side. Different aspects of the impedance measurements, taken as a function of frequency, were used to compute the various circuit elements. Low frequency values of the inductance, resonant frequencies, peak impedance values, and mid-frequency impedance values were observed from the measurements and used to calculate the parameter values.

Figure 4-1 shows a simplified version of Figure 3-1, using the configuration in which terminal B is connected to D. If this connection is made, the capacitor C_3 is eliminated from the circuit, the capacitor C_5 is in parallel with C_1 , and C_6 is in parallel with C_2 . The resulting circuit can thus be described by three capacitor values, as shown in Figure 4-1, where C_A is equal to $C_1 + C_5$, C_B is equal to $C_2 + C_6$, and C_C is equal to C_4 . This simplified circuit was used to calculate the resistive and inductive circuit components of the model and to compare predicted impedance with the measurements described in Chapter 3. Measurements using the remaining configurations were later used to define all six capacitor values shown in Figure 3-1.

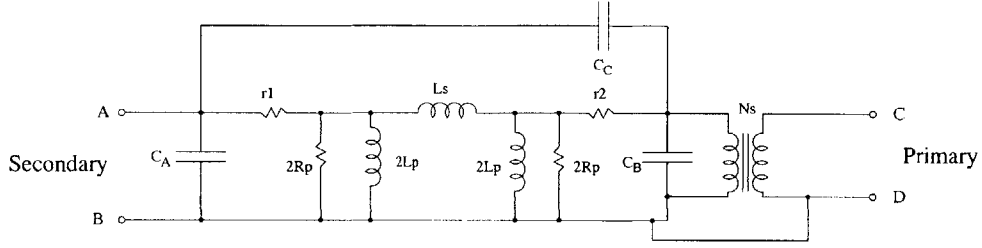


Figure 4-1: Simplified equivalent circuit model of the transformer

4.1 Modification of the equivalent circuit

The measured open circuit and short circuit impedance curves differed from those predicted by the equivalent circuit model in [3]. In particular, there was an additional series resonance in the short circuit impedance that was not found in [3], and a positive slope to the high frequency impedance in both the open and short circuit case, shown in Figures 3-4 and 3-5. These characteristics suggest that an additional inductive element was present in the measured impedance that was not accounted for in the equivalent circuit. A filter present on the measurement equipment was suspected to have caused the additional inductance.

Figure 4-2 shows a modified version of Figure 4-1. The circuit does not contain any resistive elements and has an additional inductor L_x representing the inductance of the measurement setup. In addition, to simplify the consideration of the driving point impedance seen from port AB with port CD open, the ideal coupling and the port CD are not included. Figure 4-3 shows the circuit of Figure 4-1, simplified for the case in which port CD is shorted and the driving point impedance seen from port AB is considered.

The parameters L_x , L_p , and L_s were estimated based on the impedance measurements and the circuits of Figures 4-2 and 4-3, as discussed below. The resonant frequencies of the measured impedance were used to refine the estimates of the inductances and calculate the values of the capacitors C_A , C_B , and C_C . Finally, initial estimates of the resistive parameters were refined in order to fit the measured data. The calculated values can be found in Table 4.1.

An initial estimate for the value of the unknown impedance L_x was obtained by

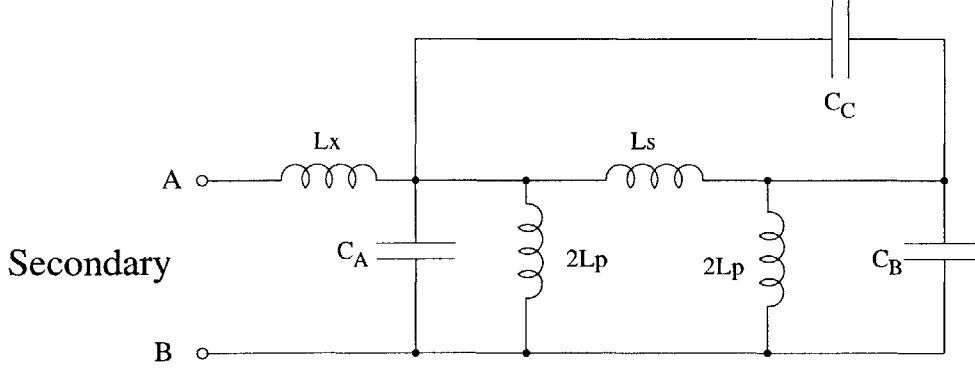


Figure 4-2: Simplified circuit with additional inductance

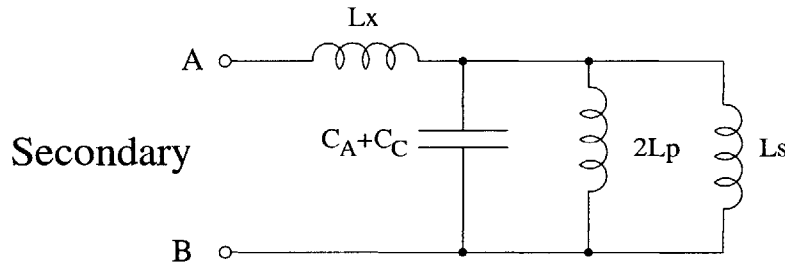


Figure 4-3: Simplified circuit with additional inductance

using the value of the measured high frequency impedance. Expressions for the low frequency open circuit inductance, L_O , and the low frequency short circuit inductance, L_c , were derived using the equivalent circuits of Figures 4-2 and 4-3.

$$L_O = L_x + 2L_p || (2L_s + 2L_p) \quad (4.1)$$

$$L_c = L_x + 2L_p || L_s \quad (4.2)$$

Based on the circuit of Figure 4-3, an expression for the frequency of the parallel resonance can be found.

$$\omega_{p,short} = \frac{1}{\sqrt{(C_A + C_C)(L_c - L_x)}} \quad (4.3)$$

The short circuit series resonance is given by

$$\omega_{s,short} = \frac{1}{\sqrt{L_x(1 - \frac{L_x}{L_c})(C_A + C_C)}} \quad (4.4)$$

A script written in Matlab iteratively determined the values of L_x , L_p , L_s , and $C_A + C_C$ which fit the measured low frequency inductance and short circuit resonant frequencies. The script is included in Appendix B.

The resonant frequencies of the open circuit model were used to determine the three capacitor values, given the constraint on the value of $C_A + C_C$. The open circuit equivalent model of Figure 4-2 has four resonant frequencies: two series resonances, or peaks in the impedance graph, and two parallel resonances, or troughs in the impedance graph. In Figure 3-4, for example, the first series and parallel resonant frequencies are easy to observe. The second two resonant frequencies occur close together and are more difficult to observe. The phase plot of the impedance is helpful in estimating the higher resonant frequencies.

Due to the complex nature of the expression for the impedance of Figure 4-2, a mathematical program was used to derive the expression, which can be found in Appendix A. A Matlab script determined the values for the capacitors C_A , C_B , and C_C which matched the measured resonant frequencies to the roots of the numerator and denominator of the impedance expression. The script is included in Appendix B. The calculated values can be found in Table 4.1.

4.1.1 Coupling coefficient

The coupling coefficient for the equivalent circuit is calculated from the low frequency open-circuit inductance seen from the secondary of the transformer and that seen from the primary. The coefficient for the ideal coupling is given by

$$N_S = \sqrt{\frac{L_{OP}}{L_{OS}}} \quad (4.5)$$

where L_{OS} and L_{OP} are the low frequency open-circuit inductance seen from the secondary and primary, respectively. The low frequency inductance of the secondary (port AB) is just $L_O - L_x$ from Equation 4.1. Similarly, the low frequency inductance of the primary (port CD) can be calculated from the measured low frequency inductance of Experiment 3 (Table 3.1) by subtracting L_x . The calculated coupling

coefficient, $N_S = \sqrt{\frac{1.16 \times 10^{-5}}{1.59 \times 10^{-3}}} = 0.0854$, closely approximates the known turns ratio of the transformer, $\frac{2}{24} = 0.0833$.

4.1.2 Loss parameters

The value of the parallel resistance R_p was determined by calculating the height of the first resonant peak in the open-circuit impedance measured from the secondary, shown in Figure 3-4. This resistance represents core losses in the transformer.

There are several possible ways of determining the DC winding resistance for each winding. One way is to note that the resistance plotted versus frequency for the open-circuit impedance of the secondary at low frequencies gives r_1 , the DC winding resistance of the secondary. The low frequency resistance calculated from the open-circuit impedance measured from the primary gives $N_S^2 r_2$, the DC winding resistance seen from the primary. This method of calculation gave $r_1 = 5.5\Omega$ and $r_2 = 2.4\Omega$. As a check, the short-circuit impedance of the secondary at low frequencies can be used to determine $r_1 + r_2$, the total DC winding resistance seen from the secondary. However, the value for $r_1 + r_2$ was calculated to be 1.5Ω . The two methods gave inconsistent results. Measurement noise and error can account for the difficulty in calculating these two values. An ohmmeter capable of determining very small resistances was used to measure the values of the low frequency resistance seen from both the primary and secondary. Even with this piece of equipment, there was a great deal of measurement noise, and the values for r_1 and r_2 are only close approximations. However, since the ohmmeter was the most direct method of measuring r_1 and r_2 , the resistance measurements were used for the initial estimates of r_1 and r_2 .

Since the resistor values R_p , r_1 , and r_2 of Figure 4-1 had only been estimated previously, a Matlab script was run which selected values for the resistor parameters. The script attempted to minimize the difference between the predicted circuit impedance and the measured points over the entire range of frequencies. The resistor values can be found in Table 4.1.

4.2 Optimization procedure

Since the impedance of the equivalent circuit is a complicated mathematical expression depending on all the circuit parameters, Matlab was used as a mathematical aid in optimizing the equivalent circuit. Scripts written in Matlab adjusted the circuit parameters to make the predicted impedance more closely match the measured impedance. The scripts would often minimize the error between the impedance of the equivalent circuit and the measured impedance data points. Initial estimates for the parameters were given to the programs as a starting point, and the script was allowed to change one or more component values in order to find a local minimum for the error.

Several attempts were made to optimize the equivalent circuit by varying all circuit parameters simultaneously. The program was given an initial set of parameter values and was able to vary those parameters until it found a minimum for the difference between the predicted and measured impedance. Since the function to be minimized was often complicated and nonlinear, the results depended heavily on the initial values given. The exact definition of the error function also played a significant role in determining the final results. For example, data points in certain frequency ranges could be weighted more heavily than others, or the program could consider the absolute or relative error of the values. The varying nature of the program output indicated a strong need for a more intelligent optimization process.

As described in Section 4.1, the values of the inductances could be determined with confidence from the measured data points. The capacitances could then be determined as well. Once those parameters were set, it was easier to determine the remaining resistor values.

Equations 4.1 through 4.4 allowed for the calculation of the inductors in the circuit, as well as the sum of the capacitor values $C_A + C_C$. Given the measured values of the low frequency inductances L_O and L_c and the resonant frequency $\omega_{p,short}$, the program used an estimated value of L_x to determine the remaining inductances and the value of $C_A + C_C$. L_x was then recalculated using the value for $\omega_{s,short}$ and an

iterative process continued until the value for L_x no longer changed.

With the inductive values already determined, the program used the four open circuit resonant frequencies to calculate C_A , C_B , and C_C . The constraint on the value of $C_A + C_C$ gave two degrees of freedom to determine the three capacitor values. A minimization script was used in this case. The function minimized the difference between the predicted and measured resonant frequencies, weighting all four resonances equally.

The three resistive parameters were determined using another minimization script. The function minimized the difference between the predicted and measured impedance in both the open and short circuit case, calculating the error over a range of data points. Since more data points were taken around the resonant frequencies of the impedance, some points around the resonant frequencies were eliminated from the minimization script. This prevented the program from giving too much weight to the value of the function near the resonant frequencies. The program took the measured R_p , r_1 , and r_2 as initial values. The error value was increased whenever the resistor values differed from their original values by more than 15 percent, thereby ensuring that the calculated values were still realistic.

Final circuit parameter values are shown in Table 4.1. It should be noted that the negative value for C_C does not pose a problem, since only capacitances which can be measured physically are required to be positive. Figures 4-4 and 4-5 show the predicted driving-point impedance of the equivalent circuit model, using the parameter values of Table 4.1. The predicted impedance is plotted with the measured data points from Figures 3-4 and 3-5.

The operating frequency of the transformer is 30 kHz. However, since the driving waveform will be a square wave with varying duty cycle, frequencies higher than 30 kHz are relevant to the operation of the transformer. Frequencies below 30 kHz may also be important as the duty cycle varies with time. The optimized circuit values match the measured impedance in a frequency range several orders of magnitude above and below the operating frequency. The optimization also yields circuit parameter values that are very close to the original calculated values. The result of the

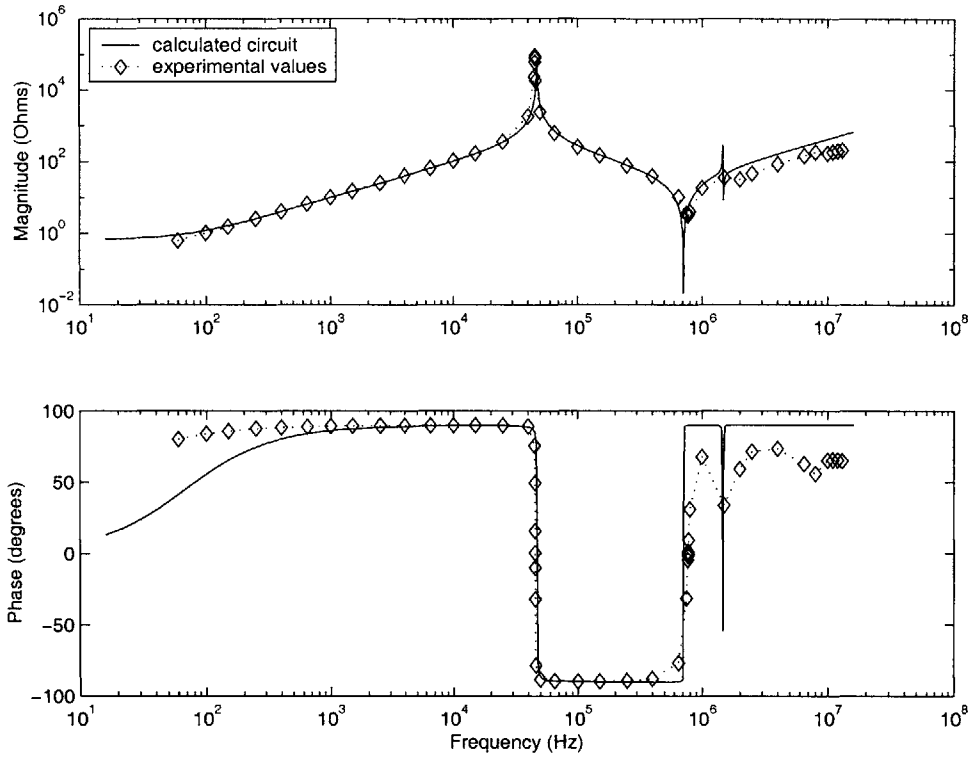


Figure 4-4: Open circuit impedance, measured and predicted

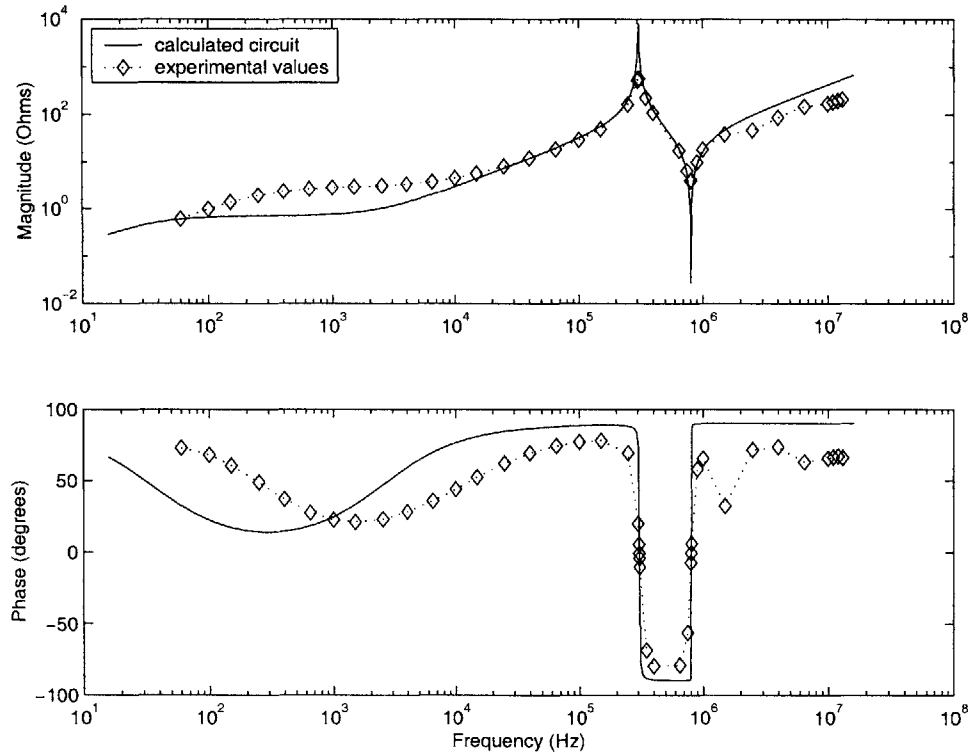


Figure 4-5: Short circuit impedance, measured and predicted

L_x	6.81 μ H
L_p	1.57mH
L_s	40.5 μ H
R_p	78.0k Ω
r_1	685m Ω
r_2	32.3m Ω
C_A	6.81nF
C_B	0.41nF
C_C	-0.088nF
N_S	0.0854

Table 4.1: Optimized circuit parameter values

optimization affirms the accuracy of the model within a wide frequency range.

There were certain tradeoffs in the optimization procedure. The new impedance curve no longer matches the magnitude of the resonant peaks as closely as it did before. However, it was considered most important to match the frequency values of the resonance and the high and low frequency inductor values.

4.3 Calculation of six capacitor values

The majority of the measurements on the transformer were taken with the configuration shown in Figure 4-1, where B on the secondary was connected to D on the primary. However, in order to calculate all six capacitor values in Figure 3-1, resonant frequencies are needed from other measurement configurations.

The first series and parallel resonant frequencies for the open and short circuit impedance was recorded for all measurement configurations described in Chapter 3 and listed in Table 3.1. The three capacitor values C_A , C_B , and C_C were determined for each case. Table 4.2 shows how the capacitor values for each measurement configuration relate to the capacitive coefficients of Equation 3.1, as described in [1]. The measurements generated thirteen equations with which to calculate the six unknown capacitances. The capacitors values are overspecified by the available information.

Since there are many redundant calculations possible for determining the six ca-

Configuration	Equations
BD	$C_A + C_B = C_{11} + N^2 C_{22} + 2NC_{12}$ $C_A + C_C = C_{11}$ $C_B + C_C = N^2 C_{22}$
AB CD	$C_{33} = C_{measured}$
AC	$C_A + C_B = C_{11} + C_{33} + 2C_{13} + N^2(C_{22} + C_{33} - 2C_{23})$ $+ 2N(C_{12} - C_{33} - C_{13} + C_{23})$ $C_A + C_C = C_{11} + C_{33} + 2C_{13}$ $C_B + C_C = N^2(C_{22} + C_{33} - 2C_{23})$
BC	$C_A + C_B = C_{11} + N^2(C_{22} + C_{33} - 2C_{23}) + 2N(C_{12} - C_{13})$ $C_A + C_C = C_{11}$ $C_B + C_C = N^2(C_{22} + C_{33} - 2C_{23})$
AD	$C_A + C_B = C_{11} + C_{33} + 2C_{13} + N^2 C_{22} + 2N(C_{12} + C_{23})$ $C_A + C_C = C_{11} + C_{33} + 2C_{13}$ $C_B + C_C = N^2 C_{22}$

Table 4.2: Equations relating capacitance values for various measurement configurations

	BD AC	BD BC	BD AD	BC AD	Best fit	C_C fit	C_A and C_B fit
C_1	124.9nF	-405.8nF	110.6nF	99.2nF	163.9nF	162.2nF	107.5nF
C_2	6.31nF	-39.6nF	4.91nF	150.1nF	24.5nF	25.7nF	40.0nF
C_3	15.3nF	-30.7nF	26.1nF	306.4nF	52.5nF	54.7nF	52.4nF
C_4	-3.52nF	-3.52nF	-3.52nF	119.2nF	-3.90nF	-.088nF	-.088nF
C_5	-114.7nF	527.5nF	-100.3nF	11.11nF	-44.2nF	-42.5nF	-100.7nF
C_6	-2.47nF	43.5nF	-13.3nF	-293.5nF	-39.7nF	-41.9nF	-39.6nF

Table 4.3: Values for six capacitors

capacitor values, the capacitors were calculated many different ways and the results were compared against each other. All calculations utilized the measurement from configuration AB CD, which gave the value for C_{33} . The first calculation combined data from when B and D from Figure 3-1 are connected together (configuration BD) and from when terminals A and C are connected together (configuration AC). The second calculation used configuration BD and configuration BC, the third configurations BD and AD, and the fourth configurations BC and AD. The resulting values are shown in Table 4.3.

It should be noted that, although a capacitance which can be directly measured can only be positive, the capacitors of the equivalent circuit are not necessarily directly related to measurable capacitances in the transformer. The six capacitors in total represent the electrostatic interactions in the transformer, and since some couplings may reduce the stored electrostatic energy, the capacitances are allowed to be negative [1].

Considering the wide variety of resultant capacitor values, it was deemed appropriate to calculate a best fit for the unknown capacitances. A set of twelve equations for the five remaining unknowns was processed by Matlab, giving equal confidence to all equations. The results appear in Table 4.3 in the column labeled “Best fit”.

Since the configuration of Figure 4-1 was more completely characterized than the other measurement configurations, there is more confidence in the capacitor values calculated from that configuration. C_C in Figure 4-1 is the same as C_4 in Figure 3-1, eliminating one of the unknowns from the set of equations. Taking this into account yields the results in column “ C_C fit”. Finally, $C_1 + C_5$ in Figure 3-1 is equal to C_A in Figure 4-1, and $C_2 + C_6$ in Figure 3-1 is equal to C_B in Figure 4-1. The values for C_A and C_B , as well as that for C_C , were matched by the final calculation. The results are in column “ C_A and C_B fit”.

The difficulty in finding a consistent set of capacitor values plays a significant role in the effectiveness of the equivalent circuit under simulation.

Chapter 5

Simulation

The measurements and calculations of the previous chapter were used to develop the circuit diagram shown in Figure 5-1 as described in [3]. Figure 5-1 is identical to Figure 3-1, but the values for the inductances, resistances, and coupling coefficient have been included in the figure. L_p represents the parallel inductance of the transformer, while L_s represents the series inductance. The resistor R_p represents core loss, and DC winding resistances are accounted for in r_1 and r_2 . The six capacitors in the circuit represent all possible capacitive couplings between the terminals. The ideal coupling of the equivalent circuit was represented in simulation by a voltage-controlled voltage source and a current-controlled current source of identical gain.

5.1 Simulation tool

Simulations of the equivalent circuit were performed using Simplorer circuit simulation software. Simplorer allows a circuit schematic to be entered with values for each of the components. An equivalent circuit can be driven by a sinusoidal source over a range of frequencies, or by a source of arbitrary waveform. Both types of analysis were used in this case, since both frequency-dependent characteristics and time-domain transient performance were important to the model. Simplorer can calculate and plot various voltages and currents for a given input. Simplorer will also calculate mathematical combinations of voltages and currents that allow calculation

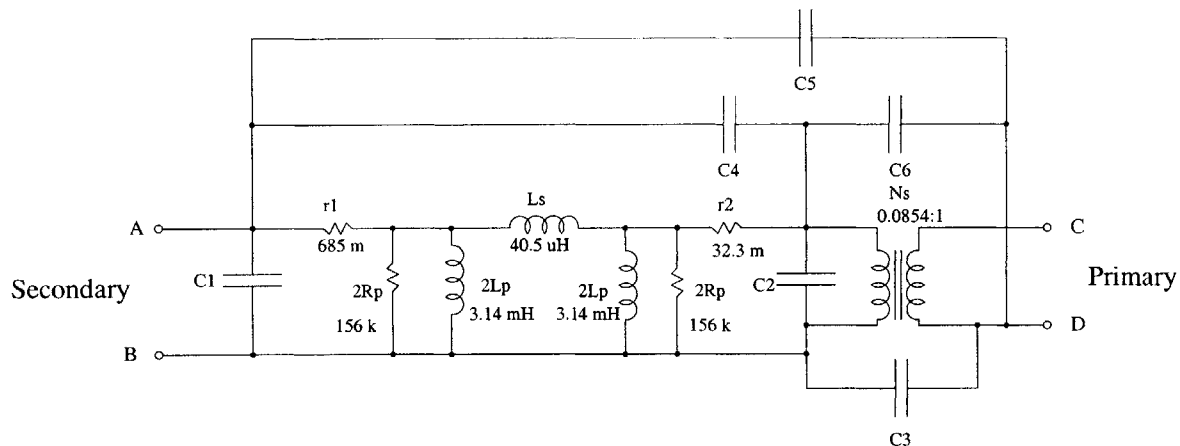


Figure 5-1: Circuit model of transformer

of other important considerations, such as magnitude and phase.

As described in Section 4.3, the capacitors in the equivalent circuit may take on negative values, provided that no capacitances which can be measured directly are negative. Simplorer accepts negative values for capacitors without giving an error. Simplorer will, however, give unstable results in transient simulation if the combination of capacitor values results in a physically impossible situation, one in which measurable capacitances in the circuit would turn out to be negative. This fact provides an additional check for the appropriateness of the capacitor values in transient simulation.

5.2 The transformer as a stand-alone circuit

In order to confirm the ability of the model to represent the transformer as it was experimentally measured, the transformer was simulated as a stand-alone circuit. AC sweep analysis was performed in order to find the voltage to current ratio seen from the secondary side of the transformer. A resistor of value 1 Megaohm placed across the primary of the transformer simulated an open circuit, while a resistor of 1 milliohm placed at that winding simulated a short circuit. The open-circuit and short-circuit impedances from the simulation were compared against the experimentally measured

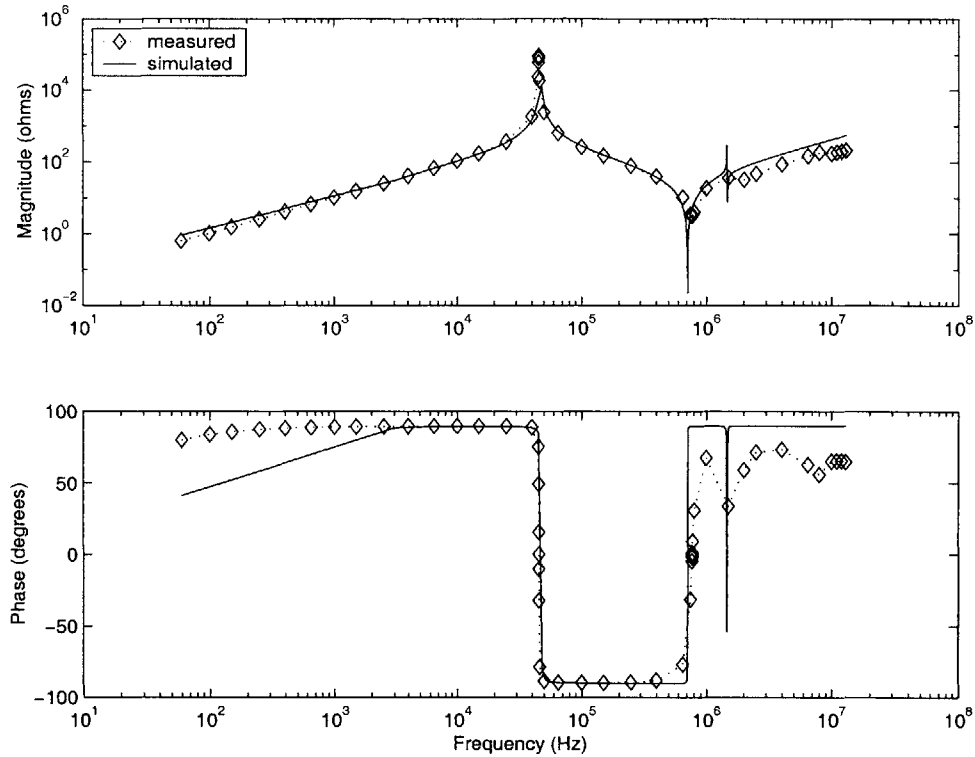


Figure 5-2: Open circuit simulation, configuration BD

values.

The measurement configuration of Figure 4-1, configuration BD, was used for the first set of simulations. Therefore, the capacitor values $C_A - C_C$ were used, rather than $C_1 - C_6$. The component L_x was included in the circuit so that it could be compared accurately to the measured data.

The simulated data is plotted with the measured data points in Figures 5-2 and 5-3. The plot closely matches the measured impedance, as predicted by the previous analysis and summarized in Figures 4-4 and 4-5.

Since the actual circuit under operation does not have terminal B connected to terminal D, it is important to consider the accuracy of the six capacitor circuit of Figure 3-1. The driving point impedance of the secondary (AB) of the six capacitor circuit was simulated and compared against a set of measurements in which no connection had been made between the secondary and primary. Since there were many possibilities for the six capacitances, the simulation was performed for each case in

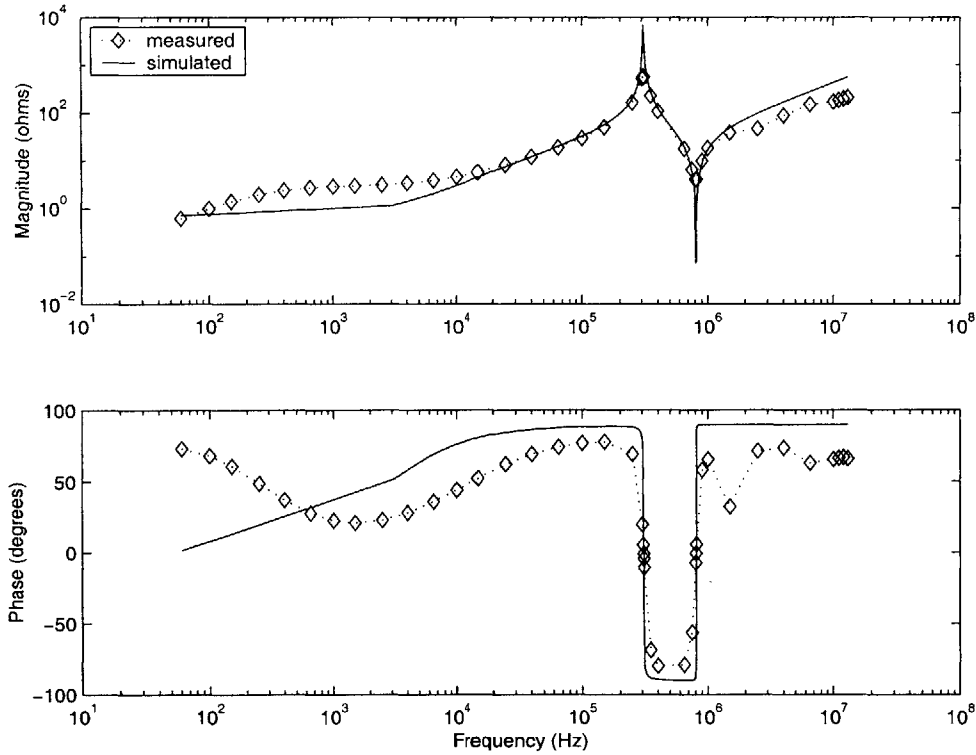


Figure 5-3: Short circuit simulation, configuration BD

Table 4.3. The simulation results for all cases are plotted together in Figure 5-4.

The resonant frequencies of the open circuit impedance do not resemble the measured values, no matter which set of capacitor values is used. The inconsistency of the six capacitor values calculated from various measurements on the transformer implied a lack of confidence in any of the capacitor values. The plot of the simulated impedance shows that the choice of capacitor values has a significant effect on the equivalent circuit behavior. Despite the close correspondence obtained for the case in which only three capacitors are significant, the equivalent circuit does not accurately predict transformer behavior for all measurement configurations.

A closer fit was obtained by arbitrarily changing capacitor values to alter the resonant frequencies. For example, it was noted that the resonant frequencies of the simulated impedance were lower than those of the measured impedance for all cases in Figure 5-4. An effort was made to increase the resonant frequency values by changing the capacitor values. Simulated impedance using the values in Table 5.1 is shown in

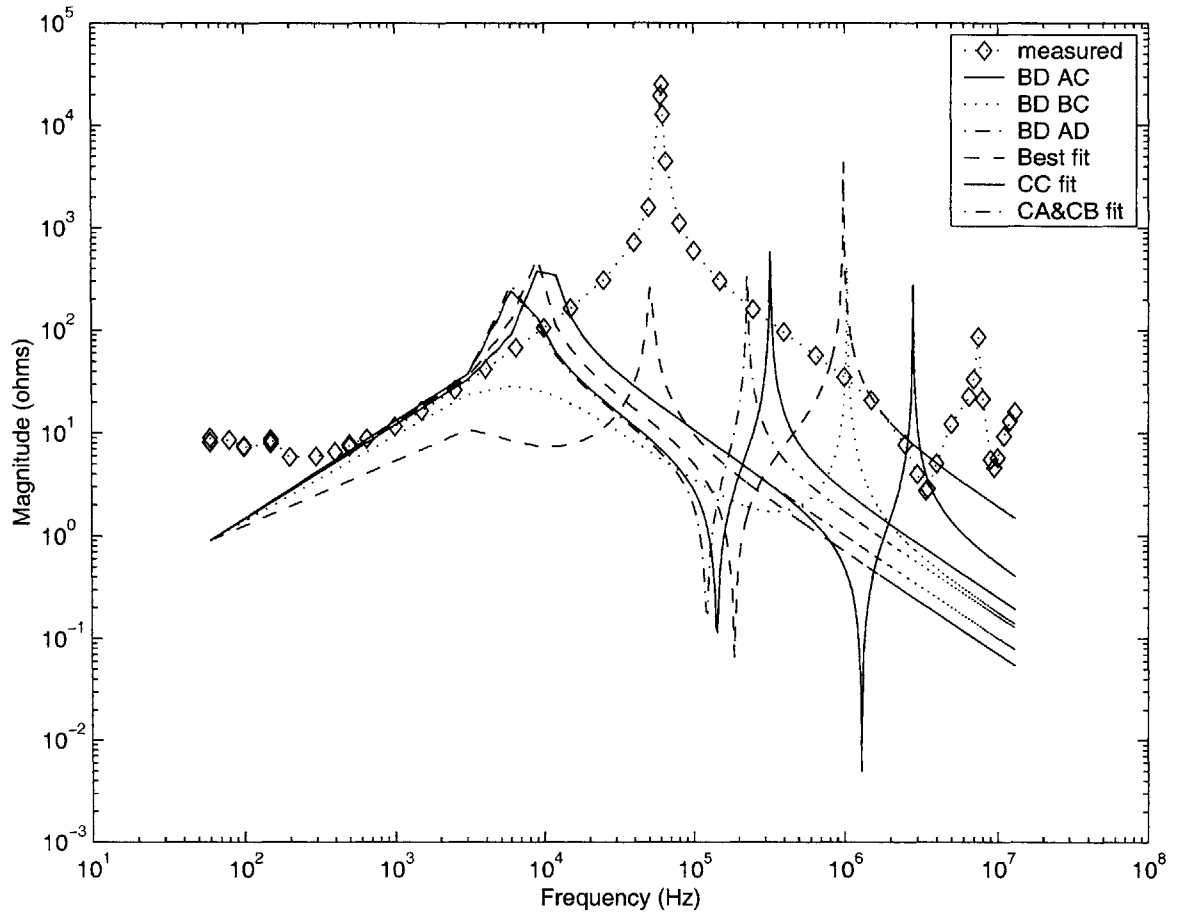


Figure 5-4: Simulated impedance from secondary, primary open, various capacitor values

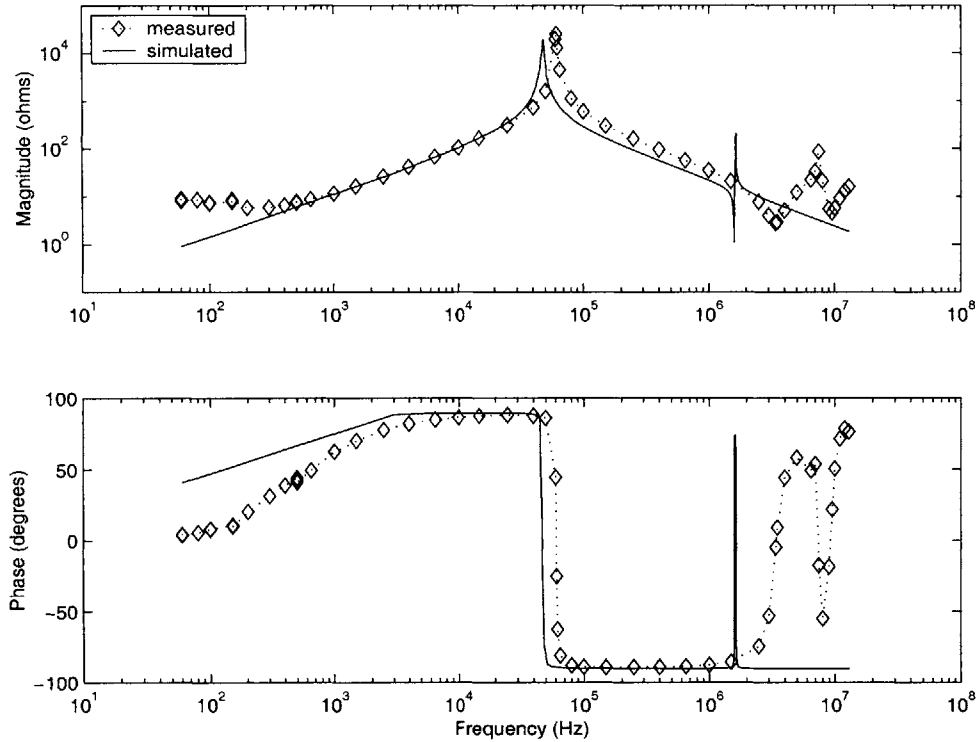


Figure 5-5: Impedance of secondary, primary open, using six capacitors from Table 5.1

Figures 5-5 and 5-6. The chosen capacitors, however, differ considerably from their original values. While the fit is improved, not all of the resonances match for this choice of capacitor values.

The altered capacitor values were simulated again in the three capacitor circuit of Figure 4-1. $C_A = C_1 + C_5$, $C_B = C_2 + C_6$, and $C_C = C_4$ define the three capacitors in terms of the six. The simulation results are shown in Figures 5-7 and 5-8. The simulation results with the altered capacitor values still match the resonant frequencies

C_1	8.5nF
C_2	10.0nF
C_3	1500nF
C_4	-.088nF
C_5	-1.7nF
C_6	-9.6nF

Table 5.1: Altered capacitor values

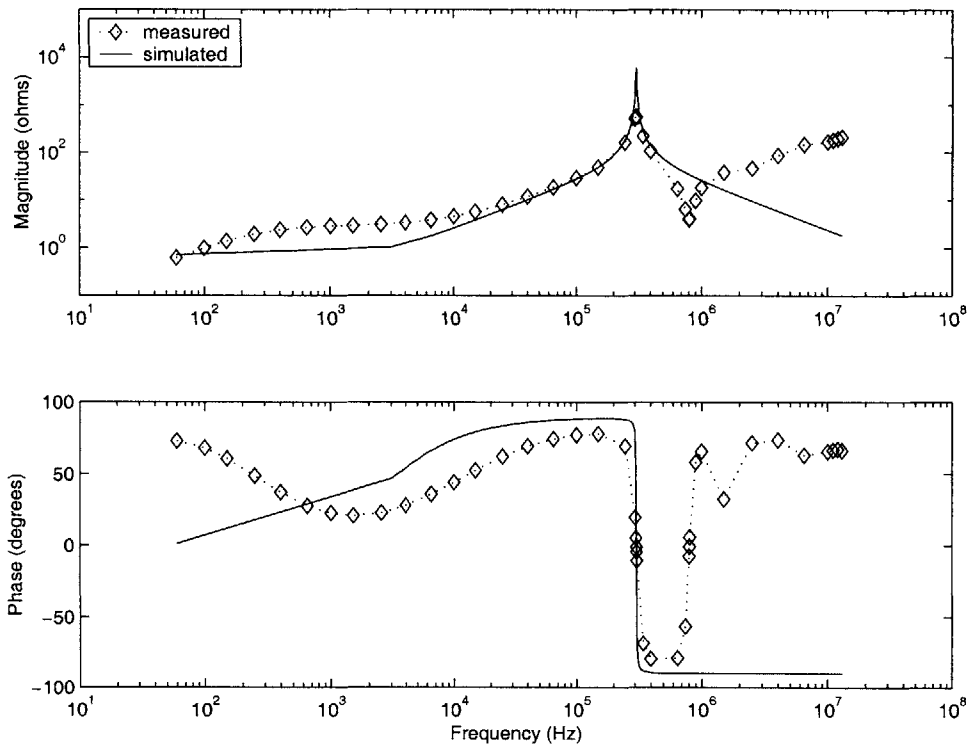


Figure 5-6: Impedance of secondary, primary shorted, using six capacitors from Table 5.1

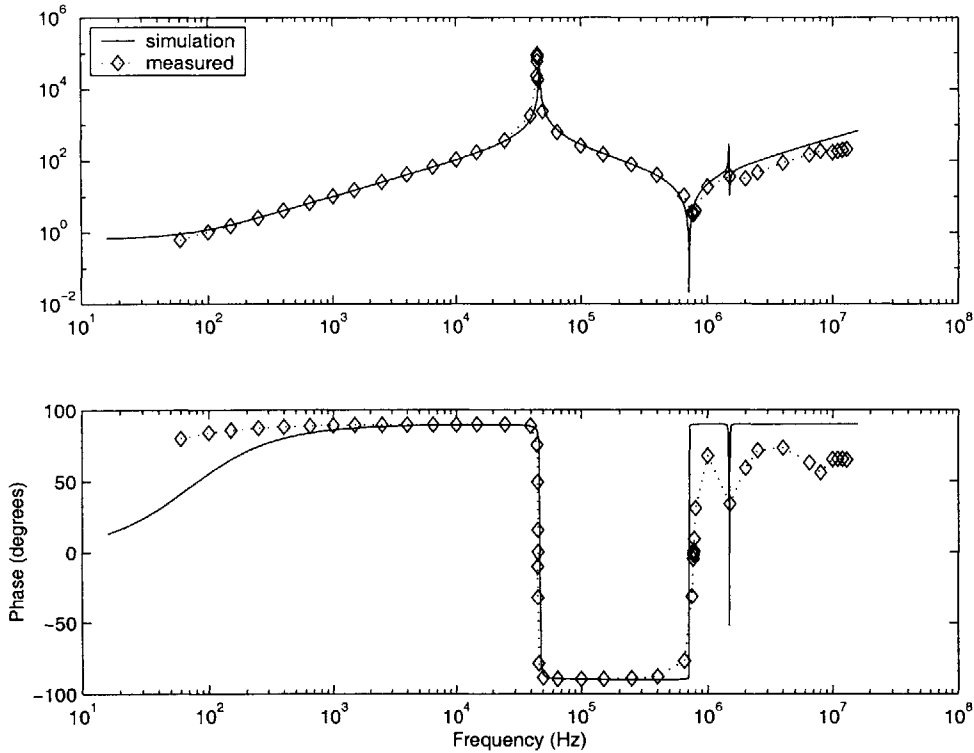


Figure 5-7: Impedance of secondary, primary open, for three-capacitor circuit

of the three capacitor circuit.

5.3 The transformer in its operational environment

The transformer equivalent circuit was combined with a circuit representation of its operating environment. The circuit of Figure 1-1 is shown connected to the transformer equivalent circuit model in Figure 5-9. The switching at the transformer primary is represented by a voltage source that presents pulses of voltage to the transformer. The load on the transformer is represented by two capacitors already charged to their steady-state operating voltage, and a resistor sized to draw the specified amount of power from the transformer.

Since only half of the transformer primary is driven at any given time, and current will flow in both halves of the secondary, the chosen configuration for representing

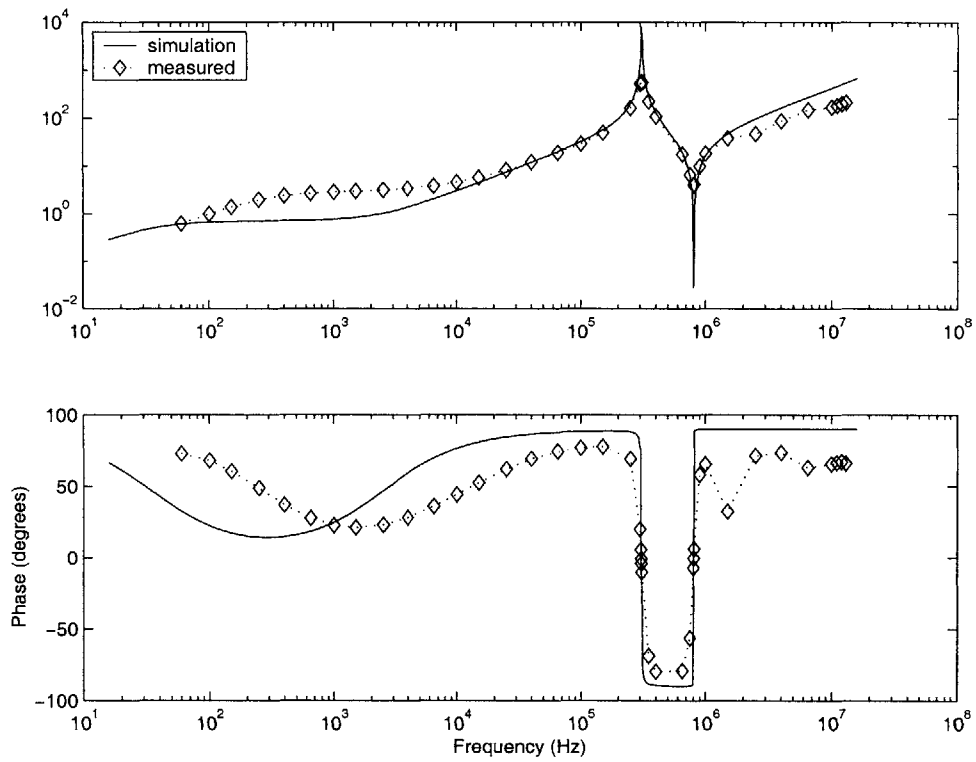


Figure 5-8: Impedance of secondary, primary shorted, for three-capacitor circuit

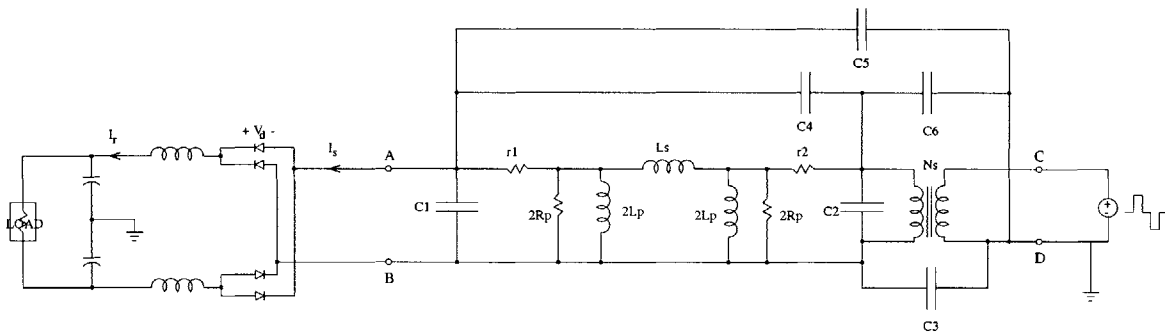


Figure 5-9: Equivalent circuit used for simulation

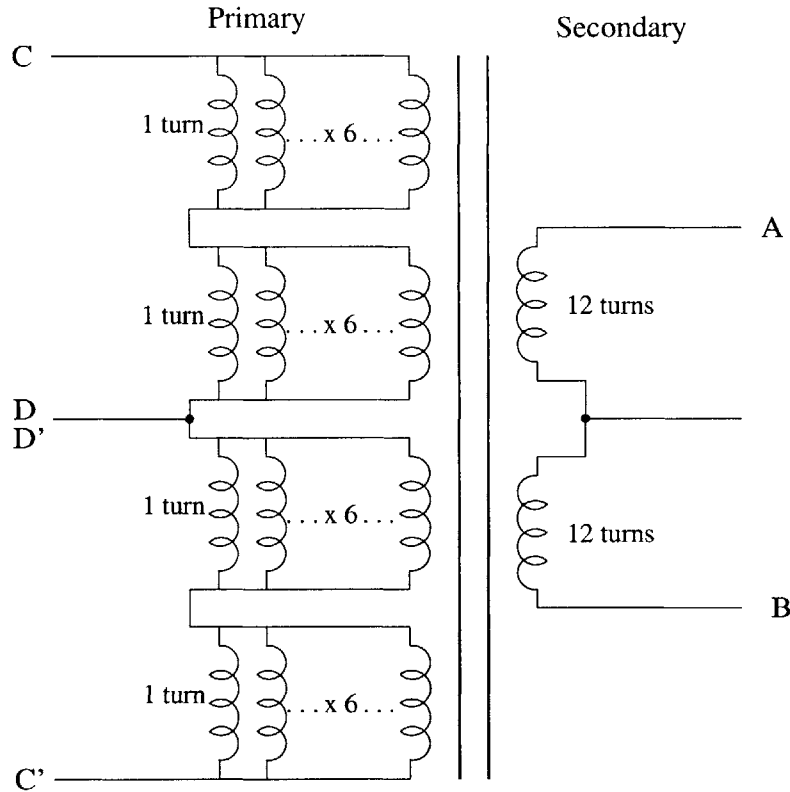


Figure 5-10: Connections to external circuit

the circuit in Simplorer was the full-secondary, half-primary configuration. Port AB in Figure 3-1 is connected across the full secondary, ignoring the center tap. Port CD represents one side of the primary, using the center tap as a connection. This is shown in Figure 5-10.

Each half of a cycle can be considered separately. The transformer primary experiences a step input for the duration of the duty cycle. The primary voltage then returns to zero. In the actual circuit, the DC bus voltage would then be applied across the other half of the transformer primary, in the opposite direction. In the simulation, this was represented by a negative voltage across the transformer primary. This simplification was never justified with a full model simulation.

Equivalent circuits from the other three possible configurations are not simulated in the transformer's operating environment. The other configurations allowed for redundant impedance calculations that tested the validity of the equivalent circuit model. They do not, however, correspond to the actual operating environment of the

transformer.

5.3.1 Transient simulation results

Sample waveforms from the testing of the transformer are shown in Figure 5-11. Channels 1 and 2 show two rectifier diode voltages at 250 volts/division. Note that the Channel 1 marker falls under the Channel 2 marker, so both diode voltages are shown together. Channel 3 is rectifier output current at 5 amps/division, and Channel 4 is the transformer secondary current at 5 amps/division. The test data is taken with 2 kilowatts of power on the output of the transformer. Figure 5-12 is another set of waveforms from a different test of the transformer, this one with 6 kilowatts on the transformer secondary. In this case, only one diode voltage is shown, using Channel 1 (whose marker is hidden behind that of Channel 4) at 250 volts/division. Channel 3 shows rectifier output current at 10 amps/division, and Channel 4 shows transformer secondary current at 10 amps/division. In both cases, the input DC voltage is 50 volts. The two sets of test data shown are a sample of the test data available for the transformer. The shape and appearance of the waveforms in Figures 5-11 and 5-12 are representative of all the available test data.

The transient waveforms from the transformer simulations were compared to actual waveforms from the transformer recorded during testing. The transformer was simulated for various combinations of capacitors, including all sets of capacitor values from Table 4.3. However, no combination of the six capacitors was able to accurately predict the transient behavior of the transformer. Some sample results follow.

The output power level of the simulation was determined by the value of the load resistor. For different simulations, the load resistor was chosen to match the output power of the test data, given the known output voltage of 215 volts. However, during the course of simulation, it was noted that the output waveforms bore little resemblance to the test data no matter what the value of the load resistor.

The waveforms of the test data were similar to those of Figures 5-11 and 5-12 for all output power levels represented by the test data, with power levels ranging from 1 to 6 kilowatts. The simulation data observed at the various output power levels exhibited

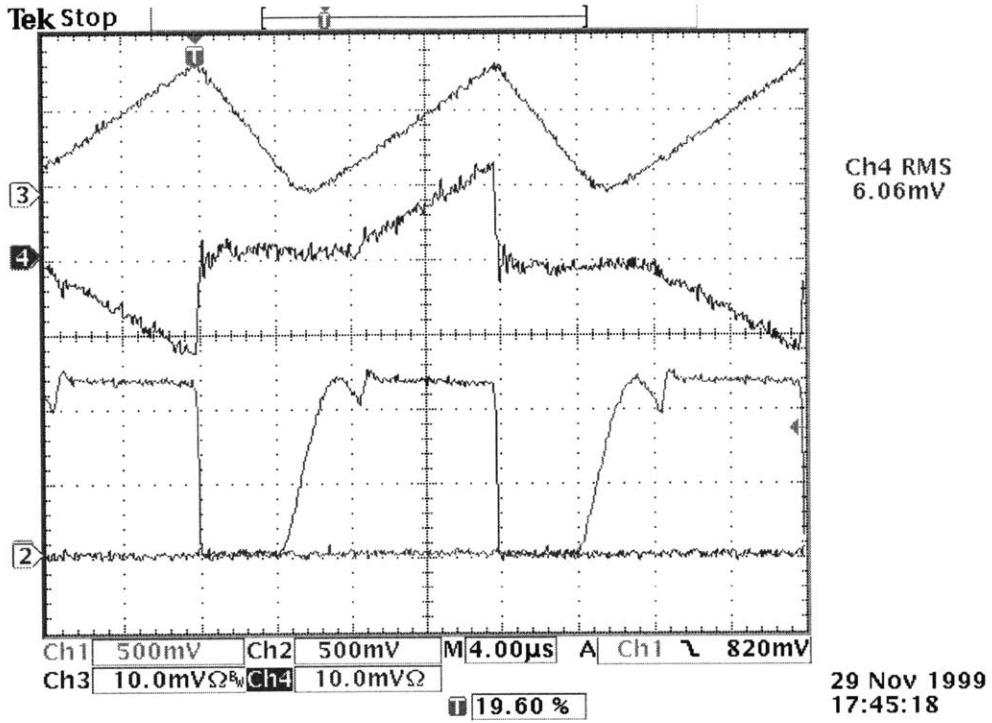


Figure 5-11: Test waveforms from the rectifier circuit, 2 kW output power

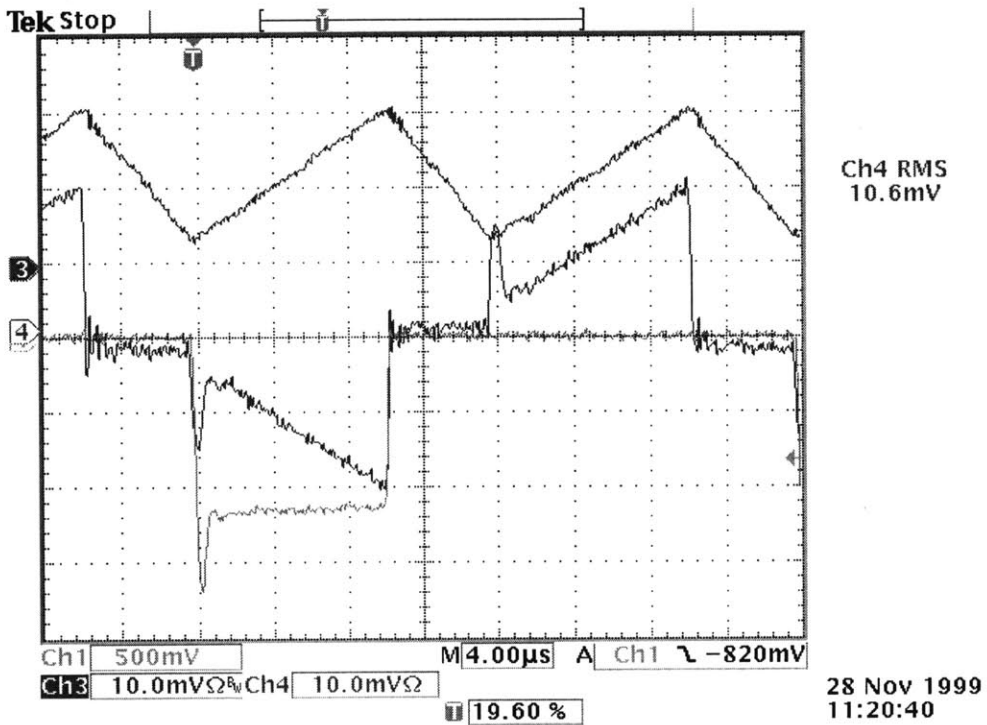


Figure 5-12: Test waveforms from the rectifier circuit, 6 kW output power

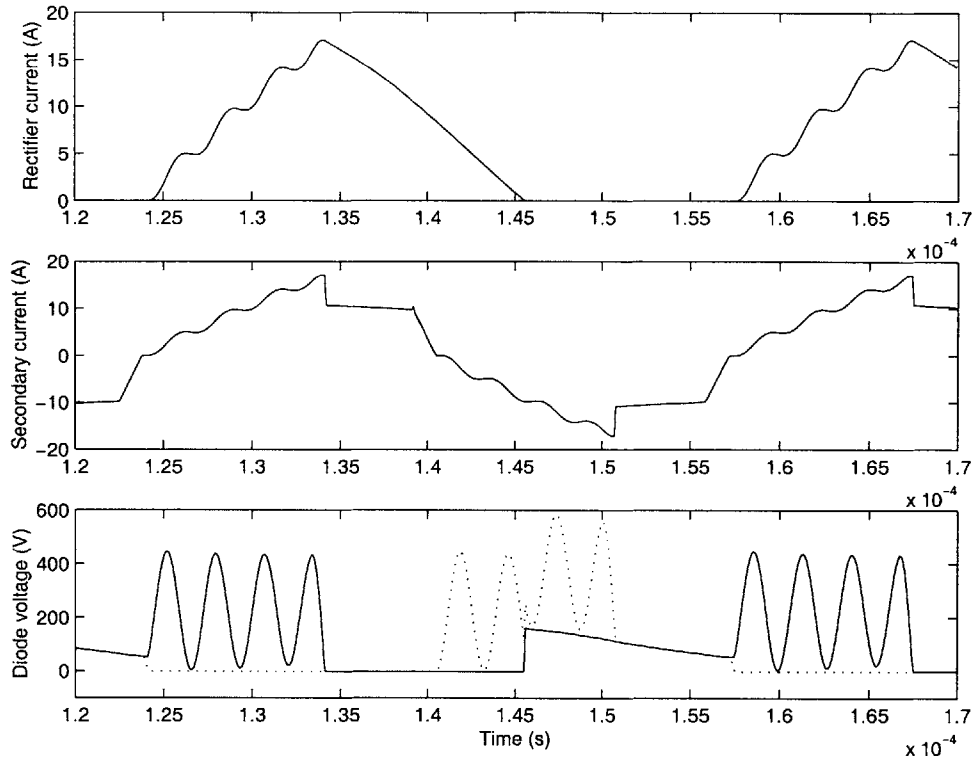


Figure 5-13: Transient simulation, 6 kW output power

the same fundamental differences between simulation waveforms and test waveforms. The simulation results that follow are a representative sample of numerous simulation attempts. They show distinct differences from all of the test data, as shown, by way of example, by the way in which the simulation results compare to both Figures 5-11 and 5-12.

The simulation shown in Figure 5-13 used the capacitor values from Table 5.1 and a resistor sized to draw 6 kilowatts of power from the transformer secondary. The simulation takes place under the conditions of Figure 5-12. Several distinct differences stand out between the simulated waveforms and the actual waveforms of Figures 5-11 and 5-12. The first is that the two rectifier diode voltages show large and relatively undamped oscillations that are not present in the measured waveforms. The second is that rectifier current I_r in the simulation exhibits a positive slope half as often as the measured rectifier current. The third is that the secondary output current does not have the exact shape of the measured waveform.

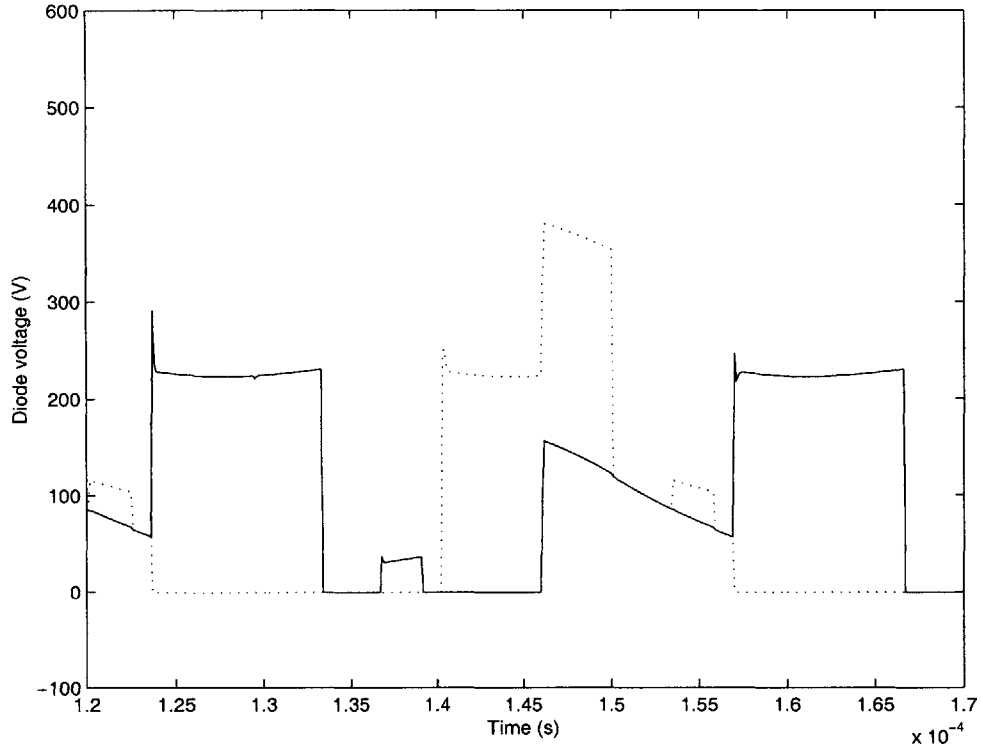


Figure 5-14: Transient simulation, $C_1 = 0.1nF$

The capacitor values of Figure 5-9 were altered and their effect on the simulated waveforms was observed. Capacitor C_1 had a significant effect on the shape of the diode voltage waveform. This is to be expected, since the location of C_1 is directly across the transformer secondary. Figures 5-14 and 5-15 show diode current when $C_1 = 0.1nF$ and $C_1 = 85nF$, respectively. Decreasing C_1 led to an increase in the frequency of the oscillations on the diode voltages, as shown by the simulation of two diode voltages in Figure 5-14. Both diode voltages, however, still contain shapes that are not found in any of the test results. Increasing the value of C_1 decreases the frequency of the oscillations. In Figure 5-15, the two diode voltages have a round, rather than square, appearance.

The original simulation using the capacitor values of Table 5.1 uses a value for C_3 that is particularly large compared to the other capacitor values. A large value for this capacitor affects the diode currents, causing less current to flow in one pair of diodes than the other. The resulting rectifier current I_r is not the same for each half

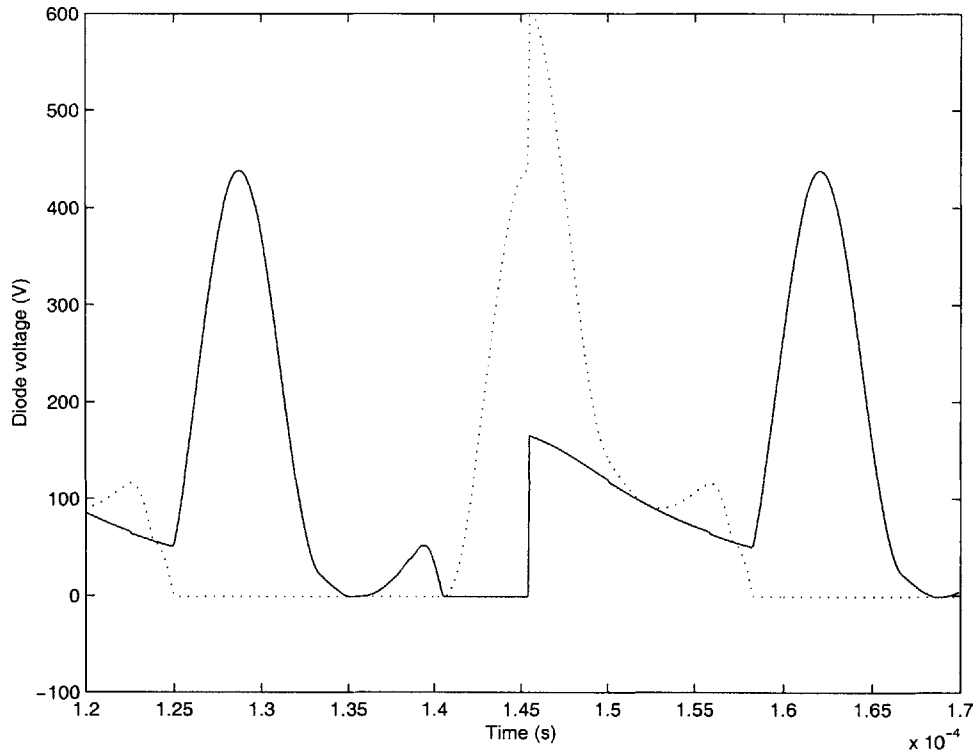


Figure 5-15: Transient simulation, $C_1 = 85nF$

of the waveform. The rectifier output current is shown in Figures 5-16 and 5-17 for $C_3 = 150nF$ and $C_3 = 15nF$. While decreasing the value of C_3 caused the rectifier current to flow for the entire output cycle, the waveform had oscillatory elements that still did not resemble the test data.

Based on the effect of individual capacitor values on the simulation data, new sets of capacitor values were chosen and simulated. The capacitor values are given in Table 5.2, and the resulting simulations are plotted in Figures 5-18 and 5-19. The motivation was that, by altering capacitor values in ways that caused the simulation waveforms to resemble the test waveforms in a qualitative sense, the equivalent circuit model could be made more correct. The simulation waveforms, however, still did not have the same shape as any of the test data to which they were compared.

Based on extensive simulation results, it is apparent that there are many possible behavior patterns that can be observed in the transformer simply by changing the six capacitor values. While small percent changes in the capacitor values do not

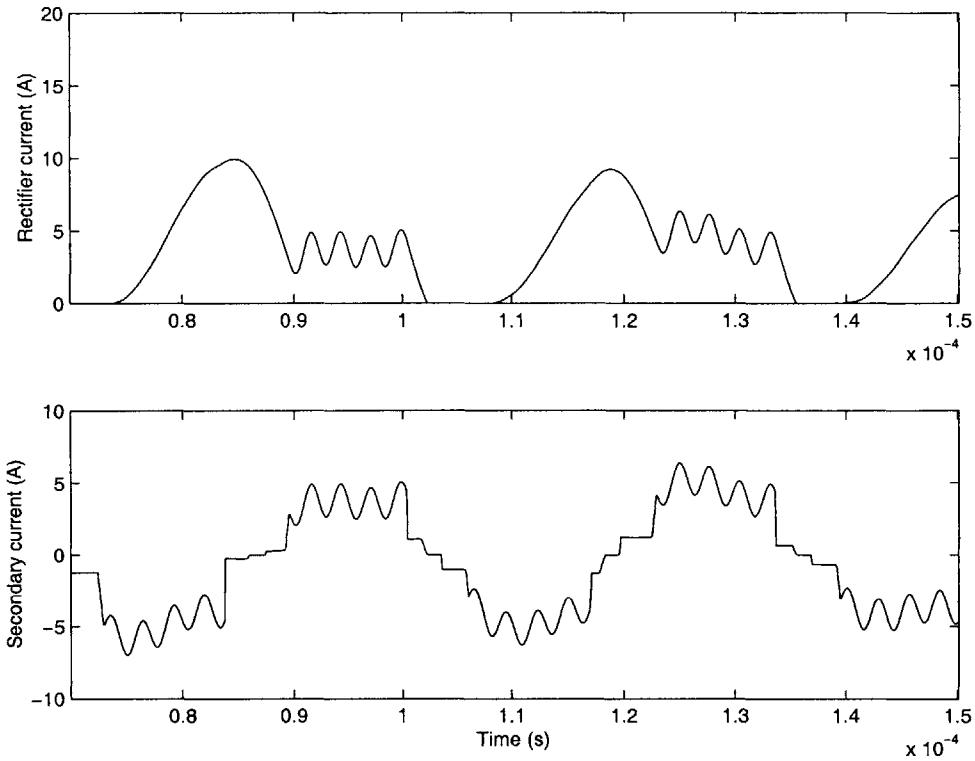


Figure 5-16: Transient simulation, $C_3 = 150nF$

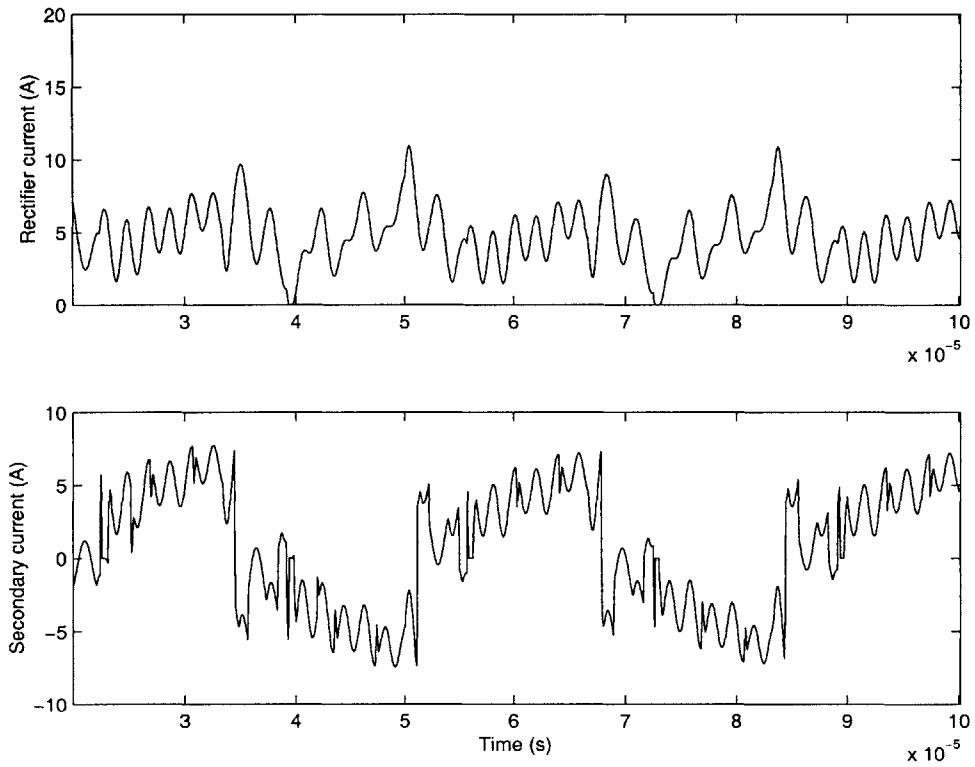


Figure 5-17: Transient simulation, $C_3 = 15nF$

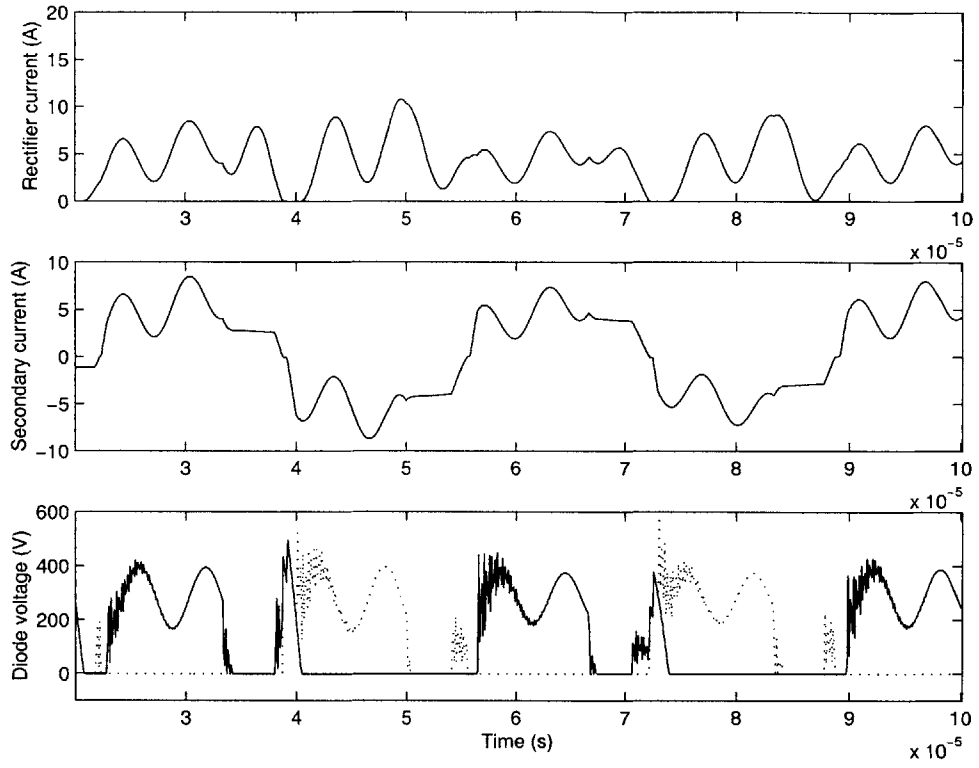


Figure 5-18: Transient simulation

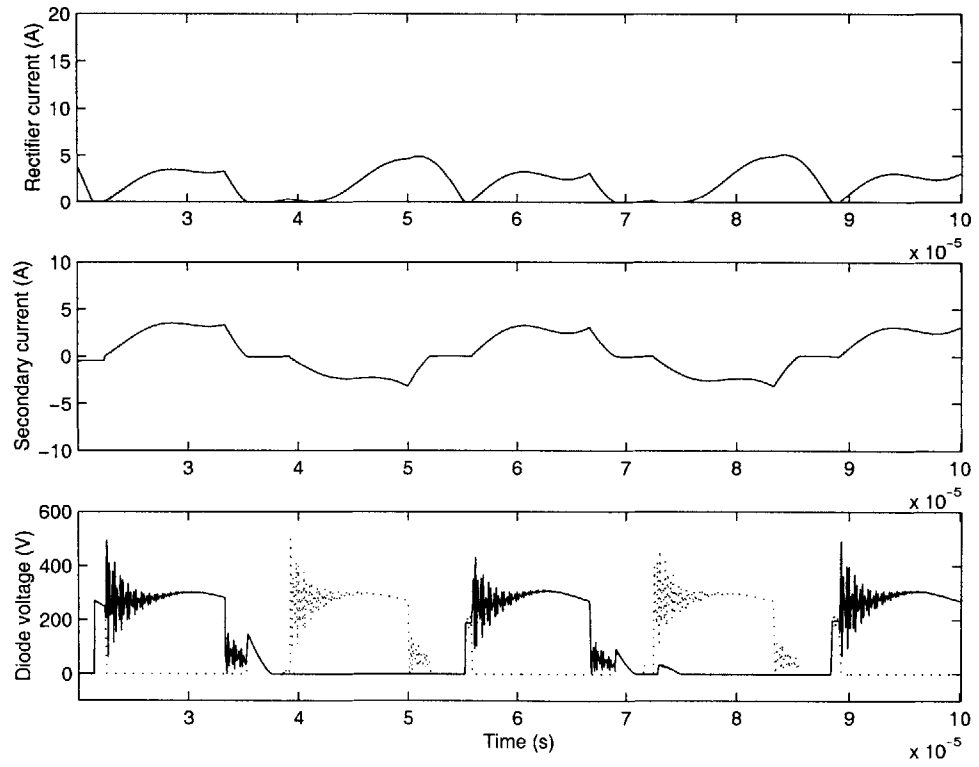


Figure 5-19: Transient simulation

C_1	0.05nF	0.05nF
C_2	10.0nF	10.0nF
C_3	25nF	75nF
C_4	0.001nF	0.0001nF
C_5	0.001nF	0.0001nF
C_6	-9.6nF	-9.6nF

Table 5.2: New capacitor values

significantly affect simulation results, a wide array of behaviors can be represented by changing the capacitor values over orders of magnitude. Both the individual capacitor values and their values relative to each other appear to have a significant effect on the output. In addition, selecting which capacitors take on negative values, and altering the relative values of positive and negative capacitors, affects the stability and the results of the model.

Chapter 6

Results and Conclusions

6.1 Interpretation of results

Values were found for the inductive, resistive, and capacitive parameters of the transformer equivalent circuit of Figure 3-1. Initial estimates for the circuit parameters were found based on plots of the open circuit and short circuit impedance of the transformer. The initial values were modified through optimization procedures in order to improve the correspondence between predicted and measured driving point impedance. A small additional inductance was found to be part of the measurement equipment and was taken into account in the calculation of the circuit parameters.

Optimization of the equivalent model allowed for a better correspondence with measured impedance. Often, noise in the measurements made it difficult to exactly determine the equivalent circuit parameters. Optimization routines allowed the parameters to be altered for closer correspondence with magnitudes or resonant frequencies. However, if too many degrees of freedom were given to the optimization procedure, the resulting parameters had a tendency to differ from their original values. As the values change too much from their initial estimation, the physical significance of the parameter to the model is called into question.

The equivalent circuit predicted impedance plots that closely resembled the measured impedance of the transformer. The calculated values, listed in Table 4.1, are close enough to their original estimates that the physical significance of each param-

eter is preserved.

The impedance plots were compared for the case in which one terminal of the primary was connected to one terminal of the secondary. The resulting equivalent circuit had three capacitor values which were determined based on the resonant frequencies of the impedance and the calculated inductor values.

The full equivalent circuit has six capacitors. There are several different ways of connecting the primary to the secondary, and each yields a unique set of three capacitors. Capacitor values from three separate configurations are sufficient to define the six capacitances of the total equivalent circuit. The six capacitances were calculated several different ways in order to have redundant measurements. However, the different calculations did not produce a consistent set of values. Due to conflicting information given by the measurements, the six capacitors could not be determined with confidence.

The equivalent circuit of the transformer was simulated in its operational environment and analyzed for its transient response. However, the capacitor values played a significant role in the behavior of the transformer, and since the capacitor values could not be determined with confidence, the equivalent circuit was unable to predict the transient behavior of the transformer.

6.2 Conclusion

The equivalent circuit described by [3] provides an excellent theoretical basis for modeling a transformer. The model is based purely on external measurements to the transformer and is independent of transformer geometry. The model is accurate over a wide range of frequencies for predicting the driving-point impedance. However, when used as part of a time simulation of the complete power circuit, the model does not produce relevant results.

The equivalent circuit model was demonstrated to be able to predict the driving point impedance characteristics of a flat-winding transformer. While the measurements were not precise enough to identify the circuit parameters exactly, simple op-

timization routines ensured that the impedance of the equivalent circuit was close to the measured values.

However, calculation of the capacitances in the model according to the method described in [3] became impossible when all of the electrostatic interactions were included. While in theory many different calculations should effectively determine the same capacitor values, in practice the values were very sensitive to the particular measurements used to calculate them. As the transient behavior of the transformer is very sensitive to the capacitor values of the equivalent circuit, the inconsistencies observed in the calculation of these capacitances and in the measurements in general make it impractical to use this model to predict the transient behavior of the device.

The difficulty in determining consistent capacitor values may be related to the low accuracy of the measurements. One very possible explanation of the inconsistencies in the measurement of the various capacitances of the model is the fact that the windings of the transformer were not mounted on a rigid supporting material. This led to the variation of the inter-turn distance during the handling of the device. The variation of this distance in turn may have led to the variation of the inter-turn capacitance.

Driving point impedance measurements were taken with the highest possible degree of precision, given the available measurement apparatus. If measurement inaccuracies are the biggest factor in the failure of the model in transient simulation, then a practical model could possibly be obtained by improving the transformer's mechanical support and using measuring equipment with well-known characteristics.

If the performance of the model in transient simulation is only dependent on the accuracy of the measurements, then attempting to run the simulation over a wide range of capacitor values may also eventually demonstrate the same behavior as the actual circuit. In this case, however, the ability of the equivalent circuit to predict transformer behavior before testing would still be in doubt.

It may also be the case that the equivalent circuit model, while demonstrating close correspondence with driving point impedance measurements, is simply not rich enough to simulate time-dependent waveforms and power transfer across the transformer. If more accurate measurement equipment is not available, or if new measure-

ments do not produce more accurate simulation results from the equivalent circuit model, a different approach to modeling the behavior of the transformer must be used.

Appendix A

Maple Code

A.1 Short-circuit impedance

```
> restart;
```

```
>
```

This is the maple script to calculate the short circuit driving point impedance of the circuit.

```
> parallel := unapply(r1*r2/(r1+r2),r1,r2);
```

$$\text{parallel} := (r1, r2) \rightarrow \frac{r1 \ r2}{r1 + r2}$$

```
> A := parallel(2*Rp,2*Lp*s);
```

$$A := 4 \frac{R_p \ L_p \ s}{2 \ R_p + 2 \ L_p \ s}$$

Calculate impedance at the input.

```
> imp := Lx*s+parallel(parallel(A,parallel(1/(CA*s),1/(CC*s))),
  r1+Ls*s+parallel(A,r2));
```

20

Simplify the impedance to an expression with a numerator and denominator.

```
> Zcc := normal(imp);
> num_impedance := numer(Zcc);
> denom_impedance := denom(Zcc);
```

Find the coefficients for each power of s for the numerator and denominator.

30

```
> coeff(num_impedance,s,6);
```

0

```
> coeff(num_impedance,s,5);
```

```
4*Lx*Ls*Rp^2*Lp^2*CC+2*Lx*Ls*Rp*Lp^2*CA*r2+2*Lx*Ls*Rp*Lp^2*CC*r2
  +4*Lx*Ls*Rp^2*Lp^2*CA
```

```
> coeff(num_impedance,s,4);
```

```
4*Lx*Rp^2*Lp^2*r2*CC+2*Lx*r1*Rp*Lp^2*CA*r2+4*Lx*r1*Rp^2*Lp^2*CC+2
  *Lx*Ls*Rp^2*Lp*CC*r2+Lx*Ls*Lp^2*r2+4*Lx*r1*Rp^2*Lp^2*CA+4*Lx
  *Rp^2*Lp^2*r2*CA+2*Lx*Ls*Lp^2*Rp+2*Lx*r1*Rp*Lp^2*CC*r2+2*Lx*Ls
  *Rp^2*Lp*CA*r2
```

```
> coeff(num_impedance,s,3);
```

```
2*Lx*r1*Lp^2*Rp+2*Lx*Ls*Rp^2*Lp+2*Lx*Ls*Rp*Lp*r2+2*Rp*Lp^2*Ls*r2
  +4*Rp^2*Lp^2*Ls+4*Lx*Rp^2*Lp^2+Lx*r1*Lp^2*r2+2*Lx*r1*Rp^2*Lp*CC
  *r2+4*Lx*Rp*Lp^2*r2+2*Lx*r1*Rp^2*Lp*CA*r2
```

```
> coeff(num_impedance,s,2);
```

```
Lx*Ls*r2*Rp^2+2*Rp*Lp^2*r1*r2+4*Rp^2*Lp^2*r2+4*Lx*Rp^2*Lp*r2+2
  *Rp^2*Lp*Ls*r2+2*Lx*r1*Rp*Lp*r2+4*Rp^2*Lp^2*r1+2*Lx*r1*Rp^2*Lp
```

```

> coeff(num_impedance,s,1);
Lx*r1*r2*Rp^2+2*Rp^2*Lp*r1*r2
50
> coeff(num_impedance,s,0);
0
> coeff(denom_impedance,s,5);
0
> coeff(denom_impedance,s,4);
2*Ls*Rp*Lp^2*CC*r2+4*Ls*Rp^2*Lp^2*CA+2*Ls*Rp*Lp^2*CA*r2+4*Ls*Rp^2
*Lp^2*CC
> coeff(denom_impedance,s,3);
4*Rp^2*Lp^2*r2*CC+4*Rp^2*Lp^2*r2*CA+2*Ls*Lp^2*Rp+Ls*Lp^2*r2+2*Ls
*Rp^2*Lp*CA*r2+2*Ls*Rp^2*Lp*CC*r2+4*r1*Rp^2*Lp^2*CA+2*r1*Rp
60
*Lp^2*CA*r2+4*r1*Rp^2*Lp^2*CC+2*r1*Rp*Lp^2*CC*r2
> coeff(denom_impedance,s,2);
4*Rp*Lp^2*r2+2*r1*Lp^2*Rp+4*Rp^2*Lp^2+2*Ls*Rp*Lp*r2+2*Ls*Rp^2*Lp
+r1*Lp^2*r2+2*r1*Rp^2*Lp*CA*r2+2*r1*Rp^2*Lp*CC*r2
> coeff(denom_impedance,s,1);
4*Rp^2*Lp*r2+Ls*r2*Rp^2+2*r1*Rp*Lp*r2+2*Rp^2*Lp*r1
> coeff(denom_impedance,s,0);
r1*r2*Rp^2
>
>
70

```

A.2 Open-circuit impedance

```

> restart;
>

```


This is the maple script to calculate the open circuit driving point impedance of the circuit.

```
> parallel := unapply(r1*r2/(r1+r2),r1,r2);
```

$$\text{parallel} := (r1, r2) \rightarrow \frac{r1 \ r2}{r1 + r2}$$

10

```
> A := parallel(2*Rp,2*Lp*s);
```

$$A := \frac{Rp \ Lp \ s}{2 \ Rp + 2 \ Lp \ s}$$

Input a test current of 1 A. Use the node method to find the voltage at the input.

```
> denom_matrix := linalg[matrix](5,5,[1/(Lx*s), -1/(Lx*s), 0, 0,
0, -1/(Lx*s), 1/r1+CA*s+CC*s+1/(Lx*s), -1/r1, 0, -CC*s, 0,
-1/r1, 1/r1+1/A+1/(Ls*s), -1/(Ls*s), 0, 0, 0, -1/(Ls*s),
1/r2+1/A+1/(Ls*s), -1/r2, 0, -CC*s, 0, -1/r2, 1/r2+CB*s+CC*s]);
```

20

```
> num_matrix := linalg[matrix](5,5,[1, -1/(Lx*s), 0, 0, 0, 0,
1/r1+CA*s+CC*s+1/(Lx*s), -1/r1, 0, -CC*s, 0, -1/r1,
1/r1+1/A+1/(Ls*s), -1/(Ls*s), 0, 0, 0, -1/(Ls*s),
1/r2+1/A+1/(Ls*s), -1/r2, 0, -CC*s, 0, -1/r2, 1/r2+CB*s+CC*s]);
```

```
> denom_impedance := linalg[det](denom_matrix);
```

30

```
> num_impedance := linalg[det](num_matrix);
```

```
> Zo := normal(num_impedance / denom_impedance);
```

```
> num_imp := numer(Zo);
> denom_imp := denom(Zo);
```

Find the coefficients for each power of s for the numerator and denominator.

```
> coeff(num_imp,s,6);
0
```

```
> coeff(num_imp,s,5);
4*CA*Lx*Rp^2*Lp^2*Ls*CB+4*CA*Lx*Rp^2*Lp^2*Ls*CC+2*CA*Lx*Rp*Lp^2
*Ls*r2*CB+2*CA*Lx*Rp*Lp^2*Ls*r2*CC+2*CA*r1*Lx*Ls*Lp^2*Rp*CB+2
*CA*r1*Lx*Ls*Lp^2*Rp*CC+CA*r1*Lx*Ls*Lp^2*r2*CB+CA*r1*Lx*Ls*Lp^2
*r2*CC+4*CC*Lx*Rp^2*Lp^2*Ls*CB+2*CC*Lx*Rp*Lp^2*Ls*r2*CB+2*CC*r1
*Lx*Ls*Lp^2*Rp*CB+CC*r1*Lx*Ls*Lp^2*r2*CB
```

40

```
> coeff(num_imp,s,4);
2*CA*Lx*Rp*Lp^2*Ls+CA*r1*Lx*Ls*Lp^2+2*CA*Lx*Rp^2*Lp*Ls*r2*CB+2*CA
*Lx*Rp^2*Lp*Ls*r2*CC+2*Lx*Ls*Lp^2*Rp*CB+4*Lx*Ls*Lp^2*Rp*CC+Lx
*Ls*Lp^2*r2*CB+Lx*Ls*Lp^2*r2*CC+4*CA*r1*Lx*Lp^2*r2*Rp*CB+4*CA
*r1*Lx*Lp^2*r2*Rp*CC+4*CA*r1*Lx*Rp^2*Lp^2*CB+4*CA*r1*Lx*Rp^2
*Lp^2*CC+4*CA*Lx*Rp^2*Lp^2*r2*CB+4*CA*Lx*Rp^2*Lp^2*r2*CC+2*CA
*r1*Lx*Ls*Rp^2*Lp*CB+2*CA*r1*Lx*Ls*Rp^2*Lp*CC+2*CA*r1*Lx*Ls*Rp
*r2*Lp*CB+2*CA*r1*Lx*Ls*Rp*r2*Lp*CC+CC*r1*Lx*Ls*Lp^2+2*CC*Lx
*Rp^2*Lp*Ls*r2*CB+4*CC*Lx*Rp^2*Lp^2*r2*CB+2*CC*r1*Lx*Ls*Rp^2*Lp
*CB+2*CC*r1*Lx*Ls*Rp*r2*Lp*CB+4*CC*r1*Lx*Lp^2*r2*Rp*CB+4*CC*r1
*Lx*Rp^2*Lp^2*CB
```

```
> coeff(num_imp,s,3);
Lx*Ls*Lp^2+4*Rp^2*Lp^2*Ls*CB+4*Rp^2*Lp^2*Ls*CC+2*Rp*Lp^2*Ls*r2*CB
+2*Rp*Lp^2*Ls*r2*CC+2*r1*Ls*Lp^2*Rp*CB+2*r1*Ls*Lp^2*Rp*CC+r1*Ls
*Lp^2*r2*CB+r1*Ls*Lp^2*r2*CC+4*Lx*Rp^2*Lp^2*CB+4*CA*Lx*Rp^2
*Lp^2+2*Lx*Ls*Rp^2*Lp*CB+4*Lx*Ls*Rp^2*Lp*CC+2*Lx*Ls*Rp*r2*Lp*CB
+2*Lx*Ls*Rp*r2*Lp*CC+2*CA*Lx*Rp^2*Lp*Ls+4*Lx*Lp^2*r2*Rp*CB+4*Lx
```

```

* $Lp^2*r2*Rp*CC+2*CA*r1*Lx*Rp*Lp*Ls+4*CA*r1*Lx*Lp^2*Rp+2*CC*r1$ 
* $Lx*Rp*Lp*Ls+CA*r1*Lx*Ls*Rp^2*r2*CB+CA*r1*Lx*Ls*Rp^2*r2*CC+4*CA$ 
* $r1*Lx*Rp^2*r2*Lp*CB+4*CA*r1*Lx*Rp^2*r2*Lp*CC+CC*r1*Lx*Ls*Rp^2$ 
* $r2*CB+4*CC*r1*Lx*Rp^2*r2*Lp*CB+4*CC*r1*Lx*Lp^2*Rp$ 
> coeff(num_imp,s,2);
2* $Rp*Lp^2*Ls+2*r1*Ls*Rp*r2*Lp*CC+2*r1*Ls*Rp^2*Lp*CB+CA*r1*Lx*Ls$ 
* $Rp^2+r1*Ls*Lp^2+2*r1*Ls*Rp^2*Lp*CC+2*Rp^2*Lp*Ls*r2*CC+4*Rp^2$ 
* $Lp^2*r2*CC+2*Lx*Rp*Lp*Ls+4*Rp^2*Lp^2*r2*CB+2*Rp^2*Lp*Ls*r2*CB$  70
+4*r1* $Rp^2*Lp^2*CC+4*r1*Lp^2*r2*Rp*CB+Lx*Ls*Rp^2*r2*CB+Lx*Ls$ 
* $Rp^2*r2*CC+4*Lx*Rp^2*r2*Lp*CC+2*r1*Ls*Rp*r2*Lp*CB+4*r1*Lp^2*r2$ 
* $Rp*CC+4*r1*Rp^2*Lp^2*CB+CC*r1*Lx*Ls*Rp^2+4*CC*r1*Lx*Rp^2*Lp+4$ 
* $Lx*Lp^2*Rp+4*CA*r1*Lx*Rp^2*Lp+4*Lx*Rp^2*r2*Lp*CB$ 
> coeff(num_imp,s,1);
2* $Rp^2*Lp*Ls+4*Rp^2*Lp^2+2*r1*Rp*Lp*Ls+Lx*Ls*Rp^2+4*r1*Rp^2*r2*Lp$ 
* $CB+4*CC*r1*Rp^2*r2*Lp+4*r1*Lp^2*Rp+r1*Ls*Rp^2*r2*CB+CC*r1*Ls$ 
* $Rp^2*r2+4*Lx*Rp^2*Lp$ 
> coeff(num_imp,s,0);
r1*Ls* $Rp^2+4*r1*Rp^2*Lp$ 
80
> coeff(denom_imp,s,5);
0
> coeff(denom_imp,s,4);
0
> coeff(denom_imp,s,3);
0
> coeff(denom_imp,s,2);
0
> coeff(denom_imp,s,1);
1/4/Lx*(4* $CA*Rp^2*Lp^2*Ls*CB+4*CA*Rp^2*Lp^2*Ls*CC+2*CA*Rp*Lp^2*Ls$  90
* $r2*CB+2*CA*Rp*Lp^2*Ls*r2*CC+2*CA*r1*Ls*Lp^2*Rp*CB+2*CA*r1*Ls$ 
* $Lp^2*Rp*CC+CA*r1*Ls*Lp^2*r2*CB+CA*r1*Ls*Lp^2*r2*CC+4*CC*Rp^2$ 

```

```

* $Lp^2 * Ls * CB + 2 * CC * Rp * Lp^2 * Ls * r2 * CB + 2 * CC * r1 * Ls * Lp^2 * Rp * CB + CC * r1$ 
* $Ls * Lp^2 * r2 * CB) / r1 / Ls / Rp^2 / Lp^2 / r2$ 
> coeff(denom_imp,s,0);
1/4/Lx*(2*Ls*Lp^2*Rp*CB+4*Ls*Lp^2*Rp*CC+Ls*Lp^2*r2*CB+Ls*Lp^2*r2
*CC+2*CA*Rp*Lp^2*Ls+CA*r1*Ls*Lp^2+CC*r1*Ls*Lp^2+2*CA*Rp^2*Lp*Ls
*r2*CB+2*CA*Rp^2*Lp*Ls*r2*CC+2*CA*r1*Ls*Rp*r2*Lp*CB+4*CA*Rp^2
*Lp^2*r2*CB+4*CA*Rp^2*Lp^2*r2*CC+2*CA*r1*Ls*Rp^2*Lp*CB+2*CA*r1
*Ls*Rp^2*Lp*CC+2*CA*r1*Ls*Rp*r2*Lp*CC+4*CA*r1*Lp^2*r2*Rp*CB+4
*CA*r1*Lp^2*r2*Rp*CC+4*CA*r1*Rp^2*Lp^2*CB+4*CA*r1*Rp^2*Lp^2*CC
+2*CC*Rp^2*Lp*Ls*r2*CB+4*CC*Rp^2*Lp^2*r2*CB+2*CC*r1*Ls*Rp^2*Lp
*CB+2*CC*r1*Ls*Rp*r2*Lp*CB+4*CC*r1*Lp^2*r2*Rp*CB+4*CC*r1*Rp^2
*Lp^2*CB)/r1/Ls/Rp^2/Lp^2/r2
>
>

```

A.3 Open-circuit resonant frequencies

```
> restart;
```

```
>
```

This is the maple script to calculate the open circuit resonant frequencies of the circuit.

```
> parallel := unapply(r1*r2/(r1+r2),r1,r2);
```

$$\text{parallel} := (r1, r2) \rightarrow \frac{r1 \ r2}{r1 + r2}$$

10

```
> s := w*I;
```

```
s := I*w
```

>

Expression for the impedance in terms of s

```
> imp := Lx*s + parallel(parallel(1/(C1*s), 2*Lp*s), parallel(Ls
  *s, 1/(C3*s)) + parallel(2*Lp*s,1/(C2*s)));
> Zoc := normal(imp);
> num_impedance := numer(Zoc);
> denom_impedance := denom(Zoc);
```

Find the coefficients of each power of w for both the numerator
and denominator

```
> a5 := coeff(num_impedance,w,5)/I;
a5 := 4*Lx*Ls*C3*Lp^2*C2+4*Lx*Ls*Lp^2*C1*C2+4*Lx*Lp^2*C1*Ls*C3
> a4 := coeff(num_impedance,w,4)/I;
a4 := 0
> a3 := coeff(num_impedance,w,3)/I;
a3 := -4*Lx*Lp^2*C2-2*Lx*Ls*Lp*C2-4*Lx*Lp*Ls*C3-4*Ls*Lp^2*C2
  -4*Lp^2*Ls*C3-4*Lx*Lp^2*C1-2*Lx*Ls*Lp*C1
> a2 := coeff(num_impedance,w,2)/I;
a2 := 0
> a1 := coeff(num_impedance,w,1)/I;
a1 := 4*Lp^2+Lx*Ls+4*Lx*Lp+2*Lp*Ls
> a0 := coeff(num_impedance,w,0);
a0 := 0
> b4 := coeff(denom_impedance,w,4);
b4 := 4*Ls*C3*Lp^2*C2+4*Ls*Lp^2*C1*C2+4*Lp^2*C1*Ls*C3
> b3 := coeff(denom_impedance,w,3);
b3 := 0
```

```

> b2 := coeff(denom_impedance,w,2);
b2 := -4*Lp*Ls*C3-4*Lp^2*C2-2*Ls*Lp*C2-2*Ls*Lp*C1-4*Lp^2*C1
> b1 := coeff(denom_impedance,w,1);
b1 := 0
> b0 := coeff(denom_impedance,w,0);
b0 := Ls+4*Lp

```

Calculate the roots of the numerator and denominator (values of 50
w for which the numerator or denominator is zero).

```

> wnsquaredplus := normal((-a3 + sqrt(a3^2-4*a5*a1)) / (2*a5));
> wnsquaredminus := normal((-a3 - sqrt(a3^2-4*a5*a1)) / (2*a5));
> wn1 = normal(sqrt(wnsquaredplus));
wn1 = 1/2*((2*Lx*Lp^2*C2+Lx*Ls*Lp*C2+2*Lx*Lp*Ls*C3+2*Ls*Lp^2*C2+2
*Lp^2*Ls*C3+2*Lx*Lp^2*C1+Lx*Ls*Lp*C1+(4*Lx^2*Lp^4*C2^2+4*Lx^2
*Lp^4*C1^2+4*Lp^4*Ls^2*C3^2+4*Ls^2*Lp^4*C2^2+4*Lx*Ls^2*Lp^3*C2
*C3-8*Lp^4*Ls*C3*Lx*C1-4*Lp^3*Ls^2*C3*Lx*C1+4*Lx^2*Lp^3*C1^2*Ls
-8*Lx^2*Lp^3*Ls*C3*C1-8*Ls*Lp^4*C2*Lx*C1-4*Ls^2*Lp^3*C2*Lx*C1-8
60 *Lx*Lp^4*C2*Ls*C3-8*Lx^2*Lp^3*C2*Ls*C1-2*Lx^2*Ls^2*Lp^2*C2*C1-8
*Lx^2*Lp^3*C2*Ls*C3+8*Ls^2*Lp^4*C2*C3+8*Lx*Lp^3*Ls^2*C3^2+4
*Lx^2*Lp^2*Ls^2*C3^2+4*Lx*Ls^2*Lp^3*C2^2+Lx^2*Ls^2*Lp^2*C2^2+8
*Lx^2*Lp^4*C2*C1+8*Lx*Lp^4*C2^2*Ls+4*Lx^2*Lp^3*C2^2*Ls+Lx^2
*Ls^2*Lp^2*C1^2)^(1/2))/Lx/Ls/Lp^2/(C3*C2+C2*C1+C1*C3))^(1/2)
> wn2 = normal(sqrt(wnsquaredminus));
wn2 = 1/2*((2*Lx*Lp^2*C2+Lx*Ls*Lp*C2+2*Lx*Lp*Ls*C3+2*Ls*Lp^2*C2+2
*Lp^2*Ls*C3+2*Lx*Lp^2*C1+Lx*Ls*Lp*C1-(4*Lx^2*Lp^4*C2^2+4*Lx^2
*Lp^4*C1^2+4*Lp^4*Ls^2*C3^2+4*Ls^2*Lp^4*C2^2+4*Lx*Ls^2*Lp^3*C2
*C3-8*Lp^4*Ls*C3*Lx*C1-4*Lp^3*Ls^2*C3*Lx*C1+4*Lx^2*Lp^3*C1^2*Ls
70 -8*Lx^2*Lp^3*Ls*C3*C1-8*Ls*Lp^4*C2*Lx*C1-4*Ls^2*Lp^3*C2*Lx*C1-8
*Lx*Lp^4*C2*Ls*C3-8*Lx^2*Lp^3*C2*Ls*C1-2*Lx^2*Ls^2*Lp^2*C2*C1-8

```

```

*Lx^2*Lp^3*C2*Ls*C3+8*Ls^2*Lp^4*C2*C3+8*Lx*Lp^3*Ls^2*C3^2+4
*Lx^2*Lp^2*Ls^2*C3^2+4*Lx*Ls^2*Lp^3*C2^2+Lx^2*Ls^2*Lp^2*C2^2+8
*Lx^2*Lp^4*C2*C1+8*Lx*Lp^4*C2^2*Ls+4*Lx^2*Lp^3*C2^2*Ls+Lx^2
*Ls^2*Lp^2*C1^2)^(1/2))/Lx/Ls/Lp^2/(C3*C2+C2*C1+C1*C3))^(1/2)
> wdsquaredplus := normal((-b2 + sqrt(b2^2-4*b4*b0)) / (2*b4));
wdsquaredplus := 1/4*(2*Lp*Ls*C3+2*Lp^2*C2+Ls*Lp*C2+Ls*Lp*C1+2
*Lp^2*C1+(4*Lp^4*C2^2+4*Lp^4*C1^2+4*Lp^3*C1^2*Ls-8*Lp^3*Ls*C3
*C1-8*Lp^3*C2*Ls*C1-2*Ls^2*Lp^2*C2*C1-8*Lp^3*C2*Ls*C3+4*Lp^2
*Ls^2*C3^2+Ls^2*Lp^2*C2^2+8*Lp^4*C2*C1+4*Lp^3*C2^2*Ls+Ls^2*Lp^2
*C1^2)^(1/2))/Lp^2/Ls/(C3*C2+C2*C1+C1*C3)
> wdsquaredminus := normal((-b2 - sqrt(b2^2-4*b4*b0)) / (2*b4));
wdsquaredminus := 1/4*(2*Lp*Ls*C3+2*Lp^2*C2+Ls*Lp*C2+Ls*Lp*C1+2
*Lp^2*C1-(4*Lp^4*C2^2+4*Lp^4*C1^2+4*Lp^3*C1^2*Ls-8*Lp^3*Ls*C3
*C1-8*Lp^3*C2*Ls*C1-2*Ls^2*Lp^2*C2*C1-8*Lp^3*C2*Ls*C3+4*Lp^2
*Ls^2*C3^2+Ls^2*Lp^2*C2^2+8*Lp^4*C2*C1+4*Lp^3*C2^2*Ls+Ls^2*Lp^2
*C1^2)^(1/2))/Lp^2/Ls/(C3*C2+C2*C1+C1*C3)
> wd1 = normal(sqrt(wdsquaredplus));
wd1 = 1/2*((2*Lp*Ls*C3+2*Lp^2*C2+Ls*Lp*C2+Ls*Lp*C1+2*Lp^2*C1+(4
*Lp^4*C2^2+4*Lp^4*C1^2+4*Lp^3*C1^2*Ls-8*Lp^3*Ls*C3*C1-8*Lp^3*C2
*Ls*C1-2*Ls^2*Lp^2*C2*C1-8*Lp^3*C2*Ls*C3+4*Lp^2*Ls^2*C3^2+Ls^2
*Lp^2*C2^2+8*Lp^4*C2*C1+4*Lp^3*C2^2*Ls+Ls^2*Lp^2*C1^2)^(1/2))
/Lp^2/Ls/(C3*C2+C2*C1+C1*C3))^(1/2)
> wd2 = normal(sqrt(wdsquaredminus));
wd2 = 1/2*((2*Lp*Ls*C3+2*Lp^2*C2+Ls*Lp*C2+Ls*Lp*C1+2*Lp^2*C1-(4
*Lp^4*C2^2+4*Lp^4*C1^2+4*Lp^3*C1^2*Ls-8*Lp^3*Ls*C3*C1-8*Lp^3*C2
*Ls*C1-2*Ls^2*Lp^2*C2*C1-8*Lp^3*C2*Ls*C3+4*Lp^2*Ls^2*C3^2+Ls^2
*Lp^2*C2^2+8*Lp^4*C2*C1+4*Lp^3*C2^2*Ls+Ls^2*Lp^2*C1^2)^(1/2))
/Lp^2/Ls/(C3*C2+C2*C1+C1*C3))^(1/2)

```

100

Appendix B

Matlab Scripts

B.1 Minimization script for inductances, capacitances, and resistances

B.1.1 lxiter.m

```
% lxiter.m
```

```
% iteratively determine Lx
```

```
global datapoints datafreqs datamag dataphaze datafreqs2 datamag2  
dataphaze2
```

```
global Lx Lp Ls wpsshort wsshort wpsopen wsopen wpsopen2 wsopen2  
C1plusC3
```

```
global C1 C2 C3
```

```
global Rp r1 r2
```

10

```
opts = optimset('MaxFunEvals',1e4,'MaxIter',1e4);
```

```
% Model selection variables
```



```

S_state = 'sfull'; % sfull, shalf
P_state = 'phalf'; % pfull, phalf
ferrite_state = 'ferriteon'; % ferriteon, ferriteoff
measurement_state = 'BD'; % float, BD, BC, AD, AC

% Data points 20
% Contained in data files labeled by model type

filename = strcat('final',S_state,'popen',ferrite_state,
    measurement_state);
load(strcat(filename, '.dat'));
evalin('caller',strcat('datapoints = ',filename,','));
filename2 = strcat('final',S_state,P_state,'short',ferrite_state,
    measurement_state);
load(strcat(filename2, '.dat'));
evalin('caller',strcat('datapoints2 = ',filename2,',')); 30

datafreqs = datapoints(:,1);
datamag = datapoints(:,2);
dataphaze = datapoints(:,3);
datafreqs2 = datapoints2(:,1);
datamag2 = datapoints2(:,2);
dataphaze2 = datapoints2(:,3);

% Initial resistive parameters
Rp = 91.8e3; 40
r1 = 425.5e-3;
r2 = 28.1e-3;

LoplusLx = 1.59e-3;

```

```

LcplusLx = 4.68e-5;
wpsshort = 307e3*2*pi;
wssshort = 805e3*2*pi;
Lx = 3.2e-6; %first guess
Lxold = 0;
while abs(Lx-Lxold)/Lx > 1e-4
    Lxold = Lx;
    Lo = LoplusLx - Lx;
    Lc = LcplusLx - Lx;
    Lp = (Lo + sqrt(Lo^2-Lo*Lc))/2;
    Ls = 2*Lp*Lc/(2*Lp-Lc);
    C1plusC3 = 1/(wpsshort^2*Lc);
    Lx = Lc / (Lc*C1plusC3*wssshort^2 - 1);
end

```

50

```

wpopen = 45.43e3*2*pi;
wsopen = 773e3*2*pi;
wpopen2 = 1.2e6*2*pi;
wsopen2 = 1.8e6*2*pi;
C1plusC2 = 1/(Lo*wpopen^2);
C2plusC3 = 1/(Lc*wsopen^2);

```

60

```

C1 = (C1plusC2 + C1plusC3 - C2plusC3)/2;
C2 = (C1plusC2 + C2plusC3 - C1plusC3)/2;
C3 = (C1plusC3 + C2plusC3 - C1plusC2)/2;

```

70

% Want wn2 = wsopen2, wn1 = wsopen, wd2 = wpopen2, wd1 = wpopen.

```

capvector = fminsearch('reserr',[C1 C2],opts);

```

```

C1 = capvector(1);
C2 = capvector(2);
C3 = C1plusC3 - C1;

fprintf('\nReactive Circuit Parameters\n');
fprintf('Lp = %7.4e; \n',Lp);
fprintf('Ls = %7.4e; \n',Ls);
fprintf('Lx = %7.4e; \n',Lx);
fprintf('C1+C3 = %7.4e; \n',C1plusC3);
fprintf('C1 = %7.4e; \n',C1);
fprintf('C2 = %7.4e; \n',C2);
fprintf('C3 = %7.4e; \n',C3);

```

80

% Now need to find resistor values

90

```

rvector = fminsearch('magnerr',[Rp r1 r2],opts);

```

```

Rp = rvector(1);
r1 = rvector(2);
r2 = rvector(3);

```

```

fprintf('\nCircuit Parameters\n')
fprintf('Lp = %7.4e; \n',Lp);
fprintf('Ls = %7.4e; \n',Ls);
fprintf('Lx = %7.4e; \n',Lx);
fprintf('C1 = %7.4e; \n',C1);
fprintf('C2 = %7.4e; \n',C2);
fprintf('C3 = %7.4e; \n',C3);
fprintf('Rp = %7.4e; \n',Rp);

```

100

```
fprintf('r1 = %7.4e; \n',r1);
fprintf('r2 = %7.4e; \n',r2);
```

B.1.2 reserr.m

```
function err = reserr(C1C2)
% function err = reserr(C1C2)
```

```
global Lx Lp Ls wpsshort wsshort wpsopen wsopen wpsopen2 wsopen2
C1plusC3
```

```
C1 = C1C2(1);
C2 = C1C2(2);
C3 = C1plusC3 - C1;
```

10

```
wn2 = 1/2*((2*Lx*Lp^2*C2+Lx*Ls*Lp*C2+2*Lx*Lp*Ls*C3+2*Ls*Lp^2*C2+2
*Lp^2*Ls*C3+2*Lx*Lp^2*C1+Lx*Ls*Lp*C1+(4*Lx^2*Lp^4*C2^2+4*Lx^2
*Lp^4*C1^2+4*Lp^4*Ls^2*C3^2+4*Ls^2*Lp^4*C2^2+4*Lx*Ls^2*Lp^3*C2
*C3-8*Lp^4*Ls*C3*Lx*C1-4*Lp^3*Ls^2*C3*Lx*C1+4*Lx^2*Lp^3*C1^2*Ls
-8*Lx^2*Lp^3*Ls*C3*C1-8*Ls*Lp^4*C2*Lx*C1-4*Ls^2*Lp^3*C2*Lx*C1-8
*Lx*Lp^4*C2*Ls*C3-8*Lx^2*Lp^3*C2*Ls*C1-2*Lx^2*Ls^2*Lp^2*C2*C1-8
*Lx^2*Lp^3*C2*Ls*C3+8*Ls^2*Lp^4*C2*C3+8*Lx*Lp^3*Ls^2*C3^2+4
*Lx^2*Lp^2*Ls^2*C3^2+4*Lx*Ls^2*Lp^3*C2^2+Lx^2*Ls^2*Lp^2*C2^2+8
*Lx^2*Lp^4*C2*C1+8*Lx*Lp^4*C2^2*Ls+4*Lx^2*Lp^3*C2^2*Ls+Lx^2
*Ls^2*Lp^2*C1^2)^(1/2))/Lx/Ls/Lp^2/((C3*C2+C2*C1+C1*C3))^(1/2); 20
```

```
wn1 = 1/2*((2*Lx*Lp^2*C2+Lx*Ls*Lp*C2+2*Lx*Lp*Ls*C3+2*Ls*Lp^2*C2+2
*Lp^2*Ls*C3+2*Lx*Lp^2*C1+Lx*Ls*Lp*C1-(4*Lx^2*Lp^4*C2^2+4*Lx^2
```

$$\begin{aligned}
& *Lp^4*C1^2+4*Lp^4*Ls^2*C3^2+4*Ls^2*Lp^4*C2^2+4*Lx*Ls^2*Lp^3*C2 \\
& *C3-8*Lp^4*Ls*C3*Lx*C1-4*Lp^3*Ls^2*C3*Lx*C1+4*Lx^2*Lp^3*C1^2*Ls \\
& -8*Lx^2*Lp^3*Ls*C3*C1-8*Ls*Lp^4*C2*Lx*C1-4*Ls^2*Lp^3*C2*Lx*C1-8 \\
& *Lx*Lp^4*C2*Ls*C3-8*Lx^2*Lp^3*C2*Ls*C1-2*Lx^2*Ls^2*Lp^2*C2*C1-8 \\
& *Lx^2*Lp^3*C2*Ls*C3+8*Ls^2*Lp^4*C2*C3+8*Lx*Lp^3*Ls^2*C3^2+4 \\
& *Lx^2*Lp^2*Ls^2*C3^2+4*Lx*Ls^2*Lp^3*C2^2+Lx^2*Ls^2*Lp^2*C2^2+8 \\
& *Lx^2*Lp^4*C2*C1+8*Lx*Lp^4*C2^2*Ls+4*Lx^2*Lp^3*C2^2*Ls+Lx^2 \quad 30 \\
& *Ls^2*Lp^2*C1^2)^{(1/2)}/Lx/Ls/Lp^2/(C3*C2+C2*C1+C1*C3))^{(1/2)};
\end{aligned}$$

$$\begin{aligned}
\text{wd2} = & 1/2*((2*Lp*Ls*C3+2*Lp^2*C2+Ls*Lp*C2+Ls*Lp*C1+2*Lp^2*C1+(4 \\
& *Lp^4*C2^2+4*Lp^4*C1^2+4*Lp^3*C1^2*Ls-8*Lp^3*Ls*C3*C1-8*Lp^3*C2 \\
& *Ls*C1-2*Ls^2*Lp^2*C2*C1-8*Lp^3*C2*Ls*C3+4*Lp^2*Ls^2*C3^2+Ls^2 \\
& *Lp^2*C2^2+8*Lp^4*C2*C1+4*Lp^3*C2^2*Ls+Ls^2*Lp^2*C1^2)^{(1/2)}) \\
& /Lp^2/Ls/(C3*C2+C2*C1+C1*C3))^{(1/2)};
\end{aligned}$$

$$\begin{aligned}
\text{wd1} = & 1/2*((2*Lp*Ls*C3+2*Lp^2*C2+Ls*Lp*C2+Ls*Lp*C1+2*Lp^2*C1-(4 \\
& *Lp^4*C2^2+4*Lp^4*C1^2+4*Lp^3*C1^2*Ls-8*Lp^3*Ls*C3*C1-8*Lp^3*C2 \quad 40 \\
& *Ls*C1-2*Ls^2*Lp^2*C2*C1-8*Lp^3*C2*Ls*C3+4*Lp^2*Ls^2*C3^2+Ls^2 \\
& *Lp^2*C2^2+8*Lp^4*C2*C1+4*Lp^3*C2^2*Ls+Ls^2*Lp^2*C1^2)^{(1/2)}) \\
& /Lp^2/Ls/(C3*C2+C2*C1+C1*C3))^{(1/2)};
\end{aligned}$$

$$\begin{aligned}
\text{err} = & \text{norm}([\log(\text{wpopen}/\text{wd1}) \log(\text{wsopen}/\text{wn1}) \log(\text{wpopen2}/\text{wd2}) \\
& \log(\text{wsopen2}/\text{wn2})]);
\end{aligned}$$

B.1.3 reserrsiml.m

function err = reserrsiml(C1C2)

% function err = reserrsimp(C1C2)

global Lx Lp Ls wpsshort wsshort wpopen wsopen C1plusC3

C1 = C1C2(1);

C2 = C1C2(2);

C3 = C1plusC3 - C1;

wn1 = 1/2*((2*Lx*Lp^2*C2+Lx*Ls*Lp*C2+2*Lx*Lp*Ls*C3+2*Ls*Lp^2*C2+2

$$\begin{aligned} & *Lp^2*Ls*C3+2*Lx*Lp^2*C1+Lx*Ls*Lp*C1-(4*Lx^2*Lp^4*C2^2+4*Lx^2 \\ & *Lp^4*C1^2+4*Lp^4*Ls^2*C3^2+4*Ls^2*Lp^4*C2^2+4*Lx*Ls^2*Lp^3*C2 \\ & *C3-8*Lp^4*Ls*C3*Lx*C1-4*Lp^3*Ls^2*C3*Lx*C1+4*Lx^2*Lp^3*C1^2 \\ & *Ls-8*Lx^2*Lp^3*Ls*C3*C1-8*Ls*Lp^4*C2*Lx*C1-4*Ls^2*Lp^3*C2*Lx \\ & *C1-8*Lx*Lp^4*C2*Ls*C3-8*Lx^2*Lp^3*C2*Ls*C1-2*Lx^2*Ls^2*Lp^2*C2 \\ & *C1-8*Lx^2*Lp^3*C2*Ls*C3+8*Ls^2*Lp^4*C2*C3+8*Lx*Lp^3*Ls^2*C3^2 \\ & +4*Lx^2*Lp^2*Ls^2*C3^2+4*Lx*Ls^2*Lp^3*C2^2+Lx^2*Ls^2*Lp^2*C2^2 \\ & +8*Lx^2*Lp^4*C2*C1+8*Lx*Lp^4*C2^2*Ls+4*Lx^2*Lp^3*C2^2*Ls+Lx^2 \\ & *Ls^2*Lp^2*C1^2)^{(1/2)})/Lx/Ls/Lp^2/(C3*C2+C2*C1+C1*C3))^{(1/2);} \end{aligned}$$

20

wd1 = 1/2*((2*Lp*Ls*C3+2*Lp^2*C2+Ls*Lp*C2+Ls*Lp*C1+2*Lp^2*C1-(4

$$\begin{aligned} & *Lp^4*C2^2+4*Lp^4*C1^2+4*Lp^3*C1^2*Ls-8*Lp^3*Ls*C3*C1-8*Lp^3*C2 \\ & *Ls*C1-2*Ls^2*Lp^2*C2*C1-8*Lp^3*C2*Ls*C3+4*Lp^2*Ls^2*C3^2+Ls^2 \\ & *Lp^2*C2^2+8*Lp^4*C2*C1+4*Lp^3*C2^2*Ls+Ls^2*Lp^2*C1^2)^{(1/2)}) \\ & /Lp^2/Ls/(C3*C2+C2*C1+C1*C3))^{(1/2);} \end{aligned}$$

err = norm([log(wpopen/wd1) log(wsopen/wn1)]);

B.1.4 magnerr.m

```
function err = magnerr(rvector)M
%function err = mangerr(rvector)

global datapoints datafreqs datamag dataphaze datafreqs2 datamag2
    dataphaze2
global Lx Lp Ls C1 C2 C3 Rp r1 r2

Rp1 = rvector(1);
r11 = rvector(2);
r21 = rvector(3);

[nZmodel,dZmodel] = finaldrivingpoint(Lx,Lp,Ls,Rp1,r11,r21,C1,C2,
    C3);
[nZshort,dZshort] = finaldrivingcc(Lx,Lp,Ls,Rp1,r11,r21,C1,C2,C3);

difference = [];
n = length(datafreqs);
for k = [1:17 22:n]
    %for k = 1:n
        magnZmodel = abs(polyval(nZmodel,2*pi*datafreqs(k)*i));
        magdZmodel = abs(polyval(dZmodel,2*pi*datafreqs(k)*i));
        magZmodel = magnZmodel/magdZmodel;
        difference(k) = abs(log(magZmodel/datamag(k)));
    end
    %for k = [1:21 24:length(datafreqs2)]
    for k = 1:length(datafreqs2)
        magnZmodel = abs(polyval(nZshort,2*pi*datafreqs2(k)*i));
        magdZmodel = abs(polyval(dZshort,2*pi*datafreqs2(k)*i));
```

10

20

```

magZmodel = magnZmodel/magdZmodel;
difference(k+n) = log(magZmodel/datamag2(k));
end

```

30

```

diff = norm(difference);
%
diff = diff + max(0,abs(r11-r1)/r1-.15) + max(0,abs(r21-r2)/r2
-.15) + max(0,abs(Rp1-Rp)/Rp-.15);

```

```

err = diff;

```

40

B.1.5 finaldrivingpoint.m

```

function [numZ, denZ] = finaldrivingpoint(Lx,Lp,Ls,Rp,r1,r2,C1,C2,
C3)
%function [numZ, denZ] = finaldrivingpoint(Lx,Lp,Ls,Rp,r1,r2,C1,
C2,C3)
%
% Driving point impedance of transformer equivalent circuit, open
% circuit on opposite side, given circuit components.
%

ns5 = 4*C1*Lx*Rp^2*Lp^2*Ls*C2+4*C1*Lx*Rp^2*Lp^2*Ls*C3+2*C1*Lx*Rp
*Lp^2*Ls*r2*C2+2*C1*Lx*Rp*Lp^2*Ls*r2*C3+2*C1*r1*Lx*Ls*Lp^2*Rp
*C2+2*C1*r1*Lx*Ls*Lp^2*Rp*C3+C1*r1*Lx*Ls*Lp^2*r2*C2+C1*r1*Lx*Ls
*Lp^2*r2*C3+4*C3*Lx*Rp^2*Lp^2*Ls*C2+2*C3*Lx*Rp*Lp^2*Ls*r2*C2+2
*C3*r1*Lx*Ls*Lp^2*Rp*C2+C3*r1*Lx*Ls*Lp^2*r2*C2;

```


$$\begin{aligned}
\text{ns4} = & 2*C1*Lx*Rp*Lp^2*Ls+C1*r1*Lx*Ls*Lp^2+2*C1*Lx*Rp^2*Lp*Ls*r2 \\
& *C2+2*C1*Lx*Rp^2*Lp*Ls*r2*C3+2*Lx*Ls*Lp^2*Rp*C2+4*Lx*Ls*Lp^2*Rp \\
& *C3+Lx*Ls*Lp^2*r2*C2+Lx*Ls*Lp^2*r2*C3+4*C1*r1*Lx*Lp^2*r2*Rp*C2 \\
& +4*C1*r1*Lx*Lp^2*r2*Rp*C3+4*C1*r1*Lx*Rp^2*Lp^2*C2+4*C1*r1*Lx \\
& *Rp^2*Lp^2*C3+4*C1*Lx*Rp^2*Lp^2*r2*C2+4*C1*Lx*Rp^2*Lp^2*r2*C3+2 \\
& *C1*r1*Lx*Ls*Rp^2*Lp*C2+2*C1*r1*Lx*Ls*Rp^2*Lp*C3+2*C1*r1*Lx*Ls \\
& *Rp*r2*Lp*C2+2*C1*r1*Lx*Ls*Rp*r2*Lp*C3+C3*r1*Lx*Ls*Lp^2+2*C3*Lx \\
& *Rp^2*Lp*Ls*r2*C2+4*C3*Lx*Rp^2*Lp^2*r2*C2+2*C3*r1*Lx*Ls*Rp^2*Lp \\
& *C2+2*C3*r1*Lx*Ls*Rp*r2*Lp*C2+4*C3*r1*Lx*Lp^2*r2*Rp*C2+4*C3*r1 \\
& *Lx*Rp^2*Lp^2*C2;
\end{aligned}$$

$$\begin{aligned}
\text{ns3} = & Lx*Ls*Lp^2+4*Rp^2*Lp^2*Ls*C2+4*Rp^2*Lp^2*Ls*C3+2*Rp*Lp^2*Ls \\
& *r2*C2+2*Rp*Lp^2*Ls*r2*C3+2*r1*Ls*Lp^2*Rp*C2+2*r1*Ls*Lp^2*Rp*C3 \\
& +r1*Ls*Lp^2*r2*C2+r1*Ls*Lp^2*r2*C3+4*Lx*Rp^2*Lp^2*C2+4*C1*Lx \\
& *Rp^2*Lp^2+2*Lx*Ls*Rp^2*Lp*C2+4*Lx*Ls*Rp^2*Lp*C3+2*Lx*Ls*Rp*r2 \\
& *Lp*C2+2*Lx*Ls*Rp*r2*Lp*C3+2*C1*Lx*Rp^2*Lp*Ls+4*Lx*Lp^2*r2*Rp \\
& *C2+4*Lx*Lp^2*r2*Rp*C3+2*C1*r1*Lx*Rp*Lp*Ls+4*C1*r1*Lx*Lp^2*Rp+2 \\
& *C3*r1*Lx*Rp*Lp*Ls+C1*r1*Lx*Ls*Rp^2*r2*C2+C1*r1*Lx*Ls*Rp^2*r2 \\
& *C3+4*C1*r1*Lx*Rp^2*r2*Lp*C2+4*C1*r1*Lx*Rp^2*r2*Lp*C3+C3*r1*Lx \\
& *Ls*Rp^2*r2*C2+4*C3*r1*Lx*Rp^2*r2*Lp*C2+4*C3*r1*Lx*Lp^2*Rp;
\end{aligned}$$

$$\begin{aligned}
\text{ns2} = & 2*Rp*Lp^2*Ls+2*r1*Ls*Rp*r2*Lp*C3+2*r1*Ls*Rp^2*Lp*C2+C1*r1 \\
& *Lx*Ls*Rp^2+r1*Ls*Lp^2+2*r1*Ls*Rp^2*Lp*C3+2*Rp^2*Lp*Ls*r2*C3+4 \\
& *Rp^2*Lp^2*r2*C3+2*Lx*Rp*Lp*Ls+4*Rp^2*Lp^2*r2*C2+2*Rp^2*Lp*Ls \\
& *r2*C2+4*r1*Rp^2*Lp^2*C3+4*r1*Lp^2*r2*Rp*C2+Lx*Ls*Rp^2*r2*C2+Lx \\
& *Ls*Rp^2*r2*C3+4*Lx*Rp^2*r2*Lp*C3+2*r1*Ls*Rp*r2*Lp*C2+4*r1*Lp^2 \\
& *r2*Rp*C3+4*r1*Rp^2*Lp^2*C2+C3*r1*Lx*Ls*Rp^2+4*C3*r1*Lx*Rp^2*Lp \\
& +4*Lx*Lp^2*Rp+4*C1*r1*Lx*Rp^2*Lp+4*Lx*Rp^2*r2*Lp*C2;
\end{aligned}$$

$$\text{ns1} = 2*Rp^2*Lp*Ls+4*Rp^2*Lp^2+2*r1*Rp*Lp*Ls+Lx*Ls*Rp^2+4*r1*Rp^2$$

$$\begin{aligned} & *r2*Lp*C2+4*C3*r1*Rp^2*r2*Lp+4*r1*Lp^2*Rp+r1*Ls*Rp^2*r2*C2+C3 \\ & *r1*Ls*Rp^2*r2+4*Lx*Rp^2*Lp; \end{aligned}$$

$$ns0 = r1*Ls*Rp^2+4*r1*Rp^2*Lp;$$

50

$$\begin{aligned} ds4 = & 4*C1*Rp^2*Lp^2*Ls*C2+4*C1*Rp^2*Lp^2*Ls*C3+2*C1*Rp*Lp^2*Ls \\ & *r2*C2+2*C1*Rp*Lp^2*Ls*r2*C3+2*C1*r1*Ls*Lp^2*Rp*C2+2*C1*r1*Ls \\ & *Lp^2*Rp*C3+C1*r1*Ls*Lp^2*r2*C2+C1*r1*Ls*Lp^2*r2*C3+4*C3*Rp^2 \\ & *Lp^2*Ls*C2+2*C3*Rp*Lp^2*Ls*r2*C2+2*C3*r1*Ls*Lp^2*Rp*C2+C3*r1 \\ & *Ls*Lp^2*r2*C2; \end{aligned}$$

$$\begin{aligned} ds3 = & 2*Ls*Lp^2*Rp*C2+4*Ls*Lp^2*Rp*C3+Ls*Lp^2*r2*C2+Ls*Lp^2*r2*C3 \\ & +2*C1*Rp*Lp^2*Ls+C1*r1*Ls*Lp^2+C3*r1*Ls*Lp^2+2*C1*Rp^2*Lp*Ls*r2 \\ & *C2+2*C1*Rp^2*Lp*Ls*r2*C3+2*C1*r1*Ls*Rp*r2*Lp*C2+4*C1*Rp^2*Lp^2 \\ & *r2*C2+4*C1*Rp^2*Lp^2*r2*C3+2*C1*r1*Ls*Rp^2*Lp*C2+2*C1*r1*Ls \quad 60 \\ & *Rp^2*Lp*C3+2*C1*r1*Ls*Rp*r2*Lp*C3+4*C1*r1*Lp^2*r2*Rp*C2+4*C1 \\ & *r1*Lp^2*r2*Rp*C3+4*C1*r1*Rp^2*Lp^2*C2+4*C1*r1*Rp^2*Lp^2*C3+2 \\ & *C3*Rp^2*Lp*Ls*r2*C2+4*C3*Rp^2*Lp^2*r2*C2+2*C3*r1*Ls*Rp^2*Lp*C2 \\ & +2*C3*r1*Ls*Rp*r2*Lp*C2+4*C3*r1*Lp^2*r2*Rp*C2+4*C3*r1*Rp^2*Lp^2 \\ & *C2; \end{aligned}$$

$$\begin{aligned} ds2 = & 4*Rp^2*Lp^2*C2+4*Ls*Rp^2*Lp*C3+2*Rp*Lp*Ls*C3*r2+4*C1*r1 \\ & *Rp^2*r2*Lp*C2+4*C1*r1*Rp^2*r2*Lp*C3+Ls*Lp^2+2*Rp*Lp*Ls*C2*r2+4 \\ & *Lp^2*r2*Rp*C3+2*Ls*Rp^2*Lp*C2+2*C1*r1*Rp*Lp*Ls+4*Lp^2*r2*Rp*C2 \\ & +4*C3*r1*Rp^2*r2*Lp*C2+4*C1*Rp^2*Lp^2+C1*r1*Ls*Rp^2*r2*C2+2*C1 \quad 70 \\ & *Rp^2*Lp*Ls+2*C3*r1*Rp*Lp*Ls+4*C1*r1*Lp^2*Rp+C3*r1*Ls*Rp^2*r2 \\ & *C2+C1*r1*Ls*Rp^2*r2*C3+4*C3*r1*Lp^2*Rp; \end{aligned}$$

$$\begin{aligned} ds1 = & 4*C3*r1*Rp^2*Lp+4*Lp^2*Rp+2*Rp*Lp*Ls+Ls*Rp^2*r2*C2+Ls*Rp^2 \\ & *r2*C3+C1*r1*Ls*Rp^2+4*Rp^2*r2*Lp*C2+4*Rp^2*r2*Lp*C3+C3*r1*Ls \end{aligned}$$

```
*Rp^2+4*C1*r1*Rp^2*Lp;
```

```
ds0 = 4*Rp^2*Lp+Ls*Rp^2;
```

80

```
%      s^5  s^4  s^3  s^2  s    1
numZ = [ ns5  ns4  ns3  ns2  ns1  ns0 ];
denZ = [      ds4  ds3  ds2  ds1  ds0 ];
```

B.1.6 finaldrivingcc.m

```
function [numZ, denZ] = finaldrivingcc(Lx,Lp,Ls,Rp,r1,r2,C1,C2,C3)
```

```
%function [numZ, denZ]=finaldrivingcc(Lx,Lp,Ls,Rp,r1,r2,C1,C2,C3)
```

```
%
```

```
% Driving point impedance of transformer equivalent circuit,
```

```
% short circuit on opposite side, given circuit components.
```

```
%
```

```
ns5 = 4*Lx*Ls*Rp^2*Lp^2*C3+2*Lx*Ls*Rp*Lp^2*C1*r2+2*Lx*Ls*Rp*Lp^2
      *C3*r2+4*Lx*Ls*Rp^2*Lp^2*C1;
```

10

```
ns4 = 4*Lx*Rp^2*Lp^2*r2*C3+2*Lx*r1*Rp*Lp^2*C1*r2+4*Lx*r1*Rp^2
      *Lp^2*C3+2*Lx*Ls*Rp^2*Lp*C3*r2+Lx*Ls*Lp^2*r2+4*Lx*r1*Rp^2*Lp^2
      *C1+4*Lx*Rp^2*Lp^2*r2*C1+2*Lx*Ls*Lp^2*Rp+2*Lx*r1*Rp*Lp^2*C3*r2
      +2*Lx*Ls*Rp^2*Lp*C1*r2;
```

```
ns3 = 2*Lx*r1*Lp^2*Rp+2*Lx*Ls*Rp^2*Lp+2*Lx*Ls*Rp*Lp*r2+2*Rp*Lp^2
      *Ls*r2+4*Rp^2*Lp^2*Ls+4*Lx*Rp^2*Lp^2+Lx*r1*Lp^2*r2+2*Lx*r1*Rp^2
```

$$*Lp*C3*r2+4*Lx*Rp*Lp^2*r2+2*Lx*r1*Rp^2*Lp*C1*r2;$$

$$\begin{aligned} ns2 = & Lx*Ls*r2*Rp^2+2*Rp*Lp^2*r1*r2+4*Rp^2*Lp^2*r2+4*Lx*Rp^2*Lp \\ & *r2+2*Rp^2*Lp*Ls*r2+2*Lx*r1*Rp*Lp*r2+4*Rp^2*Lp^2*r1+2*Lx*r1 \\ & *Rp^2*Lp; \end{aligned}$$

$$ns1 = Lx*r1*r2*Rp^2+2*Rp^2*Lp*r1*r2;$$

$$ns0 = 0;$$

$$\begin{aligned} ds4 = & 2*Ls*Rp*Lp^2*C3*r2+4*Ls*Rp^2*Lp^2*C1+2*Ls*Rp*Lp^2*C1*r2+4 \\ & *Ls*Rp^2*Lp^2*C3; \end{aligned}$$

30

$$\begin{aligned} ds3 = & 4*Rp^2*Lp^2*r2*C3+4*Rp^2*Lp^2*r2*C1+2*Ls*Lp^2*Rp+Ls*Lp^2*r2 \\ & +2*Ls*Rp^2*Lp*C1*r2+2*Ls*Rp^2*Lp*C3*r2+4*r1*Rp^2*Lp^2*C1+2*r1 \\ & *Rp*Lp^2*C1*r2+4*r1*Rp^2*Lp^2*C3+2*r1*Rp*Lp^2*C3*r2; \end{aligned}$$

$$\begin{aligned} ds2 = & 4*Rp*Lp^2*r2+2*r1*Lp^2*Rp+4*Rp^2*Lp^2+2*Ls*Rp*Lp*r2+2*Ls \\ & *Rp^2*Lp+r1*Lp^2*r2+2*r1*Rp^2*Lp*C1*r2+2*r1*Rp^2*Lp*C3*r2; \end{aligned}$$

$$ds1 = 4*Rp^2*Lp*r2+Ls*r2*Rp^2+2*r1*Rp*Lp*r2+2*Rp^2*Lp*r1;$$

$$ds0 = r1*r2*Rp^2;$$

40

$$\begin{aligned} \% \quad & s^5 \quad s^4 \quad s^3 \quad s^2 \quad s \quad 1 \\ numZ = & [ns5 \quad ns4 \quad ns3 \quad ns2 \quad ns1 \quad ns0]; \\ denZ = & [\quad ds4 \quad ds3 \quad ds2 \quad ds1 \quad ds0]; \end{aligned}$$

B.2 Determination of six capacitors

```
% allcaps.m
```

```
% Calculate all six capacitance values
```

```
%This script contains all of the functional statements of lriter.m
```

```
%but omits resistance calculation, printing of the reactive and
```

```
%resistive parameters, and plotting the resulting curve. It
```

```
%instead tries to calculate all six capacitor values.
```

```
global datapoints datafreqs datamag dataphaze datafreqs2 datamag2 10
```

```
dataphaze2
```

```
global Lx Lp Ls wpsshort wsshort wpopen wsopen wpopen2 wsopen2
```

```
global C1plusC3 C1 C2 C3
```

```
opts = optimset('MaxFunEvals',1e4,'MaxIter',1e4);
```

```
C123 = [];
```

```
A = [];
```

```
n = .0844;
```

20

```
% Model selection variables
```

```
S_state = 'sfull'; % sfull, shalf
```

```
P_state = 'phalf'; % pfull, phalf
```

```
ferrite_state = 'ferriteon'; % ferriteon, ferriteoff
```

```
measurement_state = 'BD'; % float, BD, BC, AD, AC
```

```
% Data points
```

```
% Contained in data files labeled by model type
```

```
filename = strcat('final',S_state,'popen',ferrite_state,
```

```

    measurement_state);
load(strcat(filename, '.dat'));
evalin('caller',strcat('datapoints = ',filename,','));
filename2 = strcat('final',S_state,P_state,'short',ferrite_state,
    measurement_state);
load(strcat(filename2, '.dat'));
evalin('caller',strcat('datapoints2 = ',filename2,','));
datafreqs = datapoints(:,1);
datamag = datapoints(:,2);
dataphaze = datapoints(:,3);
datafreqs2 = datapoints2(:,1);
datamag2 = datapoints2(:,2);
dataphaze2 = datapoints2(:,3);

```

% Inductance values, using BD configuration

```

LoplusLx = 1.59e-3;
LcplusLx = 4.68e-5;
wpshort = 307e3*2*pi;
wsshort = 805e3*2*pi;
Lx = 3.2e-6; %first guess
Lxold = 0;
while abs(Lx-Lxold)/Lx > 1e-4
    Lxold = Lx;
    Lo = LoplusLx - Lx;
    Lc = LcplusLx - Lx;
    Lp = (Lo + sqrt(Lo^2-Lo*Lc))/2;
    Ls = 2*Lp*Lc/(2*Lp-Lc);
    C1plusC3 = 1/(wpshort^2*Lc);
    Lx = Lc / (Lc*C1plusC3*wsshort^2 - 1);

```

end

60

% Capacitance values using BD

```
wpopen = 45.43e3*2*pi;  
wsopen = 773e3*2*pi;  
wpopen2 = 1.2e6*2*pi;  
wsopen2 = 1.8e6*2*pi;  
C1plusC2 = 1/(Lo*wpopen2);  
C2plusC3 = 1/(Lc*wsopen2);
```

```
C1 = (C1plusC2 + C1plusC3 - C2plusC3)/2;  
C2 = (C1plusC2 + C2plusC3 - C1plusC3)/2;  
C3 = (C1plusC3 + C2plusC3 - C1plusC2)/2;
```

70

% Want wn2 = wsopen2, wn1 = wsopen, wd2 = wopen2, wd1 = wopen.

```
capvector = fminsearch('reserr',[C1 C2],opts);
```

```
C1 = capvector(1);  
C2 = capvector(2);  
C3 = C1plusC3 - C1;
```

80

```
C123(1:3,1) = [C1 C2 C3]' ;
```

% using AC

```
wpsshort = 317e3;  
wpopen = 41.96e3;  
wsopen = 723e3;
```

% don't have wopen2 or wsopen2

C1plusC3 = 1/(Lc*wpshort^2);

90

C1plusC2 = 1/(Lo*wpopen^2);

C2plusC3 = 1/(Lc*wsopen^2);

C1 = (C1plusC2 + C1plusC3 - C2plusC3)/2;

C2 = (C1plusC2 + C2plusC3 - C1plusC3)/2;

C3 = (C1plusC3 + C2plusC3 - C1plusC2)/2;

% Want wn1 = wsopen, wd1 = wpopen.

capvector = fminsearch('reserrsimp1',[C1 C2],opts);

100

C1 = capvector(1);

C2 = capvector(2);

C3 = C1plusC3 - C1;

C123(4:6,1) = [C1 C2 C3]';

% using BC

wpsshort = 330e3;

110

wpopen = 51.05e3;

wsopen = 850e3;

% don't have wopen2 or wsopen2

C1plusC3 = 1/(Lc*wpshort^2);

C1plusC2 = 1/(Lo*wpopen^2);

C2plusC3 = 1/(Lc*wsopen^2);

C1 = (C1plusC2 + C1plusC3 - C2plusC3)/2;


```

C2 = (C1plusC2 + C2plusC3 - C1plusC3)/2;
C3 = (C1plusC3 + C2plusC3 - C1plusC2)/2;

```

120

```

% Want wn1 = wsopen, wd1 = wopen.

```

```

capvector = fminsearch('reserrsimp1',[C1 C2],opts);

```

```

C1 = capvector(1);

```

```

C2 = capvector(2);

```

```

C3 = C1plusC3 - C1;

```

```

C123(7:9,1) = [C1 C2 C3]';

```

130

```

% using AD

```

```

wpsshort = 337e3;

```

```

wpopen = 48.72e3;

```

```

wsopen = 814e3;

```

```

% don't have wpopen2 or wsopen2

```

```

C1plusC3 = 1/(Lc*wpsshort^2);

```

```

C1plusC2 = 1/(Lo*wpopen^2);

```

```

C2plusC3 = 1/(Lc*wsopen^2);

```

140

```

C1 = (C1plusC2 + C1plusC3 - C2plusC3)/2;

```

```

C2 = (C1plusC2 + C2plusC3 - C1plusC3)/2;

```

```

C3 = (C1plusC3 + C2plusC3 - C1plusC2)/2;

```

```

% Want wn1 = wsopen, wd1 = wopen.

```

```

capvector = fminsearch('reserrsimp1',[C1 C2],opts);

```

```

C1 = capvector(1);
C2 = capvector(2);
C3 = C1plusC3 - C1;

```

150

```

C123(10:12,1) = [C1 C2 C3]';

```

```

C33 = 12.8e-9;

```

```

% Let matlab find the closest values for C11,C22,C33,C12,C13,C23
% Already know C33, so subtract it from anywhere it might have
% been relevant.

```

160

```

% Here is the matrix with C33 as an unknown:

```

```

%A(1,1:6) = [ 1  0  0  n  0  0];
%A(2,1:6) = [ 0 n^2  0  n  0  0];
%A(3,1:6) = [ 0  0  0 -n  0  0];
%A(4,1:6) = [ 1  0 1-n  n 2-n 2*n];
%A(5,1:6) = [ 0 n^2 n^2-n n -n -2*n^2+n];
%A(6,1:6) = [ 0  0  n -n  n -n];
%A(7,1:6) = [ 1  0  0  n -n  0];
%A(8,1:6) = [ 0 n^2 n^2  n -n -2*n^2];
%A(9,1:6) = [ 0  0  0 -n  n  0];
%A(10,1:6) = [1  0  1  n  2  n];
%A(11,1:6) = [0 n^2  0  n  0  n];
%A(12,1:6) = [0  0  0 -n  0 -n];
%A(13,1:6) = [0  0  1  0  0  0];

```

170

```

% So, making the proper subtractions:

```

```

C123(4,1) = C123(4,1) - (1-n)*C33;
C123(5,1) = C123(5,1) - (n^2-n)*C33;
C123(6,1) = C123(6,1) - n*C33;

```

$$C123(8,1) = C123(8,1) - n^2 * C33;$$

$$C123(10,1) = C123(10,1) - C33;$$

180

% The matrix, without C33:

$$%A(1,1:5) = [1 \ 0 \ n \ 0 \ 0];$$

$$%A(2,1:5) = [0 \ n^2 \ n \ 0 \ 0];$$

$$%A(3,1:5) = [0 \ 0 \ -n \ 0 \ 0];$$

$$%A(4,1:5) = [1 \ 0 \ n \ 2-n \ 2*n];$$

$$%A(5,1:5) = [0 \ n^2 \ n \ -n \ -2*n^2+n];$$

$$%A(6,1:5) = [0 \ 0 \ -n \ n \ -n];$$

$$%A(7,1:5) = [1 \ 0 \ n \ -n \ 0];$$

$$%A(8,1:5) = [0 \ n^2 \ n \ -n \ -2*n^2];$$

$$%A(9,1:5) = [0 \ 0 \ -n \ n \ 0];$$

190

$$%A(10,1:5) = [1 \ 0 \ n \ 2 \ n];$$

$$%A(11,1:5) = [0 \ n^2 \ n \ 0 \ n];$$

$$%A(12,1:5) = [0 \ 0 \ -n \ 0 \ -n];$$

*%Finally, we also know C12, since C4=Cc=-n*C12*

$$C12 = -C123(3,1)/n;$$

%Subtracting the proper factors of C12 from the vector

$$C123 = C123 - n * C12 * [1 \ 1 \ -1 \ 1 \ 1 \ -1 \ 1 \ 1 \ -1 \ 1 \ 1 \ -1]';$$

% The matrix, this time with C12 also gone:

$$A(1,1:4) = [1 \ 0 \ 0 \ 0];$$

$$A(2,1:4) = [0 \ n^2 \ 0 \ 0];$$

200

$$A(3,1:4) = [0 \ 0 \ 0 \ 0];$$

$$A(4,1:4) = [1 \ 0 \ 2-n \ 2*n];$$

$$A(5,1:4) = [0 \ n^2 \ -n \ -2*n^2+n];$$

$$A(6,1:4) = [0 \ 0 \ n \ -n];$$

$$A(7,1:4) = [1 \ 0 \ -n \ 0];$$

$$A(8,1:4) = [0 \ n^2 \ -n \ -2*n^2];$$

$$A(9,1:4) = [0 \ 0 \ n \ 0];$$

$$A(10,1:4) = [1 \ 0 \ 2 \ n];$$

```
A(11,1:4) = [0 n^2 0 n];
A(12,1:4) = [0 0 0 -n];
```

210

```
C112233 = A \ C123;
% The order of this vector:
% C11 C22 {C33} {C12} C13 C23
C11 = C112233(1);
C22 = C112233(2);
C13 = C112233(3);
C23 = C112233(4);
```

220

```
% Now that we have C11, C12, C13, C22, C23, and C33,
% use those to find C1-C6.
c1 = C11 + n*C12 + C13;
c2 = n^2*C22 + n*C12 + n*C23;
c3 = C33 + C13 + n*C23;
c4 = -n*C12;
c5 = -C13;
c6 = -n*C23;
C123456 = [c1 c2 c3 c4 c5 c6]';
```

230

Appendix C

Equivalent Model for Remaining Transformer Configurations

There were four possible models that could be developed for the transformer under study, depending on whether the center tap was used as a connection. The measurements could utilize half or all of the primary or secondary winding. The model using the full secondary winding and half of the primary winding was chosen for study due to its significance in later simulations in the operating environment of the transformer. For completeness and to verify the accuracy of the modeling method, measurements were recorded for the three other transformer models.

C.1 Measured Data

The experiments of Table 3.1 were performed for all possible transformer models. Plots of the measured driving point impedance for configuration BD are shown below. Resonant frequencies for the other configurations are included in Table C.1. It should be noted that driving-point measurements taken from the transformer secondary with the primary open are the same whether the full or half primary is being used for the model. The redundant measurements are not repeated.

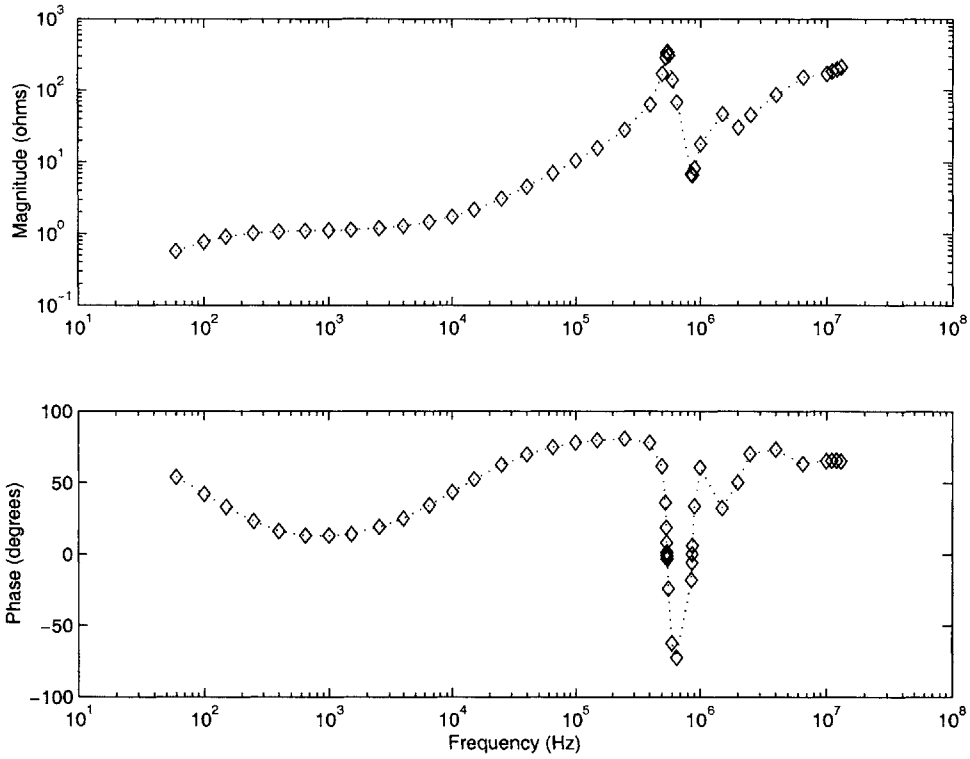


Figure C-1: Impedance of full secondary, full primary shorted

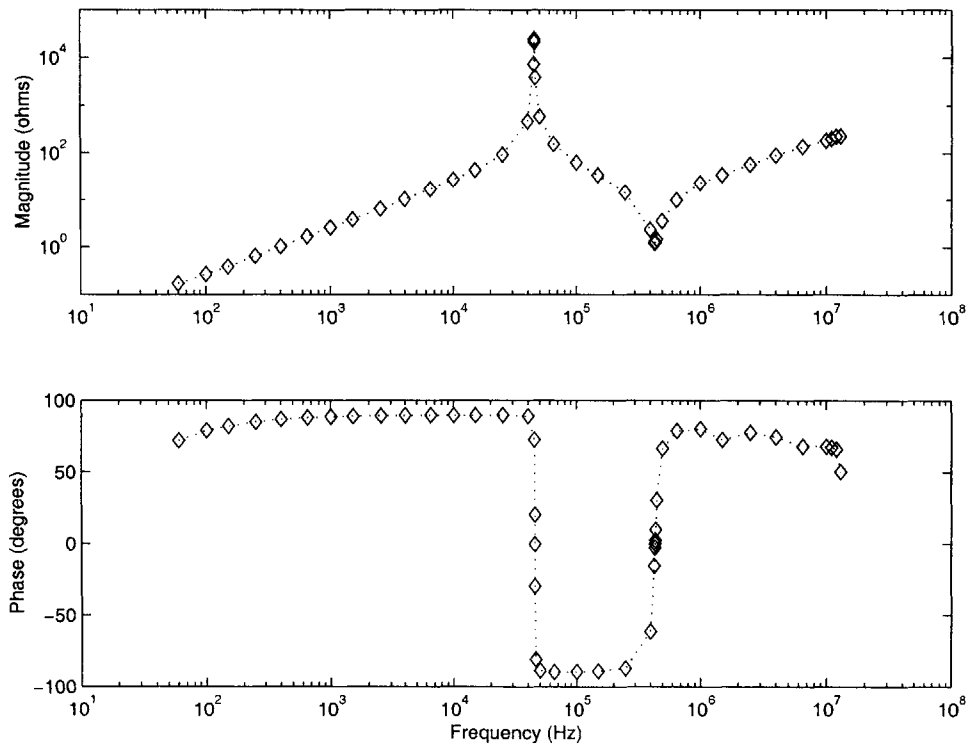


Figure C-2: Impedance of half secondary, primary open

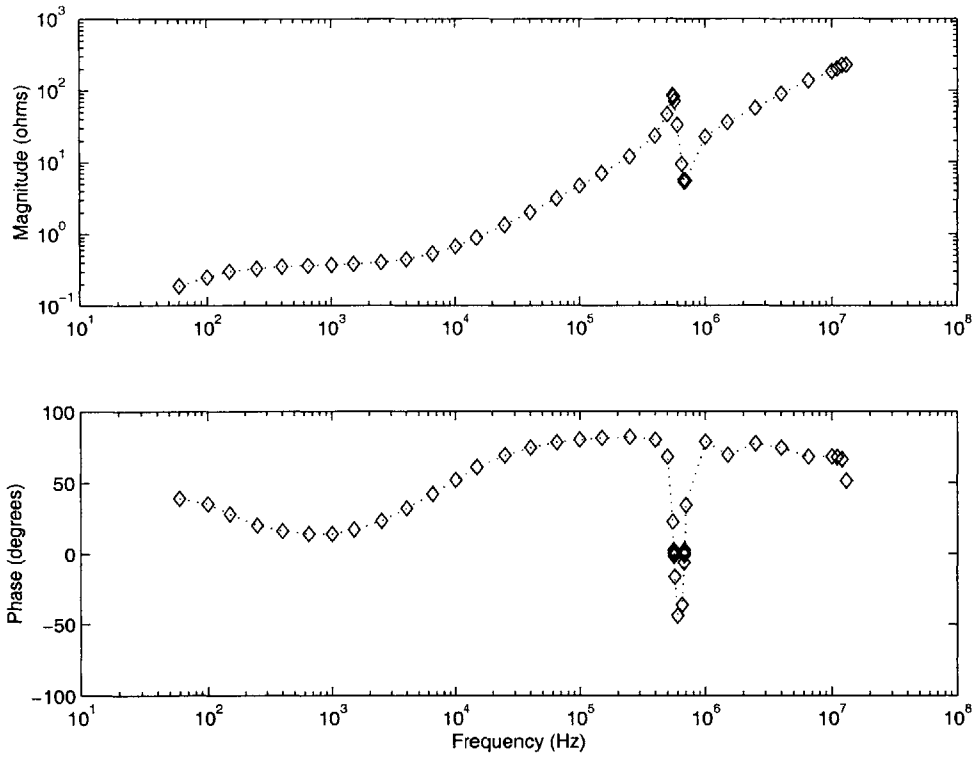


Figure C-3: Impedance of half secondary, full primary shorted

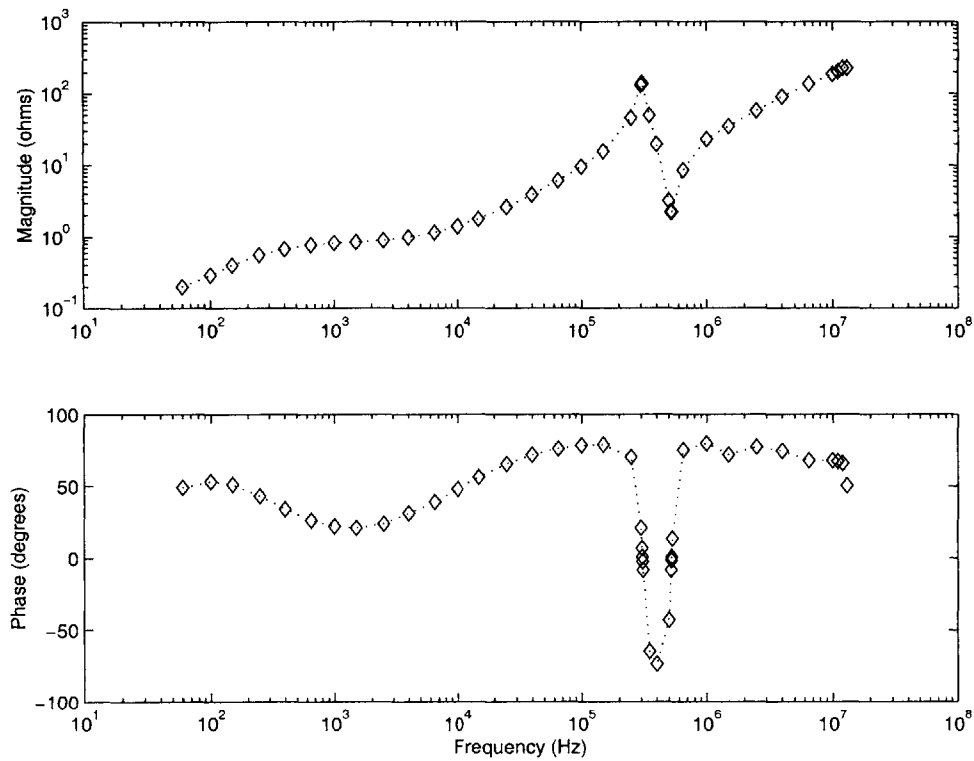


Figure C-4: Impedance of half secondary, half primary shorted

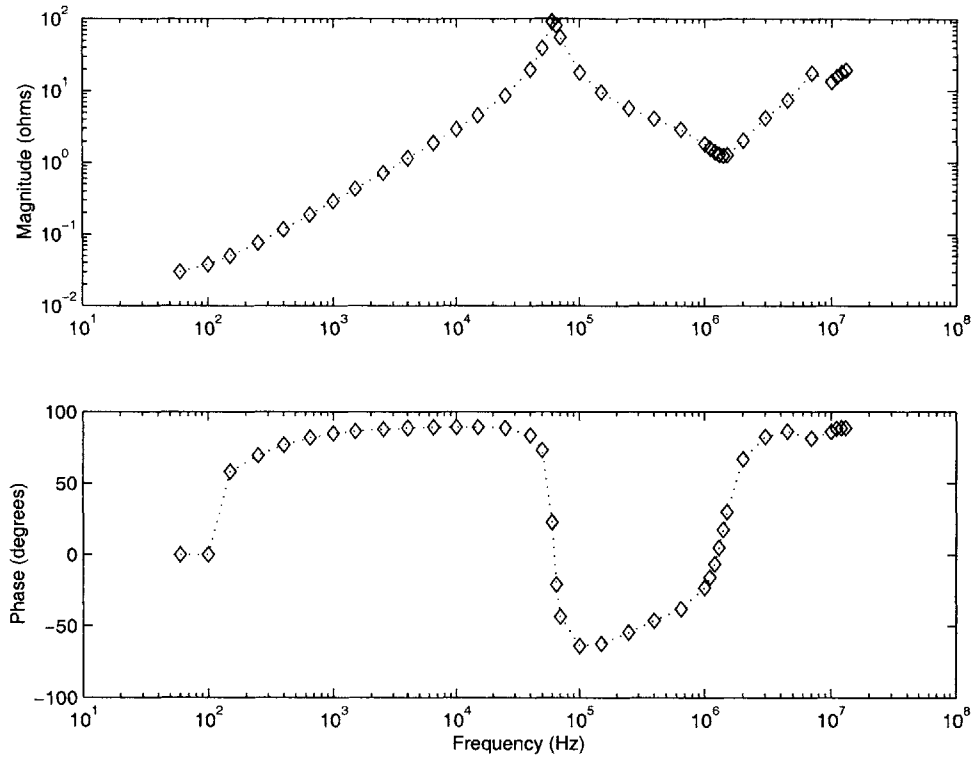


Figure C-5: Impedance of full primary, secondary open

	Configuration	$f_{p,open}$	$f_{s,open}$	$f_{p,short}$
Full secondary, full primary	BD	45.43kHz	773kHz	549kHz
	AC	41.96kHz	723kHz	565.5kHz
	BC	51.05kHz	850kHz	624kHz
	AD	48.72kHz	814kHz	590kHz
Half secondary, full primary	BD	45.34kHz	561kHz	436kHz
	AC	63.19kHz	845kHz	628kHz
	BC	52.70kHz	645kHz	510kHz
	AD	64.35kHz	870kHz	639kHz
Half secondary, half primary	BD	45.34kHz	307kHz	436kHz
	AC	63.19kHz	450kHz	628kHz
	BC	52.70kHz	328kHz	510kHz
	AD	64.35kHz	455kHz	639kHz

Table C.1: Measured resonant frequencies

	Full secondary, full primary	Half secondary, full primary	Half secondary, half primary
L_x	6.57 μ H	5.05 μ H	5.01 μ H
L_p	1.58mH	0.404mH	0.403mH
L_s	9.76 μ H	2.36 μ H	9.70 μ H
R_p	78.0k Ω	20.9k Ω	20.9k Ω
r_1	489m Ω	6.56m Ω	6.56m Ω
r_2	375m Ω	95.0m Ω	8.13m Ω
C_A	7.21nF	-23.0nF	28.1nF
C_B	-0.204nF	41.6nF	0.802nF
C_C	1.42nF	57.3nF	-0.066nF
N_S	0.166	0.331	0.168

Table C.2: Optimized circuit parameter values

C.2 Equivalent Circuit Model

The values of the equivalent circuit model components are shown in Table C.2 for each model.

Each transformer model was simulated as a stand-alone circuit to show its driving-point impedance. The predicted impedance is compared to the measured impedance in the following figures.

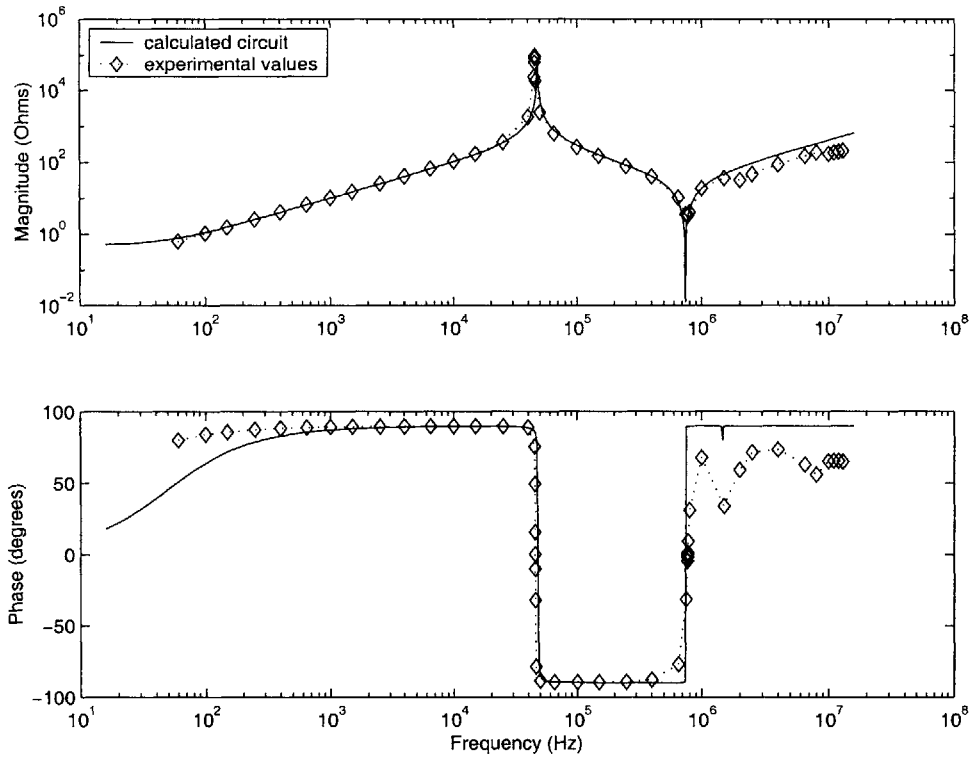


Figure C-6: Full secondary, full primary. Impedance of secondary, primary open

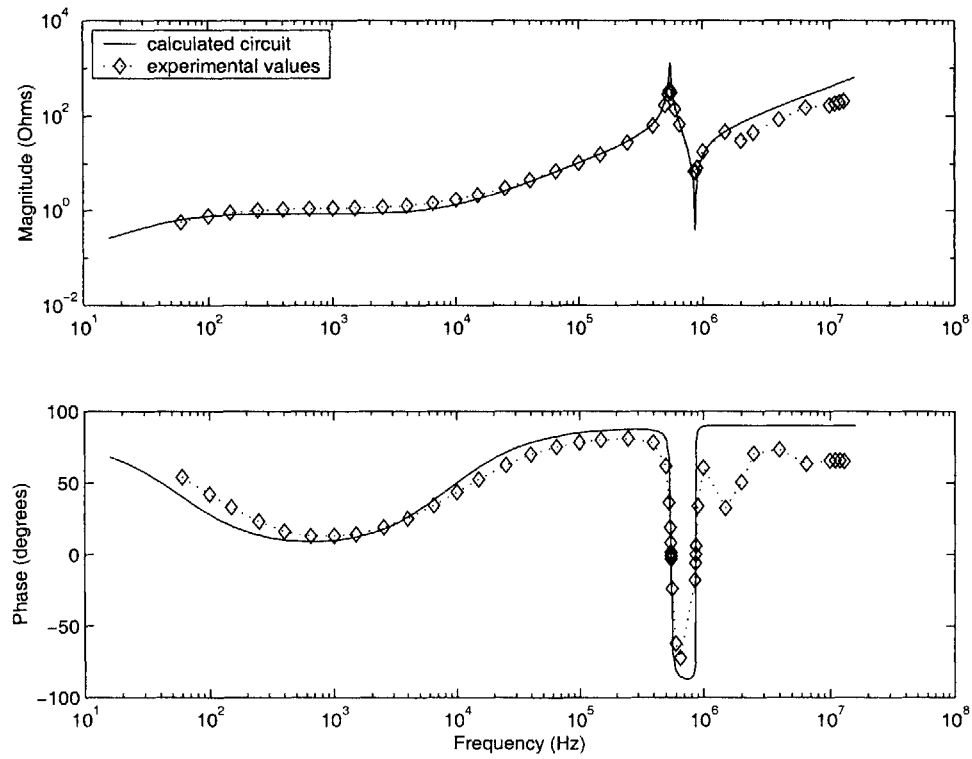


Figure C-7: Full secondary, full primary. Impedance of secondary, primary shorted

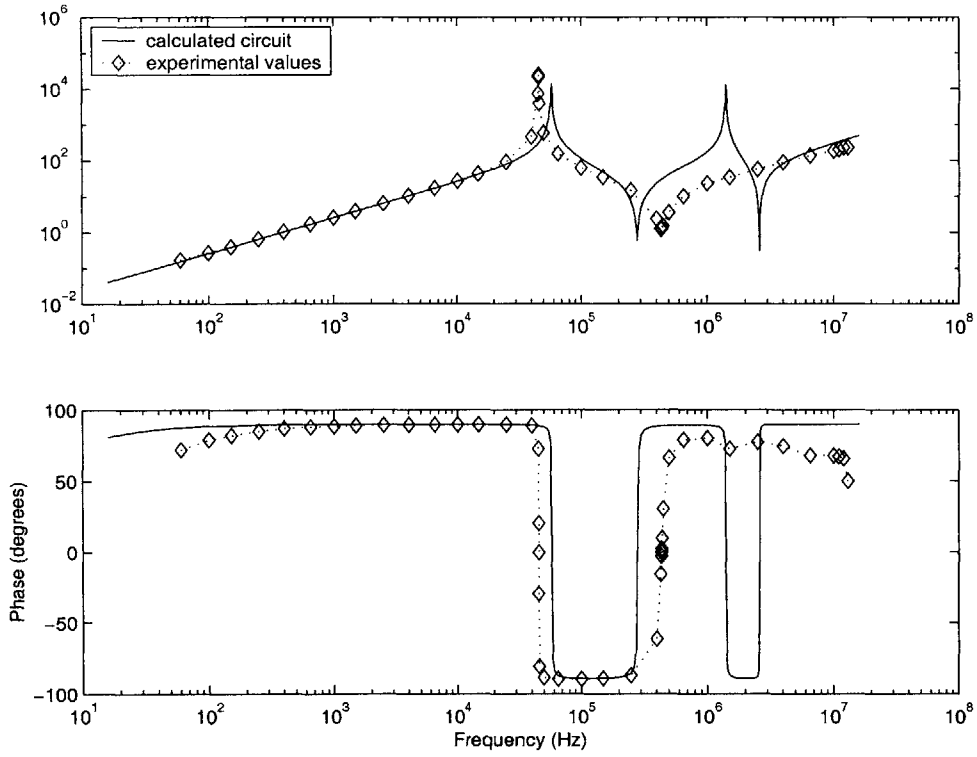


Figure C-8: Half secondary, full primary. Impedance of secondary, primary open

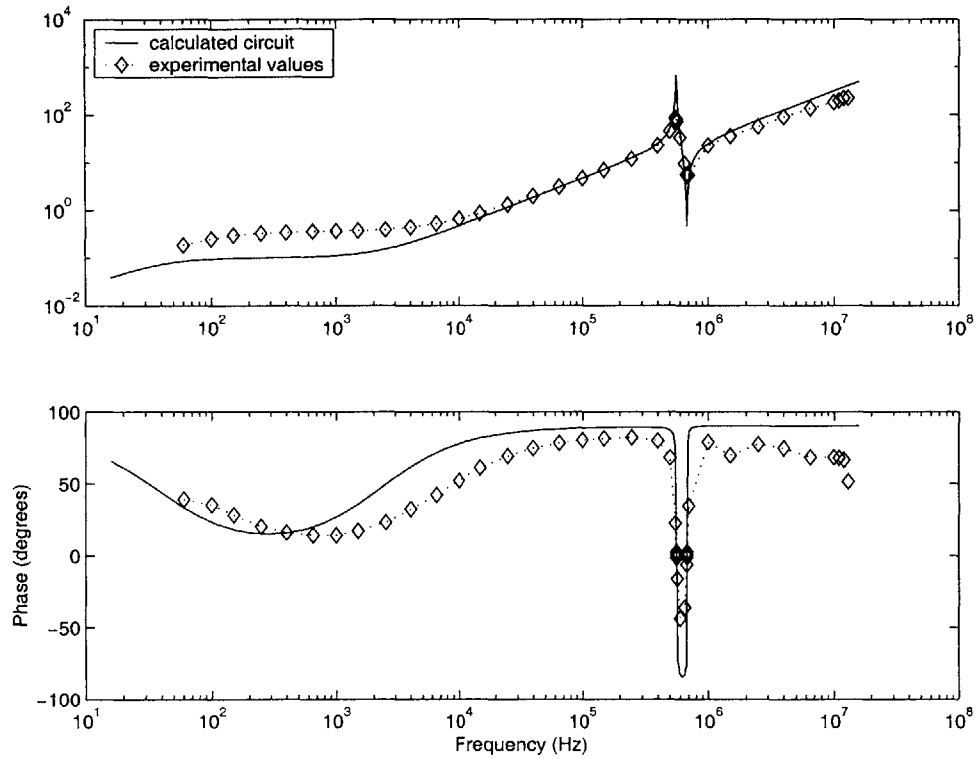


Figure C-9: Half secondary, full primary. Impedance of secondary, primary shorted

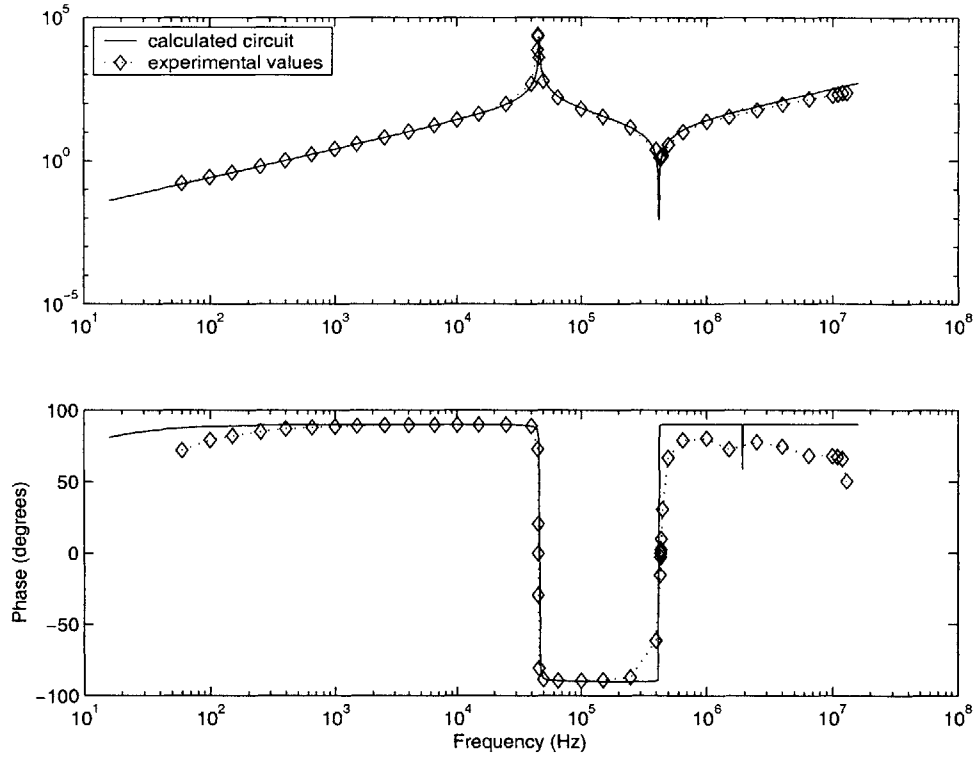


Figure C-10: Half secondary, half primary. Impedance of secondary, primary open

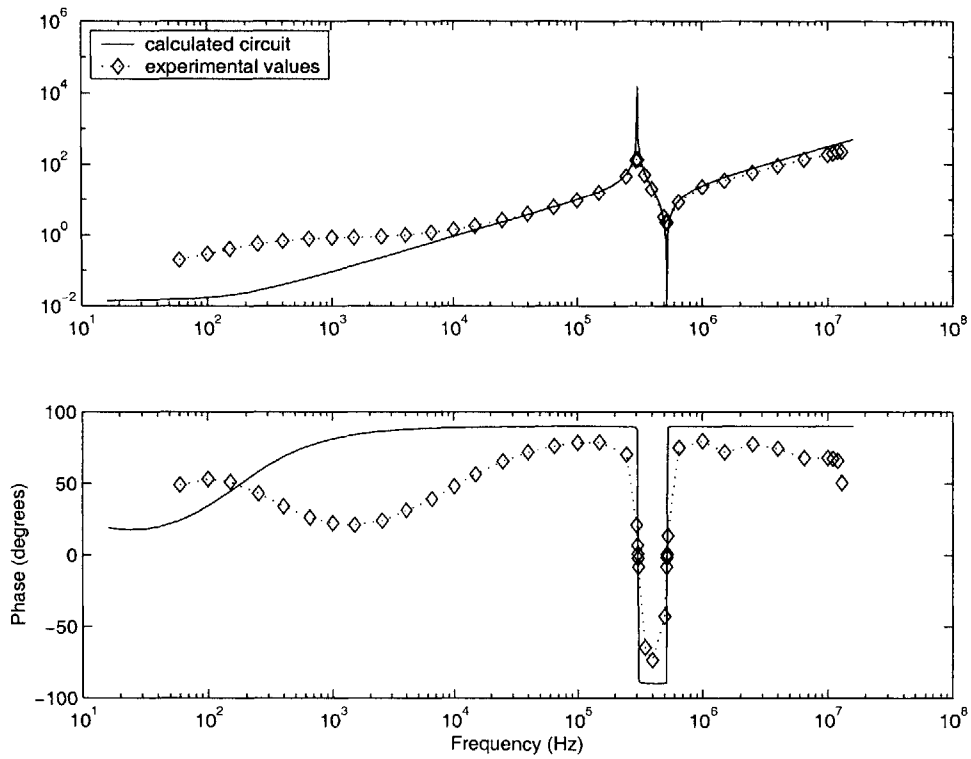


Figure C-11: Half secondary, half primary. Impedance of secondary, primary shorted

Bibliography

- [1] F. Blache, J.P. Keradec, and B. Cogitore. Stray capacitances of two winding transformers: equivalent circuit, measurements, calculation and lowering. *Industry Applications Society Annual Meeting, 1994., Conference Record of the 1994 IEEE*, 2:1211–1217, October 1994.
- [2] Q. Chen, F. Lee, J.Z. Jiang, and M. Jovanovic. A new model for multiple-winding transformer. *Power Electronics Specialists Conference, PESC '94 Record., 25th Annual IEEE*, 2:864–871, 1994.
- [3] B. Cogitore. *Recherche de circuits equivalents pour les composants magnetiques haute frequence*. Doctoral thesis, Institut National Polytechnique de Grenoble, France, July 1994.
- [4] B. Cogitore, J.P. Keradec, and J. Barbaroux. The two-winding transformer: an experimental method to obtain a wide frequency range equivalent circuit. *IEEE Transactions on Instrumentation and Measurement*, 43(2), April 1994.
- [5] J. Kirtley. Surge voltage distribution in helical high voltage armature windings. *IEEE Transactions on Power Apparatus and Systems*, PAS-102(9), September 1983.
- [6] V.A. Niemela, H.A. Owen, and T.G. Wilson. Frequency-independent-element cross-coupled-secondaries model for multiwinding transformers. *Power Electronics Specialists Conference, 1992. PESC '92 Record., 23rd Annual IEEE*, 2:1261–1268, 1992.

- [7] A. Schellmanns, K. Berrouche, and J.P. Keradec. Multiwinding transformers: a successive refinement method to characterize a general equivalent circuit. *IEEE Transactions on Instrumentation and Measurement*, 47(5), October 1998.
- [8] J. Wang, A. Witulski, J. Vollin, T.K. Phelps, and G.I. Cardwell. Derivation, calculation and measurement of parameters for a multi-winding transformer electrical model. *Applied Power Electronics Conference and Exposition, 1999. APEC '99. Fourteenth Annual*, 1:220–226, 1999.

5962-27